



UNIVERSITÀ
DEGLI STUDI
DI PADOVA

Sede Amministrativa: Università degli Studi di Padova

Dipartimento di *Ingegneria Industriale*

SCUOLA DI DOTTORATO DI RICERCA IN : INGEGNERIA INDUSTRIALE
INDIRIZZO: INGEGNERIA CHIMICA
CICLO XXV

***SYNTHESIS AND CHARACTERIZATION OF FLUORINATED
COMPOUNDS FOR INDUSTRIAL APPLICATIONS***

Direttore della Scuola : Ch.mo Prof. Paolo Colombo

Coordinatore d'indirizzo: Ch.mo Prof. Alberto Bertucco

Supervisore :Ch.mo Prof. Lino Conte

Dottorando : Flavio Ceretta

General introduction

The presence of fluorine atoms in the structure of an organic molecule alters in an extraordinary way its physico-chemical properties and the countless applications of organo-fluorine compounds are a strong testimony of it.

The unique properties of fluorinated surfaces (low surface tension, dielectric constant, friction coefficient) derive from the particular features of the C-F bond (Chapter 1).

Thanks to their exceptionally low intermolecular interactions, fluorinated compounds produce surfaces with very low interfacial energies which are hardly wet by aqueous and organic liquids, have anti-adhesive properties and low friction coefficients. Thanks to these unique properties fluoro-polymers play an important role in various fields of modern industry.

Fluorinated thermoplastic polymers endowed with high thermal stability, low dielectric constants, excellent chemical resistance, very low surface tensions have now become commonly used both in the industrial practice and in *everyday life* applications (non-stick cookware, waterproof and breathable fabrics, optical fibers, to name a few).

In 2006 the EPA (Environmental Protection Agency) demonstrated the bio-accumulative effects of several perfluoro organic compounds with long perfluoro alkyl chain (and their derivatives). This environmental aspect led to the progressive banning of all long chain fluorotelomers compounds within 2015 (Chapter 2). Many of these compounds are currently comprised in the candidate list for SHVC (substances of very high concern) enclosed in the CLP Regulation. As a consequence of these decisions companies involved in the manufacture and marketing of fluoro-compounds for surface treatment are replacing long perfluorinated alkyl compounds with shorter ones.

The shortening of the chain length of the fluorinated moiety has posed challenging technological issues because of the dramatic loss of performances.

The goal of researchers is to find new molecular solutions able to maintain the same performances of “old” long chain molecules with shorter compounds.

In this work the study of alternative fluorinated polymers, obtained by controlled radical polymerization techniques (Chapter 3) were investigated. In particular, the synthesis of fluoroalkyl styrene monomer with short fluorinated chain was carried out (Chapter 4) and the optimization of the synthesis of its precursor, 4'-nonafluorobutyl acetophenone, was also studied. The fluoroalkyl styrene monomer was polymerized by conventional radical polymerization and controlled radical polymerization (Chapter 5).

Further, the telomerization of polyvinylidene fluoride in presence of 1-iodoperfluorobutane and trifluoromethyl iodide as chain transfer agents were investigated. The telomers synthesized were characterized by NMR analyses and the structure of the telomers chains were determined (Chapter 6).

Introduzione generale

La presenza di atomi di fluoro all'interno di una molecola organica è in grado di alterarne le proprietà chimico-fisiche in modo significativo e le innumerevoli applicazioni dei composti fluorurati ne sono la prova.

Le proprietà superficiali dei composti fluorurati sono attribuibili alle particolari caratteristiche del legame C-F. (Capitolo 1).

Le basse interazioni intermolecolari proprie dei composti fluorurati conferiscono alle superfici proprietà chimico-fisiche uniche: difficile bagnabilità da parte di liquidi acquosi ed organici, spiccate proprietà anti-adesive e basso coefficiente d'attrito. I composti fluorurati giocano pertanto un ruolo importante in svariati ambiti dell'industria moderna. I polimeri termoplastici fluorurati sono dotati di alta stabilità termica, bassa costante dielettrica, eccellente resistenza chimica, bassissima tensione superficiale.

Nel 2006 l'EPA (Environmental Protection Agency) dimostrò gli effetti di bio-accumulo di diversi composti perfluoroorganici dotati di una lunga catena perfluoroalchilica (e relativi derivati). Gli aspetti ambientali hanno portato alla progressiva dismissione di tutte le molecole fluorocarburiche a catena lunga entro il 2015 (capitolo 2). Alcuni di questi composti sono già presenti nella candidate list per le SVHC (substances of very high concern) del Regolamento CLP.

In conseguenza di queste decisioni le aziende coinvolte nella produzione e commercializzazione di prodotti fluorurati hanno cercato di adeguarsi rimpiazzando i prodotti fluorurati a lunga catena fluorocarburica con prodotti a catena corta.

L'accorciamento della catena fluorocarburica ha posto un problema tecnologico legato alla perdita delle performance dei nuovi composti fluorurati. Lo scopo dei ricercatori è quello di sintetizzare nuove molecole, in grado di mantenere le stesse performance dei vecchi composti a catena lunga e che non ne presentino più le caratteristiche di bioaccumulo e tossicità.

In questo lavoro di ricerca si è studiata un'alternativa ai composti fluorurati a lunga catena per applicazioni superficiali utilizzando tecniche di polimerizzazione radicalica controllata di monomeri a corta catena fluorurata (Capitolo 3). In particolare, si è studiata la sintesi di un monomero fluoroalchil stirenico a catena fluorocarburica corta, ottimizzando la sintesi del suo precursore, il 4'-nonafluorobutil acetofenone (Capitolo 4). Il monomero fluoroalchil stirenico è stato quindi polimerizzato attraverso una reazione di polimerizzazione radicalica convenzionale e controllata (Capitolo 5).

Infine, si è studiata la telomerizzazione del vinilidene fluoruro in presenza di 1-iodoperfluorobutano e trifluorometilioduro come *chain transfer agents*. I telomeri sintetizzati sono stati caratterizzati attraverso misure di spettroscopia NMR, le quali hanno permesso di determinare la struttura delle catene (Capitolo 6).

Contents

Chapter 1. Characteristics and properties of fluorinated compounds	11
1.1 Introduction.....	11
1.2 The properties of fluorine	11
1.3 The C-F system.....	12
1.3.1 Electronegativity and Density	12
1.3.2 Boiling point.....	12
1.3.3 The steric effect	13
1.3.4 Acidity and basicity	14
1.3.5 Thermal stability.....	15
1.3.6 Surface properties	15
1.4 Applications of fluorinated compounds.....	16
1.4.1 Refrigerants	16
1.4.2 Fire-fighting agents	16
1.4.3 Lubricants	17
1.4.4 Medical and pharmaceutical applications.....	17
1.4.5 Surfactants	18
1.4.6 Polymers	19
Appendix A: the surface tension	20
Physical models and basic equations.....	20
The measure of the contact angle	22
The measure of solid-liquid interfacial tension	23
Bibliography	25
Chapter 2. The environmental problems associated to perfluorinated compounds	27
2.1 Perfluorooctanoic acid (PFOA) and perfluorooctanoic sulfonate (PFOS)	27
2.2 Source of exposure of PFOA/PFOS	28
2.3 Health effects caused by PFOA/PFOS	29
2.4 The 2010/2015 PFOA Stewardship Program	30

2.5	Final considerations.....	31
Chapter 3.	The Fluorinated Polymers.....	35
3.1	General characteristics of fluoropolymers	35
3.2	Synthesis and polymerization of commercial fluorinated monomers	36
3.2.1	Tetrafluoroethylene.....	36
3.2.2	Vinylidene fluoride ^{8,11}	37
3.2.3	Chlorotrifluoroethylene ^{9,10}	38
3.2.4	Vinyl fluoride ⁸	39
3.2.5	Hexafluoropropylene ⁹	39
3.2.6	Fluorinated (meth)acrylic monomers ⁸	40
3.3	Fluorinated copolymers.....	41
3.3.1	Fluorinated elastomers.....	41
3.3.2	Copolymers containing heteroatoms in the chain.....	43
3.4	Polymerization of fluoromonomers.....	44
3.4.1	Telomerization.....	45
3.4.2	Controlled Radical Polymerization.....	46
3.5	Iodine transfer polymerization.....	47
Chapter 4.	Synthesis of 4'-nonafluorobutyl styrene.....	55
4.1	Introduction.....	55
4.2	The introduction of the phenyl ring.....	57
4.3	Cross-coupling reaction in presence of perfluoroalkyl iodide.....	58
4.4	Synthesis of 4'-nonafluorobutyl acetophenone (1).....	59
4.4.1	Materials and Methods.....	59
4.4.2	General procedure for the synthesis of 4'-nonafluorobutylacetophenone, C ₄ F ₉ C ₆ H ₄ COCH ₃ (1).....	59
4.4.3	Chemical characterization of 4'-nonafluorobutylacetophenone.....	60
4.5	Results and discussion.....	64
4.5.1	Effect of the metal catalyst.....	64
4.5.2	Effect of the solvent.....	66
4.5.3	Effect of the ligand.....	67

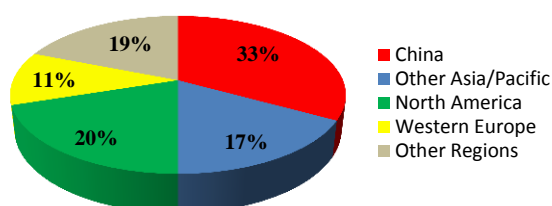
4.5.4	Effect of temperature	68
4.6	Conclusion	69
4.7	Synthesis of 4'-nonafluorobutyl ethanol (2).....	69
4.7.1	Materials	69
4.7.2	General procedure for the synthesis of 4'-nonafluorobutyl phenylethanol C ₄ F ₉ C ₆ H ₄ CH(OH)CH ₃	70
4.7.3	Chemical characterization of 4'-nonafluorobutyl phenylethanol.....	70
4.7.4	General procedure for the synthesis of 4'-nonafluorobutyl styrene C ₄ F ₉ C ₆ H ₄ CHCH ₂	73
4.7.5	Chemical characterization of 4'-nonafluorobutyl styrene.....	73
Chapter 5.	Polymerization of 4'-nonafluorobutyl styrene: surface and thermal characterizations of the resulting polymer.....	79
5.1	Synthesis of poly(4'-nonafluorobutyl styrene).....	79
5.1.1	Materials	80
5.1.2	Radical polymerization of 4'-nonafluorobutyl styrene by conventional radical polymerization.....	80
5.1.3	Radical polymerization of 4'-nonafluorobutyl styrene by iodine transfer polymerization.....	81
5.2	Characterization	81
5.3	Kinetics of iodine transfer polymerization of 4'-nonafluorobutyl styrene (3)	84
5.4	Contact angle assessment.....	88
5.5	Conclusion	90
	Appendix B: the Tobolsky's equation.....	92
Chapter 6.	Telomerization of VDF in presence of CF ₃ I and C ₄ F ₉ I as chain transfer agents. 97	
6.1	Introduction.....	97
6.2	The mechanism of the telomerisation of VDF.....	99
6.3	Telomerization of VDF with R _F I as chain transfer	101
6.3.1	Materials and methods.....	101
6.3.2	Telomerization of VDF using TBPP as initiator	102
6.3.3	Telomerization of VDF using (Perkadox [®] 16s) as initiator	103

6.3.4	Characterization of the telomers	103
6.4	Results and discussion.....	104
6.4.1	Telomerization of VDF with C ₄ F ₉ I as chain transfer.....	106
6.4.2	Telomerization of VDF using TBPP as initiator and C ₄ F ₉ I as chain transfer agent 107	
6.4.3	¹ H and ¹⁹ F NMR of C ₄ F ₉ -(VDF)-I and C ₄ F ₉ -(VDF) ₂ -I telomers	107
6.5	Synthesis of C ₄ F ₉ -(VDF) ₂ -CH ₂ -CH ₂ -CH ₂ -OH.....	111
6.5.1	Materials.....	111
6.5.2	Synthesis of C ₄ F ₉ -CH ₂ CF ₂ -CH ₂ CF ₂ -CH ₂ -CHI-CH ₂ -OH (2)	111
6.5.3	Synthesis of C ₄ F ₉ -CH ₂ CF ₂ -CH ₂ CF ₂ -CH ₂ -CH ₂ -CH ₂ -OH (3)	111
6.5.4	Chemical characterization of C ₄ F ₉ -CH ₂ CF ₂ -CH ₂ CF ₂ -CH ₂ -CHI-CH ₂ -OH (2) and C ₄ F ₉ -CH ₂ CF ₂ -CH ₂ CF ₂ -CH ₂ -CH ₂ -CH ₂ -OH (3).....	112
6.6	Conclusion.....	116
	Appendix C: half-life of initiators.....	117
Chapter 7.	Instruments.....	121
7.1	Nuclear Magnetic Resonance	121
7.2	Infrared and GC-MS.....	122
7.3	Surface characterizations.....	122
7.4	Gas chromatography (GC)	123
7.5	Gel permeation chromatography (GPC).....	124
7.6	Thermogravimetric analyses (TGA)	124
7.7	Differential scanning calorimetry.....	124
	General conclusion.....	125

Chapter 1. Characteristics and properties of fluorinated compounds

Introduction

Global demand of fluorine-containing chemicals is forecast to rise 3.9 percent per year to 3.5 million tons in 2016, valued at \$19.6 billion¹. The growing success of fluorinated compounds is due to the unique properties of the carbon-fluorine bond that affects the characteristics of



the fluorinated materials. In this chapter the chemical and physical aspects of the fluorine atom and fluoro-carbon bond is presented. The F-C bonds are the basic “brick” for the building of fluorinated organic compounds investigated in this work.

The properties of fluorine

Numerous properties typical of fluorinated materials can be anticipated by comparing the fundamental properties of fluorine with those of other elements (Table 1)². The low polarizability combined with the high ionization potential and small Van der Waals radius of fluorine imply very weak intermolecular reactions. For instance, the bond energy of fluorine molecule (F-F) is only 157 kJ/mol, weaker than the bond energies of hydrogen H-H (434 kJ/mol) and chlorine Cl-Cl (242 kJ/mol)³. Conversely, the bond energy of C-F in CF₄ is 546.0 kJ/mol, higher than the bond energy of C-H in CH₄ (446.4 kJ/mol) or C-Cl in CCl₄ (305 kJ/mol). The higher energy of C-F bond is due to its strong polarization ($\delta^+C-F\delta^-$) due to the very high electronegativity of fluorine which produce a strong electron-withdrawing effect when bonded to carbon. For these reasons the formation of C-F bonds is difficult and it explain the fact that in nature only 12 compounds containing C-F bonds have been found⁴. The greater strength of carbon-fluorine over the carbon-hydrogen bond leads to a considerable thermal stability for perfluorocarbon systems. The ionization potential (IP) is the highest except for those of helium and neon. Therefore, electrons are drawn strongly toward the fluorine nucleus. For this reason the electro dipole of fluorine atoms is small. As consequence, intermolecular Van der Waal’s attractive force between fluorine-containing compounds, is small. Moreover, the electronic configuration of fluorine with non-bonding *p*-electrons, shield the carbon backbone from attack giving to fluorinated materials anti-corrosive and stability towards oxidation.

Atom	IP ^a [kcal/mol]	EA ^b [kcal/mol]	α_v ^c [Å ³]	r_v ^d [Å]	χ_p ^e
H	313.6	17.7	0.667	1.20	2.20
F	401.8	79.5	0.557	1.47	3.98
Cl	299.0	83.3	2.18	1.75	3.16
Br	272.4	72.6	3.05	1.85	2.96
I	241.2	70.6	4.7	1.98	2.66

Table 1.1 Atomic physical properties. a) ionization potential; b) electronic affinity; c) atom polarizability; d) Van der Waals radius; e) Pauling's electronegativity.

The C-F system

1.1.1 Electronegativity and Density

Fluorine is the highest electronegative atom and for this reason it is always electron-withdrawing when bound to carbon. Consequently the C-F system is polarized and have a strong ionic character. All these properties ensure to C-F bond the highest bond energy compared to the other C-X systems (Table 1.2)³.

	H	F	Cl
Bond energies of C-X in C-X ₄ [kJ·mol ⁻¹]	446.4	546.0	305.0

Table 1.2. Comparison between the bond energies of some compounds.

Saturated perfluorocarbons have densities typically about 2.5 times those of corresponding hydrocarbons and they have greater compressibility and viscosities.

1.1.2 Boiling point

The boiling points of perfluorocarbons are close to the homologous hydrocarbons. Conversely, if we compare the molecular weight of this two categories of compounds, such as CF₄ (PM = 88) and n-hexane (PM = 78), the boiling points are very different: -128 °C and -161 °C respectively (Table 1.3).

	Boiling point [°C]									
	n = 1	n = 2	n = 3	n = 4	n = 5	n = 6	n = 7	n = 8	n = 9	n = 10
<i>n</i> -C _n F _{2n+2}	-128	-78	-38	-1	29	57	82	104	125	144
<i>n</i> -C _n H _{2n+2}	-161	-88	-42	-0.5	36	69	98	126	151	174

Table 1.3. Boiling points of linear perfluorocarbons and alkanes.

In contrast with hydrocarbons, the branching on perfluorinated systems does not significantly affect the boiling point of the molecules as reported in Figure 1.1

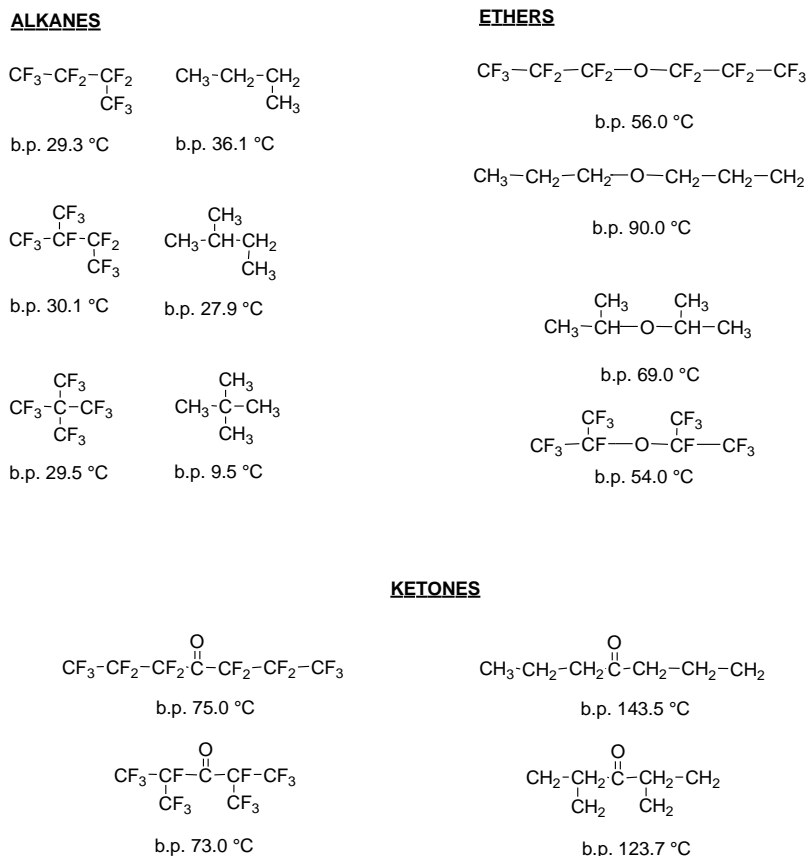


Figure 1.1 Effect of the branching on the boiling points of perfluorocarbons and hydrocarbons.

In the case of perfluoro ethers and perfluoroketones the difference of boiling point is more enhanced and it is due to the low intermolecular force.

1.1.3 The steric effect

Replacing hydrogen in organic molecule by fluorine modify the steric effect of the systems. In fact, the Van der Waals radii of hydrogen is 1.20 Å, for fluorine is 1.40 Å. Also, the C-F length (1.38 Å) is longer than those of C-H (1.09 Å). Consequently, the CF₃ group is more sterically demanding than methyl substituent group (Figure 1.2) with a Van der Waals volume of 16.8 Å³ for CH₃ and 42.6 Å³ for CF₃.⁵

The steric effect influence the behavior of fluorinated molecules that differ from the “classical” chemistry. For instance, the spatial configuration of polyethylene is all-trans, while for PTFE is helical⁶.

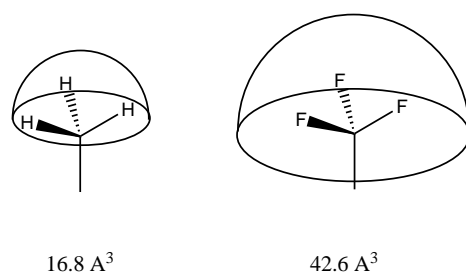


Figure 1.2. Comparison between the Van Der Waals volume of CH_3 and CF_3 substituent.

1.1.4 Acidity and basicity

The introduction of perfluoroalkyl group into the backbone of organic acid such as alcohols and carboxylic acids increase the acidity of the system and this is due to the high electronegativity of the fluorine.

Alcohol	n° fluorine	pK _a	Carboxylic acid	n° fluorine	pK _a
$\text{CH}_3\text{CH}_2\text{OH}$	-	15.9	CH_3COOH	-	4.76
$\text{CF}_3\text{CH}_2\text{OH}$	3	12.4	CH_2FCOOH	1	2.59
$(\text{CH}_3)_3\text{COH}$	-	19.2	CHF_2COOH	2	1.34
$(\text{CF}_3)_3\text{COH}$	9	5.1	CF_3COOH	3	0.52

Table 1.4. pK_a values of some organic acids and alcohols. The introduction of fluorinated atoms in the carbon chain increase the acidity of the substances.

The substitution of one hydrogen with fluorine in carboxylic acid increases the acidity of about 100 times while the presence of trifluoromethyl group increase the acidity 1000 times (Table 1.4). All the secondary and tertiary fluorinated alcohols were strongly acidic because of the cumulative inductive effect of the fluorine atom present in the molecules⁷. Interesting, the acidity of perfluoro-*t*-butanol is comparable with the acidity of acetic acid.

Correspondingly, fluoroalkyl groups lower the strength of bases, examples for amines are reported in Table 1.5.

Amine	n° fluorine	pK _b
$\text{CH}_3\text{CH}_2\text{NH}_2$	-	10.6
$\text{CF}_3\text{CH}_2\text{NH}_2$	3	5.7
$\text{C}_6\text{H}_5\text{NH}_2$	-	4.6
$\text{C}_6\text{F}_5\text{NH}_2$	5	-0.36

Table 1.5. pK_b values of some amines. The introduction of fluorinated atoms in the carbon chain decrease the basicity of the substances.

The lack of basicity decrease the reactivity of secondary perfluoro amines $(R_F)_2NH$ that do not react, for example, with boron trifluoride, hydrogen chloride or trifluoroacetic acid⁸. Also the oxygen atoms in perfluoro-ethers and perfluoro-ketones are poor electron donor⁹. For example, hexafluoroacetone is so no basic and it cannot be protonated in solution by superacids².

1.1.5 Thermal stability

In monohaloalkanes, the C-F bond is about 25 kcal mol⁻¹ stronger than C-Cl bond and this is due to the poor leaving-group ability of fluoride ion. Therefore, alkylfluorides are 102-106 times less reactive than the corresponding alkylchloride in typical S_N1 or S_N2 reactions. Table 6 summarize the bond dissociation energies for ethanes. From the data is remarkable that α -fluorination always increases C-F and C-O bond strengths but does not have significantly influence on the other atoms. Conversely, β -fluorination increases C-H bond but does not influence the C-F bonds.

X	BDE [kcal mol ⁻¹]			
	CH ₃ CH ₂ -X	CH ₃ CF ₂ -X	CF ₃ CH ₂ -X	CF ₃ CF ₂ -X
H	100.1	99.5	106.7	102.7
F	107.9	124.8	109.4	126.8
Cl	83.7	-	-	82.7
Br	69.5	68.6	-	68.7
I	55.3	52.1	56.3	52.3

Table 1.6. Bond dissociation energies (BDE) of ethanes.

The thermal stability of perfluorocarbons decrease with increasing the chain length or chain branching. Indeed, the most thermo stabile perfluorocarbons is the CF₄ whose C-F bond thermolyze over 2000 °C. Conversely, perfluorocarbons with tertiary C-C bonds thermolyze around 300 °C. Perfluoroethers are more thermally stable than PCFs, thanks to the presence of strong C-O bonds. For example, poly-(CF₂CF₂O) decompose at 585 °C, 10 times slower than poly-(CF₂CF₂). Hydrofluorocarbons are less thermally stable than their PFCs counterparts and this is due to the rapidly elimination of HF that starts above about 350 °C⁶.

1.1.6 Surface properties

The perfluorinated ethers and amines have low surface tensions (see appendix), typically 15-16 mN·m⁻¹. The surface tensions of hydrocarbons are always greater than those of corresponding perfluorocarbons (Table. 1.7)².

Structure	Surface tension [dyn·cm ⁻¹]	
	Perfluorocarbons (X = F)	Hydrocarbons (X = H)
<i>n</i> -C ₅ X ₁₂	9.4 ^a	15.2 ^a
<i>n</i> -C ₆ X ₁₄	11.4 ^a	17.9 ^a
<i>n</i> -C ₈ X ₁₈	13.6 ^a	21.1 ^a
C ₆ X ₆	22.6 ^b	28.9 ^c

Table 1.7. Surface tension of perfluorocarbons and hydrocarbons measured at 25 °C (^a), 23 °C (^b) and 20 °C (^c).

Applications of fluorinated compounds

The unique properties of fluorinated compounds mentioned above have continuously increased the use of these materials in a wide range of industrial applications. In this paragraph a non-exhaustive list of examples of commercial applications will be mentioned.

1.1.7 Refrigerants

A fluid for mechanical refrigeration must be thermally and chemically stable and non-corrosive and should possess suitable vapor-pressure characteristics. Further it should be non-toxic and non-flammable. Until 30's, when there was the advent of chlorofluorocarbons (CFCs)¹⁰ there was no fluid displaying these properties all together. The principal CFCs used were CF₂Cl₂, CFCl₃, CHFCl₂. Their volatility and inertness posed environmental issues because they dissociate under short wavelength up to the stratosphere, releasing chlorine atoms which catalyze the decomposition of ozone. Consequently, the CFCs were replaced with the HFCs such as CF₃CFH₂ (HFC-134a) which are chlorine free and are not dangerous for the ozone.

1.1.8 Fire-fighting agents

Fire extinguishing foams of various types are known for use against fire for polar and non-polar flammable liquids such as hydrocarbon solvents, kerosene, crude oil and so on. Often, these foams additionally provide the ability to form a film on the surface of a liquid. The film formed should inhibit the re-ignition of the flammable liquids. Aqueous film forming foam (AFFF) concentrates are concentrated aqueous solutions that can be diluted and used as extinguish flammable liquids fire. The concentrates can contain fluorinated surfactants in low concentration (usually 6-8 %) which contribute to improve the extinguishing power of the fire-fighting agents. Further the extremely low interfacial tension obtained with fluorinated surfactants allows an easy spreading of the foam on surfaces facilitating the extinguishing procedure in case of fire in closed and narrow places such as planes or tanks. Different examples of fluorinated agents are reported in literature¹¹⁻¹⁵.

1.1.9 Lubricants

Perfluoropolyethers (PFPEs) with high molecular weights are commercialized as lubricants (see Figure). The characteristics of these compounds are the long liquid range, they remain fluid from -100 °C to 350 °C. consequently they find application in the lubrication of precision instruments, from the mechanism of watches to computer discs.

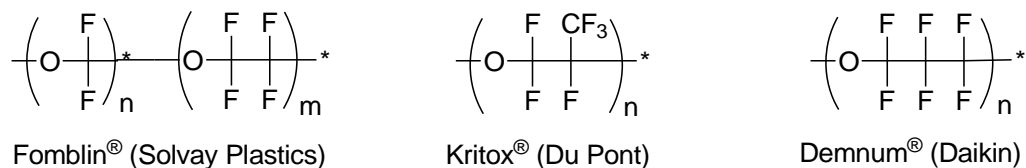


Figure 1.3. Some examples of commercialized lubricants based on PFPEs.

1.1.10 Medical and pharmaceutical applications

Perfluorocarbons are inert to microbiological attack and can dissolve significant amounts of oxygen, for these reason perfluorocarbons can be used as artificial blood¹⁶. The incorporation of fluorine into a biologically active molecule may modulate the absorption, the transport through membranes before reaching the correct site of action and produce the desired effect on the appropriate enzyme site¹⁷. Also, the presence of fluorinated groups in the drugs can increase their acidity or decrease their basicity. For example, the presence of the trifluoromethyl groups can enhance the lipophilicity of an aromatic substrate to facilitate the transport of the drug. In Figure 1.4 are reported some examples of commercialized drugs that contain fluorinated groups.

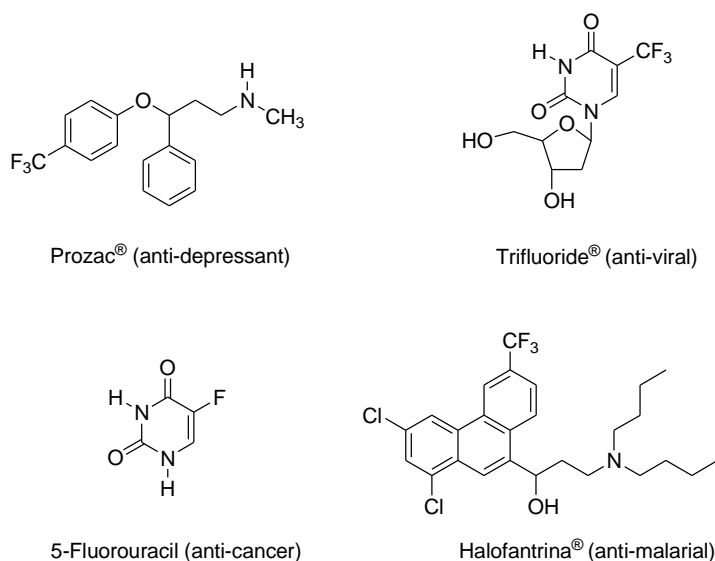


Figure 1.4. Examples of commercial drugs containing fluorinated moieties.

1.1.11 Surfactants

Molecules that bear both hydrophobic and hydrophilic parts are called surfactants. These compounds can be classified either cationic, anionic, amphoteric or non-ionic¹⁸. Fluorinated surfactants, thanks to the fluorinated moieties, contribute to increase the hydrophobic behaviour of the molecules. In particular, fluorinated surfactants have a lower surface tension respect to hydrocarbon counterpart and for these reason sometimes they are called “super surfactants” and exhibit a lower critical micellar concentration (c.m.c.)¹⁹. Historically the production of perfluorosurfactants began in 1949 by 3M with the production of perfluorooctane sulfonyl fluoride (C₈F₁₇SO₂F). From 1949 to 2002 3M manufactured approximately 3665 t of PFOS²⁰. The whole of perfluorosulfonates (PFSAs, C_nF_{2n+1}SO₂F) such as the mentioned perfluorooctane sulfonate (PFOS), and the perfluorocarboxylic acids (PFCAs, C_nF_{2n+1}COOH) represent the most known class of perfluorosurfactants. The physical and chemical properties, such as persistence and volatility, vary depending on the length of the functional groups.

Because of their environmental and health toxicity the production of surfactants based on PFOA and PFOS has almost ceased (see Chapter 2).

Thanks to both hydrophobicity and oleophobicity, join to their chemical and thermal inertness, fluorosurfactants are used in more than 200 applications²⁰⁻²⁴ including soil and stain-repellents, fire fighting foams, paints, lubricants, clothing fabrics, textile, leather, carpets, and paper coatings, electroplating, photographic emulsifiers, pressure sensitive additives, waxes, polishes, pharmaceuticals, insecticides, or involved in cosmetics formulations.

1.1.12 Polymers

Unlike organofluorine chemistry, the chemistry of fluoropolymers is rather recent. In 1934 poly(chlorotrifluoroethylene), $-(CF_2-CFCl)_n-$ was synthesized, then in 1938 Plunkett discovered poly(tetrafluoroethylene), (PTFE) $-(CF_2-CF_2)_n-$, known with the commercial name of Teflon[®] by DuPont de Nemours Co. Later, different homopolymers were synthesized, most from fluorinated olefins such as tetrafluoroethylene (TFE), vinylidene fluoride (VDF), vinyl fluoride (VF), and chlorotrifluoroethylene (CTFE). Perfluorinated homopolymers exhibit too high crystallinity rates, compromising their solubility in common organic solvents. Further, they are cross-linkable with difficulty. For this reason in the last decades a large number of co-polymers were developed²⁵. Co-polymers are composed of a mixture of co-monomers that can insert bulky side groups or may induce a certain disorder in the molecule that reduce the high crystallinity of homopolymers. For examples, fluorinated thermoplastics obtained by the copolymerization of VDF with HFP, such as KF Polymer[®], Kynar[®], and Solef[®] (manufactured respectively by Kureha, Arkema, and Solvay) are widely produced. In contrasts, fluoroelastomers such as Dyneon Elastomer[®], Viton[®], Daiel[®], and Technoflon[®], are produced by Dyneon, DuPont Performance Elastomers, Daikin or Solvay Speciality Polymers respectively. In general, fluoropolymers possess variable morphologies, from thermoplastics to elastomers and can be semicrystalline or totally amorphous.

Fluoropolymers have found a large number of applications in chemical industries (high performance membranes), building industries (paints and coatings), petrochemicals and automotives, aerospace and aeronautics (elastomers used as packings, O-rings or diaphragms devote for extreme temperatures close to liquid hydrogen or hydrazine tanks in the booster of space shuttles), for optics (optical fibers), textile, fabrics or stone treatment (coating of old monuments), microelectronics²⁵⁻²⁷. More details about mechanism and strategies for the synthesis of fluoropolymers will be described in Chapter 3.

Appendix A: the surface tension

Physical models and basic equations

Consider a molecule P1 positioned in the bulk (Figure 1.5) of a liquid. The resultant of the forces acting on P1 is zero because the molecules positioned all around P1 interact with it with the same force. P1 is thus in equilibrium. A molecule P2 located at the air-liquid interface is still in equilibrium but a different force resultant exists and an additional force must be invoked in order to compensate the asymmetrical attraction exercised by neighbors. This additional force is called surface tension between the liquid and vapor phases, γ_{LV} (sometimes it is indicated only as γ_L).

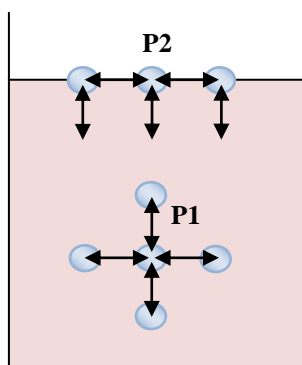


Figure 1.5 Equilibrium of the forces that act on a molecule in the bulk and at the surface of a liquid.

When a droplet of water is deposited on a solid surface three interfaces exist: solid-liquid (γ_{SL}), vapor-liquid (γ_{LV}), vapor-solid (γ_{SV}). The balance between these three interfacial forces determines the shape of the drop and the value of the contact angle (Figure 1.6).

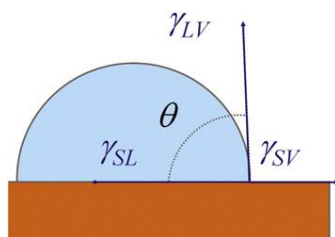


Figure 1.6 Model of a drop on a solid surface. The scheme shows the three interfacial forces in three phase contact angle.

The contact angle is a very common measure of the hydro-phobicity of a solid surface. The relationship between surface tension and contact angle was first recognized by Young. At equilibrium, the contact angle is obtained by the balance of the surface tension forces:

$$\gamma_{SV} = \gamma_{SL} + \gamma_{LV} \cos \theta_Y \quad \text{Eq. 1.1}$$

This is called Young's equation and θ_Y represents the contact angle. The quantity γ_{LV} (or γ_L) can be easily measured directly by specific methods such as the Du Nouy ring or Wilhelmy plate. The measure of the contact angle and γ_{SL} are describe in the next paragraphs. γ_{SV} (or γ_S) is the only factor that is not directly measurable.

The Young's equation requires that the solid surface must be smooth, flat, homogeneous, inert, insoluble, non-reactive, and non-deformable. A surface with all this properties is referred as an ideal surface. However, most of the surfaces are non-ideal, and the measure of the contact angle with the Young's equation is considered "apparent". This means that the value of contact angle measured by the Young's equation falls into an interval between the advancing (the largest) and the receding (the smallest) contact angle. The difference between these extremes is called contact angle hysteresis. The most important factors affecting the non-ideality of a surface are: contamination of either the liquid and solid surface, the surface roughness, and surface immobility on a macromolecular scale.

Wenzel investigated the effect of roughness on the measure of the static contact angle which causes a hydrophobic fluid to behave as if it were more hydrophobic and a hydrophilic fluid to behave as if it were more hydrophilic. Wenzel highlighted the importance of the effect of the geometry of the surface. When a drop is sufficiently large compared with the roughness scale, and if the liquid completely penetrates into the roughness grooves of the solid surfaces, the measure of the contact angle can be evaluated as:

$$\cos\theta_W = r \cos\theta_Y \quad \text{Eq. 1.2}$$

Where θ_W is the Wenzel contact angle, and r is the average roughness ratio, defined as the ratio between the true and apparent surface area of the solid.

A more accurately description of the contact angle phenomena for heterogeneous and rough surfaces was done by Cassie and Baxter. The apparent contact angle is related to the ideal contact angle by the equation:

$$\cos\theta_C = f_1 \cos\theta_1 + f_2 \cos\theta_2 \quad \text{Eq. 1.3}$$

Where f_1, f_2 are the fractional area of the surface with contact angle θ_1 and θ_2 respectively. The value θ_C is the Cassie's contact angle, and Eq. 1.3 is called Cassie's equation. In the case of non-wetting situation for a porous surface f_2 is the fraction of air spaces which makes $\cos\theta_2 = -1$, as $\theta_2 = 180^\circ$ (e.g. : hydrophobic):

$$\cos\theta_c = f_1 \cos\theta_1 - f_2 \quad \text{Eq. 1.4}$$

Eq. 1.4 is called the Cassie-Baxter's equation.

The theory proposed by Wenzel and Cassie is consistent and they have been widely used to predict the real surface behavior. The main problem that limit these theories is the evaluation of the average roughness and the accurately determination of the parameters f_1 and f_2 . For these reasons the determination of contact angle of the polymers synthesized in this thesis is based on the Young's model.

The measure of the contact angle

The measure of the contact angle is performed using a Drop Shape Analysis. The general method used to determine the contact angle is the *sessile drop method*. The surface of the solid should be as flat as possible. A liquid drop of fixed volume is deposited on the solid surface with the aid of a syringe. In this way the measure is independent from the size of the drop. The determination of the contact angles is based on the adaptation of the drop in the region of three-phase contact point to the solid surface. The instrument used for the measure has a camera which registers the shape of the drop. The software of the instrument use various functions and system of equations to calculate the shape of the drop. Once the proper function has been chosen, the contact angle can be determine from its derivative. The derivative of this equation at the baseline gives the slope at the three phase contact point and thus the contact angle.

In this thesis the equation of a conical section was choice to adapt the shape of the drop.

The measure of the contact angle can be differentiated in *static contact angle* and *dynamic contact angle*. In the measure of the static contact angle the drop is deposited on the surface and its shape and contact-angle is assumed to be time-independent. The dynamic contact angle describes the time evolution of both the shape and contact angle of drop at the liquid-solid boundary during the wetting and dewetting processes. The dynamic contact angle measure is composed by two phases, the advancing and receding contact angle. Conversely from the static measurement in this case the syringe remains in the drop during the whole of the measurement. A drop of fixed volume is deposited on the solid surface and then it is slowly enlarged by adding more liquid. The contact angle initially increases, then the drop starts to wander over the solid surface: the contact angle is measured during the slow advance across the liquid surface. Once joint the fixed volume, the siring start to suk back the liquid from the drop and the system records the contact-angle between the liquid front and the wetted surface. The difference between the advancing and receding contact angle is called

hysteresis and it is a direct measure of the wettability of the surface: the smaller the hysteresis the smaller the surface wettability.

The measure of solid-liquid interfacial tension

Considering two phases with interfacial tension γ_1 and γ_2 respectively, the interfacial tension between them can be described as:

$$\gamma_{12} = |\gamma_1 - \gamma_2| \quad \text{Eq. 1.5}$$

Where γ_{12} is the interfacial tension between the two phases.

Good and Girifalco²⁸ improve Eq. 1.5 with the introduction of a new parameter φ , a complicate function of the molecular size and determined empirically.

$$\gamma_{12} = \gamma_1 + \gamma_2 - 2 \varphi \sqrt{\gamma_1 \gamma_2} \quad \text{Eq. 1.6}$$

Fowkes²⁹ took into account the dispersion forces (γ_1^d, γ_2^d) present in all atoms and molecules (caused by the temporary asymmetrically charge distribution)

$$\gamma_{12} = \gamma_1 + \gamma_2 - 2 \sqrt{\gamma_1^d \gamma_2^d} \quad \text{Eq. 1.7}$$

Owens and Wendt³⁰ considered the contribute of the polar forces that involve certain molecules and originated by the electronegative of different atoms:

$$\gamma = \gamma^d + \gamma^p \quad \text{Eq. 1.8}$$

Eq. 1.8 express the interfacial tension as the sum of the interfacial tension due to the polar contribution and to the dispersive contribution.

Assuming the parameter $\varphi = 1$ combining Eq. 1.6-1.8 is possible to obtain the expression of the interfacial tension according to Owens-Wendt:

$$\gamma_{12} = \gamma_1 + \gamma_2 - 2 \left(\sqrt{\gamma_1^d \gamma_2^d} + \sqrt{\gamma_1^p \gamma_2^p} \right) \quad \text{Eq. 1.9}$$

If the value of polar and dispersive components of one phase is known (commonly those of liquid) then the polar and dispersive components of the second phase can be calculated from the value of the contact angle.

Mathematically, Eq. 1.9 is a geometric mean, is also possible to use different expression using the harmonic mean or the geometric-harmonic mean. Such method provides different results, the choice of the mean depends on the kind of system studied³¹.

The method of Owens-Wendt use Eq. 1.9, that can be rewrite:

$$\gamma_{SL} = \gamma_S + \gamma_L - 2 \left(\sqrt{\gamma_S^d \gamma_L^d} + \sqrt{\gamma_S^p \gamma_L^p} \right) \quad \text{Eq. 1.10}$$

Considering the Young's equation (Eq. 1.1) and transforming this relationship as a straight line equation $y = mx + b$:

$$x = \frac{\sqrt{\gamma_L - \gamma_L^d}}{\gamma_L^d} = \frac{\sqrt{\gamma_L^p}}{\sqrt{\gamma_L^d}}$$

$$y = \frac{1 + \cos\theta}{2} \frac{\gamma_L}{\sqrt{\gamma_L^d}} \quad \text{Eq. 1.11}$$

$$m = \sqrt{\gamma_S^p}$$

$$b = \sqrt{\gamma_S^d}$$

If the values γ_L , γ_L^d , γ_L^p are known for various test liquids and if the contact angles θ to the solid surface have been measured then, a straight line can be build by points (x1, y1), (x2, y2), etc.. Once the straight line have been drawn is possible to determine the slope m and intercept b , which the value γ_S^p , γ_S^d are obtain. Usually, for this method two different liquids are used: distilled water and diiodomethane.

Bibliography

- (1) Feedonia *World Fluorochemicals- Industry Study with Forecast for 2016 & 2021*. www.feedoniagroup.com **2012**,
- (2) Smart, B. E., *Organofluorine Chemistry. Principle and Commercial Applications*. ed. B. E. Smart R. E. Banks, J. C. Tatlow 1994, Plenum: New York. pp. 57-88.
- (3) Chambers, R.D., *Fluorine in Organic Chemistry*. 2004, Blackwell Publishing-CRC Press: Oxford (UK). pp. 1-22.
- (4) D. O'Hagan, D.B. Harper *Nat. Prod. Rep.* **1994**, 11, 123-133.
- (5) Seebach, D. *Angew. Chem.* **1990**, 29, 1320-1367.
- (6) Wall, L. A., *Fluoropolymers*. High Polymers. Vol. XXV 1972, Wiley: New York.
- (7) W.J. Middleton, R.V. Lindsey *J. Am. Chem. Soc.* **1964**, 86, 4948-4952.
- (8) J.A. Young, S.N. Tsoukalas, R.D. Dresdner *J. Am. Chem. Soc.* **1958**, 80, 3604-3606.
- (9) Chambers, R.D., *Fluorine in Organic Chemistry*, ed. Blackwell Publishing Ltd. 2004, Oxford (UK): CRC Press.
- (10) T. Midgley, A. L. Henne *Ind. Eng. Chem.* **1930**, 22, 542-545.
- (11) Francen, V. **1973**, Minnesota Mining & MFG.
- (12) R. Bertocchio, L. Foulletier, A. Lantz **1991**, Ugine Kuhlmann.
- (13) G. Garcia, E. Morillon, C. Varescon, C. Kalinka, I. Devaux **1994**, Atochem ELF SA.
- (14) M.R. Stern, P.L. Blagev, W.Q. Fan **1997**, Minnesota Mining & MFG.
- (15) M.C. Candido, L. Conte, A. Zaggia **2008**, Sicit Chemitech s.p.a.
- (16) Riess, J.G. *Chem. Rev.* **2001**, 101, 2797-2919.
- (17) D. O'Hagan, H.S. Rzepa *J. Chem. Soc., Chem. Commun.* **1997**, 7, 645-652.
- (18) Kissa, E., *Fluorinated Surfactants and Repellents*. 2nd ed. Hubbard 2001, Marcel Dekker: New York.
- (19) Taylor, C. *Annual Surfactant Review* **1999**, 2, 271-296.
- (20) A.G. Paul, K.C. Jones, A.J. Sweetman *Environ. Sci. Technol.* **2009**, 43, 386-392.
- (21) M.-P. Krafft, J.G. Riess *J. Polym. Sci., Part A: Polym. Chem.* **2007**, 45, 1185-1198.
- (22) G. Kostov, F. Boshet, B. Ameduri *J. Fluorine Chem.* **2009**, 130, 1192-1199.
- (23) Riess, J.G. *Curr. Opin. Colloid Interf. Sci.* **2009**, 14, 294-304.
- (24) A. Zaggia, B. Ameduri *Curr. Opin. Colloid Interf. Sci.* **2012**, 17, 188-195.
- (25) B. Ameduri, B. Boutevin, *Well-Architected Fluoropolymers: Synthesis, Properties and Applications*. ed. Elseviers 2004: Amsterdam.
- (26) Scheirs, J., *Modern Fluoropolymers*. 1997, Wiley: New York.
- (27) Feiring, A.E., *Organofluorine Chemistry: Principles and Commercial Applications*. R.E. Banks and B. Smart ed., ed. Plenum Press 1994: New York. pp. 339-372.
- (28) R.J. Good, L.A. Girifalco *J. Phys. Chem.* **1960**, 64, 561-565.
- (29) Fowkes, F.M. *J. Phys. Chem.* **1964**, 66, 382.

- (30) D.K. Owens, R.C. Wendt *J. Appl. Polym. Sci.* **1969**, 13, 1741-1747.
- (31) Zenkiewicz, M. *J. Achieve Mater. Manuf. Eng.* **2007**, 24, 137-145.

Chapter 2. The environmental problems associated to perfluorinated compounds

As shown in the previous chapter the particular physico-chemical properties associated with perfluorinated compounds allow their wide spread use every day-life, industrial and institutional applications. In the early 90's many studies demonstrated the accumulation of fluorinated compounds in the environment and in human tissues¹. The U. S. Environmental Protection Agency (EPA) in agreement with the eight major companies involved in the production of fluorinated compounds through the voluntary 2010/2015 PFOA Stewardship Program aim to the complete elimination of 'long-chain' perfluorochemicals by 2015.

Perfluorooctanoic acid (PFOA) and perfluorooctanoic sulfonate (PFOS)

Perfluorinated chemicals (PFCs) are a class of organic compounds characterized by a completely fluorinated moiety and a functional group. PFCs do not occur naturally, and they have been produced and used in commercial and industrial applications for over 60 years². PFCs are extremely persistent and the high energy bond of the C-F bond contrast the typical environmental degradation processes³. Perfluorooctanoic acid (PFOA) and perfluorooctanoic sulfonate (PFOS) are the reference compounds in the environmental studies of bioaccumulation of PFCs. PFCs could be classified in 'short-chain' compounds (when the number of perfluorinated carbon atoms is less than six and 'long-chain' (when the number of perfluorinated carbon atoms is higher than 6) such as PFOA and PFOS.

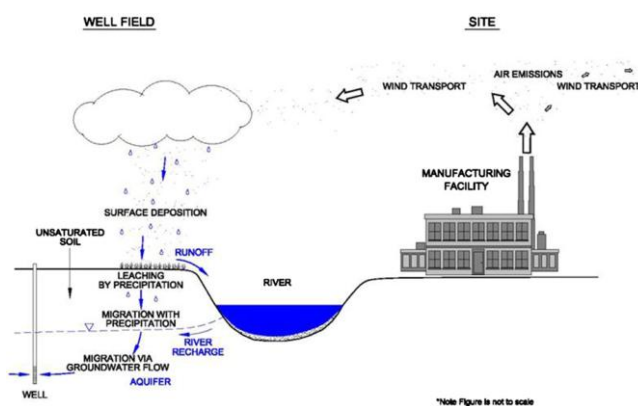


Figure 2.1. PFOA and PFOS transport near discharge source⁸.

Source of exposure of PFOA/PFOS

PFOA is used as polymerization aid in the production of fluoropolymers such as Teflon[®]. The possible PFOA/PFOS route to the environment are mainly two: direct exposure and indirect exposure. The main direct PFOA source of contamination is the manufacturing and

use of ammonium perfluorooctanoate (APFO). PFOS emissions are produced directly by the manufacture, use, and application of perfluoroalkyl sulfonate (PFAS). In particular, direct sources of exposure of PFOA and PFOS are mainly due by released in wastewater streams of repellent treated carpets, waterproof apparel, and aqueous fire fighting foams. About 85% of the emission are caused by the disposal from consumers of carpets, clothes, paper, and packaging⁵. An example of indirect PFOA and PFOS source of exposure are fluorotelomer alcohols (FTOHs) and perfluorooctane sulfonyl fluoride (POSF)-based chemicals which can degrade in PFOA and PFOS respectively^{4,6,7}.

PFOA properties are different from other persistent and bioaccumulative pollutants such as polychlorinated dioxine, furans, and pesticides (like chlordane and DDT). In contrast with other pollutants, PFOA and PFOS are water-soluble does not bind well to soil or sediments, and bioaccumulate in serum rather in fat. For these reasons PFOA and PFOS are distinctive as persistent and bioaccumulative organic compounds

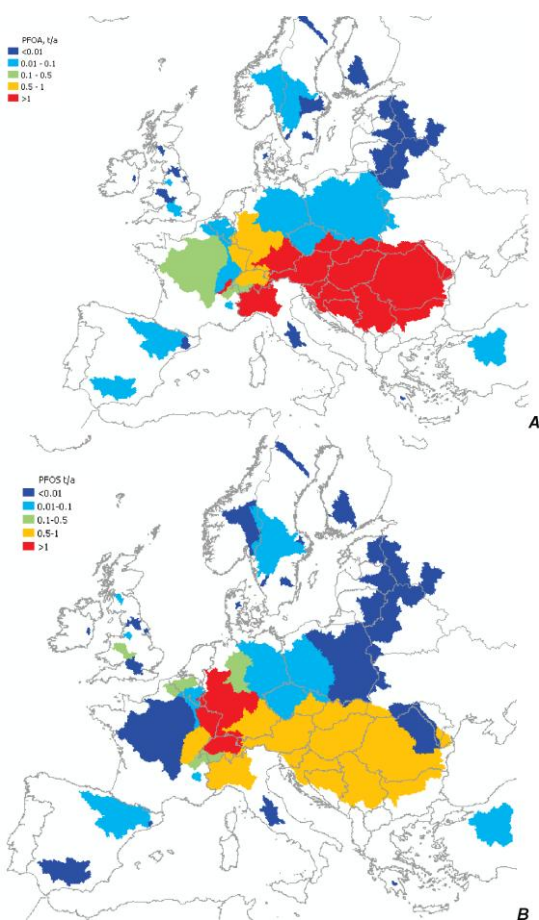


Figure 2.2. Map of PFOA (A) and PFOS (B) emissions (t/a) for monitored catchments in Europe⁸.

that are important drinking water contaminants⁸. PFOA and PFOS migrates from air emissions from industrial facilities onto soil, followed by migration through the solid to groundwater (Figure 2.1). As consequence, drinking water is one of the most important source of human exposure of PFOA. Further, researchers demonstrate that the wastewater treatment plant effluents are one of the major sources of PFOA and PFOS^{9,10}. Pistocchi and Loos¹¹, estimate a map of European emissions of PFOA and PFOS (Figure 2.2). Skutlarek et al.¹² evidenced the contamination of PFOA and other PFCs in the Mohenne and Ruhr Rivers, important source of drinking water. PFOA was detected up to 33,900 ng/L in a creek near the site of contamination upstream of these rivers, and at up to 519 ng/L in drinking water from

the Mohenne River. Also, in Catalonia, Spain, PFOA was detected at up to 0.85 ng/L in 65% of 40 municipal water systems¹³.

PFOA present in drinking water is not removed by standard water treatment processes such as coagulation, sand filtration, sedimentation, ozonation, or chlorination but it is removed by activate carbon^{14,15}. The sources of exposure to PFOA or its precursors include not only drinking water but also food, migration of food packaging into food, treated fabrics (carpets, clothing), house dust, ski waxes¹⁶. Migration into food from PTFE-coated cookware is not considered to be significant exposure source¹⁷. Most of the studies confirm that the predominant exposure source is the diet. Unfortunately, the quantitative data are uncertain because there are few data on PFOA level in food, and PFOA levels differ from sample of the same foods obtained from different locations. For these reasons in Flanders, Belgium, estimates a PFOA dietary exposure of 6.1 ng/kg/day¹⁸, in Norway 0.6 ng/kg/day¹⁹, and in Netherlands 0.2 ng/kg/day²⁰. PFOA was detected in several samples of foods including bread, milk, microwave popcorn, meats, fish, butter, vegetables²¹

Health effects caused by PFOA/PFOS

Given the widespread production and the use of fluorinated organics, it is not surprising that organic fluorine has been detected in the blood of individuals from the general public as well as industrial workers^{22,23}. For workers handling fluoroorganics, organic fluorine levels of 1.0-71.0 ppm have been reported in their blood serum. In individuals that have not been exposed to industrial fluorochemicals the concentration of organic fluorine range from 0.0 to 13.0 ppm. Guy et al.²⁴ suggested that there is a widespread contamination of human tissues with organofluorine compounds derived from commercial sources of PFOA. Two studies estimate the half-life of PFOA in humans: one²⁵ considered 26 retired workers employed in the production of fluoroorganics chemicals, the median half life (followed up for 5 years) was 3.4 years, the second¹⁴ is based on 200 people who had been exposed via public water supplies and followed for 1 year, the mean of half life of PFOA was 2.3 years. PFOA is completely absorbed by oral exposure²⁶, through skin²⁷, and by dust inhalation²⁸. Most of the information on health effects in humans and animals are recent. Overt toxicity or mortality has not been reported in humans after accidental or intentional acute exposure to PFOA at concentration higher than those encountered in the workplace²⁹. In 2009 the *C8 Health Study* provided information on the exposure to PFOA present in drinking water, serum level and biological changes on a large community (about 70,000 Ohio and West Virginia resident) exposed at wide range of PFOA levels (≥ 50 ng/L to over 3000 ng/L). For the first time many health endpoints have been significantly associated with PFOA levels³⁰. These include elevated cholesterol and other serum lipid parameters, increased risk of elevated uric acid in adults, change in several indicators of inflammatory and immune response, delayed puberty in girls,

early menopause, thyroid disease in women. Forthcoming studies will evaluate other endpoints, including cancer incidence in this population. Studies on workers exposed directly to both PFOA and PFOS showed some consistency of increased cancer mortality and/or incidence, including bladder, kidney, and prostate cancer³¹. More data are available in case of animals. PFOA induce tumours of the testicles, liver, and pancreas in rodents^{32,33}.

The 2010/2015 PFOA Stewardship Program

After the numerous studies conducted on PFOA/PFOS, the U.S. EPA concluded that evidence was suggestive that PFOA is carcinogenic in humans. In its review of that risk assessment in 2006 U.S. EPA concluded that PFOA is “likely to be carcinogenic for humans”³⁴. In the same year U.S. EPA initiated the 2010/2015 PFOA Stewardship Program³⁵, in which the eight major companies involved in the production of fluorinated organic chemicals, committed voluntary to reduce facility emission and product content of PFOA and related chemicals. The two goals of the PFOA Stewardship Program were:

- 1) To commit to achieve, not later than 2010, a 95% reduction, measured from a year 2000 baseline, in both: facilities emissions to all media of PFOA, precursors chemicals that can break down to PFOA, and related high homologue chemicals.
- 2) To commit working toward the elimination of PFOA, PFOA precursors, and related higher homologue chemicals from emission and products by five years thereafter, or no later than 2015.

To ensure transparency, companies submit each year annual public reports on their progress toward the goals. Global production of PFOA was phased out in the last years, U.S. serum levels have declined markedly, from a geometric mean of 30.4 ng/mL in 1999-2000 to 13.2 ng/mL in 2001-2008³⁶. As part of the voluntary stewardship effort by major manufacturers to reduce the use of PFOA, new fluorinated and polyfluorinated compounds, including short chain length PFCs, are being developed as alternatives to PFOA, PFOS and other long chain perfluorinated compounds³⁷. In 2011 U.S. EPA proposed the third Unregulated Contaminant Monitoring Rule finalized to determining the concentration and spatial distribution of contaminants in public drinking water. In this list are proposed not only PFOA and PFOS but also perfluorononanoic acid (PFNA), perfluoroheptanoic acid (PFHpA), perfluorohexansulfonic acid (PFHxS) and perfluorobutanesulfonic acid (PFBS). PFBS shows low toxicity based on substantial toxicological database. While PFBS is persistent in the environment, it has a relatively short half life in humans, based on a study of production workers²⁵, the half life in human blood averaged 28 days, substantially shorter than the half-life of the other ‘long-chain’ PFCs. Despite PFBS with four completely fluorinated carbon atoms is considered a ‘short chain’ perfluorinated compound U.S. EPA decide to put it in the list of monitored substances. This can be explained because, after the banning of long chain

PFCs, producers used ‘short chain’ perfluorinated compounds, specially PFBS, as alternatives to PFOA and PFOS. The increasing use of PFBS suggest to U.S. EPA to put this compound in the list of the monitoring contaminant of drinking water.

Final considerations

The use of fluorinated organic compounds has increased throughout this century, and they are ubiquitous environmental contaminants. PFCs are contaminants that differ in several ways from most other well-studied organic pollutants for its extreme resistance to environmental degradation. In particular, perfluorooctanoic acid (PFOA) and perfluorooctan sulfonate (PFOS), present in different source of exposure, persist in humans with an half-life of several years and are widespread found in the serum of population worldwide. Considering the numerous health endpoints associated with human PFOA exposure, the U.S. EPA classified PFOA as “likely to be carcinogenic in humans” and, in agreement with the major companies involved in the production of fluorinated chemicals, the C8 and their precursors were banned by the 2010/2015 PFOA Stewardship Program.

Nowadays, the companies substitute their ‘long-chain’ perfluorinated carbon products with ‘short-chains’ ones. Conversely, this replacement caused a decay in the chemical-physical performances of these compounds. For this reasons the goal of this research is the design of new molecules with ‘short-chains’ perfluorinated carbon atoms, but with well-defined architecture able to guarantee similar performances to ‘long-chains’. In the next chapters will be explained the ways adopted to reach the synthesis of C4 fluorinated compounds with particular chemical structure able to guarantee physical-chemical properties closed with the “long-chain” commercial products.

Bibliography

- (1) B.D. Key, R.D. Howell, C.S. Criddle *Environ. Sci. Technol.* **1997**, 31, 2445-2454.
- (2) Lindstrom, A.B.; Strynar, M.J.; Libelo, E.L. *Environ. Sci. Technol.* **2011**, 45, 7954-7961.
- (3) Vaalgamaa, S.; Vahatalo, A.V.; Perkola, N.; Huhtala, S. *Sci. Total Environ.* **2011**, 409, 3043-3048.
- (4) Prevedouros, K.; Cousins, I.T.; Buck, R.C.; Korzeniowski, S.H. *Environ. Sci. Technol.* **2006**, 40, 32-44.
- (5) A.G. Paul, K.C. Jones, A.J. Sweetman *Environ. Sci. Technol.* **2009**, 43, 386-392.
- (6) Armitage, J.; Cousins, I.T.; Buck, R.C.; Russell, M.H.; MacLeod, M.; Korzeniowski, S.H. *Environ. Sci. Technol.* **2006**, 40, 6969-6975.
- (7) Armitage, J.M.; MacLeod, M.; Cousins, I.T. *Environ. Sci. Technol.* **2009**, 2009, 1134-1140.
- (8) Davis, K.L.; Aucoin, M.D.; Larsen, B.S.; Kaiser, M.A; Hartten, A.S. *Chemosphere* **2007**, 67, 2011-2019.
- (9) Huset, C.A.; Chiaia, A.C.; Barofsky, D.F.; Jonkers, N.; Kohler, H.-P.E. *Environ. Sci. Technol.* **2008**, 42, 6369-6377.
- (10) Becker, A.M.; Gerstmann, S.; Frank, H.; *Chemosphere* **2008**, 72, 115-121.
- (11) Pistocchi, A.; Loos, R. *Environ. Sci. Technol.* **2009**, 43, 9237-9244.
- (12) D. Skutlarek, M. Exner, H. Farber *Environ. Sci. Pollut. Res. Int.* **2006**, 13, 299-307.
- (13) I. Ericson, J.L. Domingo, M. Nadal, E. Bigas, X. Llebaria, B. Van Bavel, G. Lindstrom *Arch. Environ. Contam. Toxicol.* **2009**, 57, 631-638.
- (14) S.M. Bartell, A.M. Calafat, C. Lyu, K. Kato, P.B. Ryan, K. Steenland *Environ. Health Perspect.* **2010**, 118, 222-228.
- (15) S. Takagi, F. Adachi, K. Miyano, Y. Koizumi, H. Tanaka, I. Watanabe, S. Tanabe, K. Kannan *Water Res.* **2011**, 45, 3925-3932.
- (16) G.B. Post, P.D. Cohn, K.R. Cooper *Environ. Res.* **2012**, 116, 93-117.
- (17) D. Trudel, L. Horowitz, M. Scheringer, I.T. Cousins, K. Hungerbuehler *Risk Anal.* **2008**, 28, 251-269.
- (18) C. Cornelis, W. D'Hollander, L. Roosens, A. Covaci, R. Smolders, R. Van Den Heuvel, E. Govarts, K. Van Campenhout, H. Reynders, L. Bervoets *Chemosphere* **2012**, 86, 308-314.
- (19) L.S. Haug, S. Salihovic, I.E. Jogsten, C. Thomsen, B. Van Bavel, G. Lindstrom, G. Becher *Chemosphere* **2010**, 80, 1137-1143.
- (20) C.W. Noorlander, S.P. Van Leeuwen, J.D. Te Biesebeek, M.J. Zeilmaker *Agric. Food Chem.* **2011**, 59, 7496-7505.
- (21) Domingo, J.L. *Environ. Int.* **2012**, 40, 187-195.

- (22) J. Belisle *Science* **1981**, 212, 1509-1510.
- (23) F.D. Gilliland, J.S. Mandel *Am. J. Ind. Med.* **1996**, 29, 560-568.
- (24) W.S. Guy, D.R. Taves, W.S. Brey, *Biochemistry Involving Carbon-Fluorine Bonds*. ed. American Chemical Society. Vol. 28 1976: Washington DC.
- (25) G.W. Olsen, J. Burris, D. Ehresman, J. Froehlich, A. Seacat, J. Butenhoff, L.R. Zobel *Environ. Health Perspect.* **2007**, 115, 1298-1305.
- (26) S.G. Hundley, A.M. Sarrif, G.L. Kennedy *Drug Chem. Toxicol.* **2006**, 29, 137-145.
- (27) J. Franko, B.J. Meade, H.F. Frasch, A.M. Barbero, S.E. Anderson *J. Toxicol. Environ. Health A* **2012**, 75, 50-62.
- (28) G.L. Kennedy, J.L. Buthenhoff, G.W. Olsen. J.C. O'Connor, A.M. Seacat, R.G. Perkins, L.B. Biegel, S.R. Murphy, D.G. Farrar *Crit. Rev. Toxicol.* **2004**, 34, 351-384.
- (29) Registry, Agency for Toxics Substances and Disease. Available from: <http://www.atsdr.cdc.gov/toxprofiles/tp200.pdf> [accessed: 6 November 2012]
- (30) S.J. Frisbee, A.P. Brooks, A. Maher, P. Flensburg, S. Arnold, T. Fletcher, K. Steenland, A. Shankar, S.S. Knox, C. Pollard, J.A. Halverson, V.M. Vieira, C. Jin, K.M. Leyden, A.M. Ducatman *Environ. Health Perspect.* **2009**, 117, 1873-1882.
- (31) R.C. Leonard, K.H. Kreckmann, C.J. Sakr, J.M. Symons *Ann. Epidemiol.* **2008**, 18, 15-22.
- (32) L.B. Biegel, M.E. Hurtt, S.R. Frame, J.C. O'Connor, J.C. Cook *Toxicol. Sci.* **2001**, 60, 44-55.
- (33) U.S. EPA (Environmental Protection Agency). 2005 Available from: <http://www.epa.gov/oppt/pfoa/pubs/pfoarisk.pdf> [accessed: 7 November 2012]
- (34) U.S. EPA (Environmental Protection Agency). 2006 Available from: http://www.epa.gov/sab/pdf/sab_06_006.pdf [accessed: 7 November 2012]
- (35) U.S. EPA (Environmental Protection Agency). 2006 Available from: <http://www.epa.gov/oppt/pfoa/pubs/stewardship/pfoastewardshipbasics.html> [accessed: 7 November 2012]
- (36) K. Kato, L.Y. Wong, L.T. Jia, Z. Kuklenyik, A.M. Calafat *Environ. Sci. Technol.* **2011**, 45, 8047-8045.
- (37) U.S. EPA (Environmental Protection Agency). 2010 Available from: <http://www.epa.gov/oppt/pfoa/pubs/altnewchems.html> [accessed: 7 November 2012]

Chapter 3. The Fluorinated Polymers

This chapter describes the synthesis of the most important fluorinated monomers industrially produced. Furthermore, examples of fluorinated polymers and co-polymers commercially available are supplied.

General characteristics of fluoropolymers

Fluoropolymers are attractive because of their high versatility: they can be either thermoplastic, elastomeric, semicrystalline or totally amorphous. Highly fluorinated polymers exhibit high thermal, chemical, aging, and weather resistance, excellent inertness to solvents, hydrocarbons, acids and alkalis, low surface energy (oil and water repellency), low dielectric constants, low flammability and low refractive index¹. The high dissociation energy of the strong C-F bond (see Chapter 1) imparts outstanding resistance to oxidation and to hydrolytic decomposition². However, fluoropolymers have several drawbacks: the homopolymers are often crystalline, which hence induces a low solubility in common organic solvents. Further they are not easily curable or crosslinkable³. This disadvantage can be exceeded by using fluorinated copolymers with sterically hindered side groups which produce a disorder in the

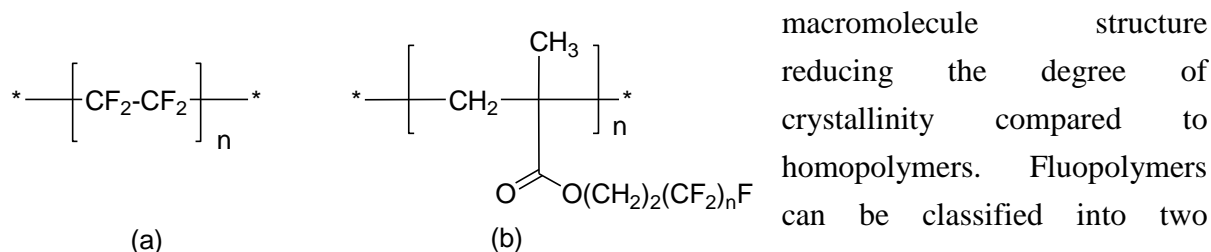


Figure 3.1. Examples of fluoropolymers: high fluorinated fluoropolymers (a) PTFE, and FA (b) poly(fluoroalkyl methacrylate)s.

macromolecule structure reducing the degree of crystallinity compared to homopolymers. Fluopolymers can be classified into two

categories: (a) high fluorinated polymers with a fluorinated backbone or with only short and highly fluorinated side groups (such as tetrafluoroethylene (TFE), hexafluoropropylene (HFP), perfluoromethyl vinyl ether (PFVE), and vinylidene fluoride (VDF)), and (b) perFluoroAlkyl (FA)⁴ polymers, having an hydrocarbon backbone and a long perfluorinated pendant chain such as $\text{F}(\text{CF}_2)_n$ with $n = 4-18$ (Figure 3.1).

Despite their high price, fluoropolymers have been successfully used in many industrial applications such as: chemical resistant coatings in chemical and petrochemicals processes, high performances membranes in fluids separations, transmission fluids in automotive, elastomeric and plastic materials for harsh environments in space and aerospace applications, in cores and claddings of optical fibers, as stain resistant coatings for textiles, stone, paper, wood and metal treatments, microelectronics^{2,5-8}.

Synthesis and polymerization of commercial fluorinated monomers

Industrially relevant fluorinated monomers are olefins and alkenes containing one or several fluorine atoms. The synthesis of fluorinated monomers is expensive, often involving extreme and dangerous reaction conditions. Most of them are gaseous and their polymerization requires to be carried out in high pressure autoclaves.

Fluoroalkenes commercially available in greater amounts are tetrafluoroethylene (TFE), vinylidene fluoride (VDF), chlorotrifluoroethylene (CTFE), hexafluoropropene (HFP), vinyl fluoride (VF), and fluorinated acrylates.

3.1.1 Tetrafluoroethylene

Tetrafluoroethylene (TFE) (b.p. = -76 °C) is the most used fluorinated monomers in homo- and co-polymerization. It is produced by a noncatalytic gas-phase pyrolysis of chlorodifluoromethane at 600-900°C at atmospheric or subatmospheric pressure. In these conditions difluorocarbene is formed which undergoes a dimerization reaction quasi-instantaneously (Scheme 3.1). Although this process requires a CFC as starting point, this method is still currently used by the main manufacturing companies (3M, Du Pont, Asahi, Solvay-Solexis, Daikin, etc.)⁹. TFE is an explosive monomer and it must be handled with care. Its homopolymer, polytetrafluoroethylene (PTFE), is commercial available with different names such as Teflon[®] (DuPont), Algorflon[®] (Solvay-Solexys), Fluon[®] PTFE (Asahi Glass), Hostaflon[®] (Dyneon), and Polyflon[®] (Daikin)^{9,10}.



Scheme 3.1. Synthesis of TFE.

TFE is polymerized with extremely high molecular weight, in order to limit the crystallinity in the final product and to give the desired mechanical properties. The initially prepared, high molecular weight PTFE has a crystallinity of over 90% and a melting point of about 341°C. It displays remarkable properties such as thermostability, good stability to fire, very good surface properties. PTFE is insoluble in most of the solvents, acids, base and fuels. Besides, this polymer keeps a good flexibility even at low temperatures and displays low friction coefficient, dielectric constant, and dissipation factor, but has high volumic resistance and it is quite resistant to UV and to aging^{9,10}.

	T_g [°C]	T_m [°C]	T_{dec} [°C]	T_{Me} [°C]	T_{sc} [°C]	d [g/dm ³]	ϵ	γ_c [mN/m]
$C_2H_4-CF_2=CFCl$ (ECTFE)	-	240	320	275	158	1.65	2.5	-
$C_2H_4-C_2F_4$ (ETFE)	-	275	345	335	175	1.77	2.2	22
$C_2F_4-C_3F_6$ (FEP)	-	265	330	318	200	2.15	2.0	18
$C_2F_4-CF_2=CF-$ OC_3F_7 (PFA)	-	305	385	370	260	2.16	2.0	18
$CF_2=CFCl$ (PCTFE)	50	214	315	285	165	2.13	2.4	31
C_2F_4 (PTFE)	(-100)	327	395	380	270	2.18	2.1	18
$CF_2=CH_2$ (PVDF)	-40	170	342	225	150	1.76	8.0	25
$CH_2=CHF$ (PVF)	48	200	245	220	110	1.40	6.5	28

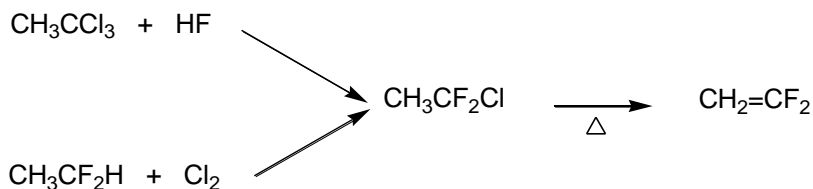
Table 3.1. Properties of some fluorinated thermoplastics. T_g (glass transition temperature), T_m (melting temperature), T_{dec} (decomposition temperature), T_{Me} (processing temperature), T_{sc} (continuous use temperature), d (density), ϵ (dielectric constant), γ_c (critical surface tension).

3.1.2 Vinylidene fluoride^{8,11}

Vinylidene fluoride (VDF) (b.p. -82 °C) has several advantages compared to TFE: it is less toxic and it is not explosive. VDF is easily homopolymerizes and co-polymerizes in presence of radicals. There are two routes for the synthesis of VDF: (1) starting from trichloroethane or (2) from HFC-152a (CH_3-CF_2H) (Scheme 3.2).

The homopolymerization of vinylidene fluoride produces polyvinylidene fluoride (PVDF), which is a thermoplastic exhibiting interesting physical and electrical properties. PVDF is well-known for its high piezoelectricity, but also for its pyroelectric properties. PVDF has a typical degree of crystallinity of 50-70% with five crystalline polymorphisms. The spatial conformation created by the alternance of CF_2 and CH_2 groups all along the polymeric chain

confer to PVDF a particular polarity and an exceptional dielectric constant (8.0, see Table 3.1).

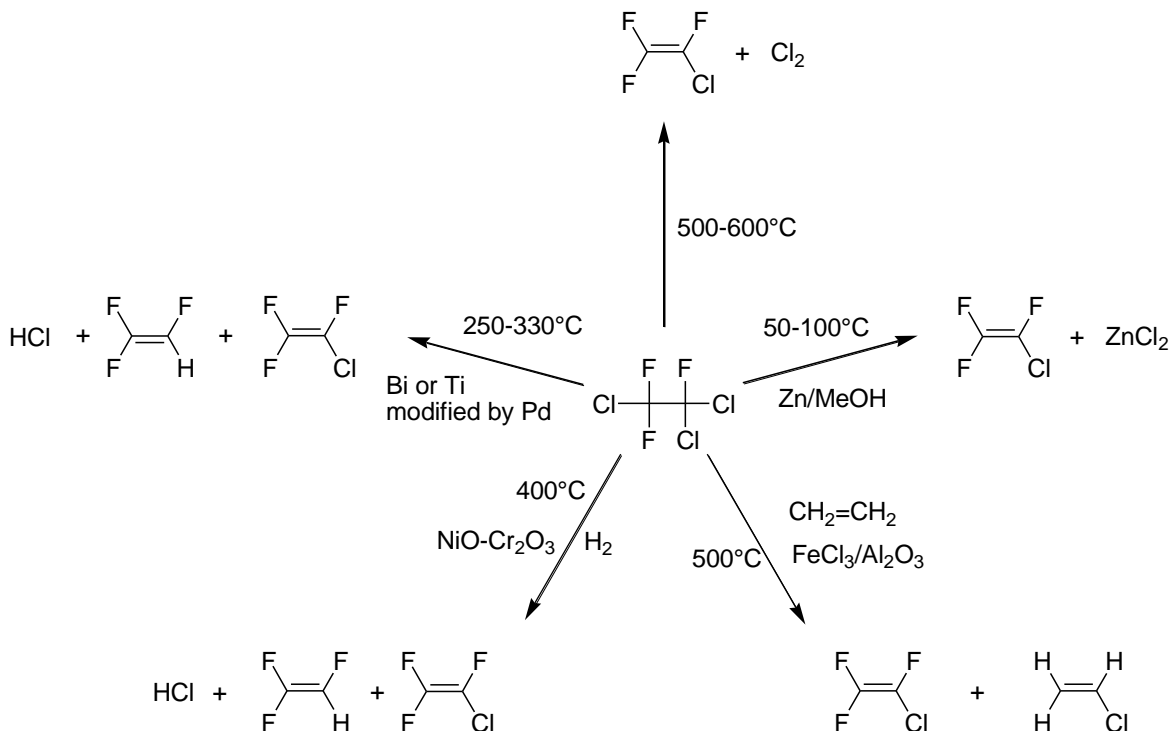


Scheme 3.2. Synthesis of vinylidene fluoride.

PVDF is inert to many solvents, oil, fuels and strong acids and shows low permeability to gases and liquids. It is resistant to UV, to aging and to ionizing radiations. However it is sensitive to bases which induce the dehydrofluorination of the $-\text{CF}_2-\text{CH}_2-$ group yielding an insaturation. The T_g of PVDF is about -40°C , while its melting point ranges from 158°C to 197°C depending on molecular weight and number of chain defects.

3.1.3 Chlorotrifluoroethylene^{9,10}

Chlorotrifluoroethylene (CTFE) (b.p. -27.8°C) is commonly used as refrigerant. Many reaction pathways for its synthesis are available (Scheme 3.3). The most frequently used is carried out in two steps: (a) fluorination of hexachloroethane with HF, catalyzed by antimony complex, followed by (b) dechlorination.

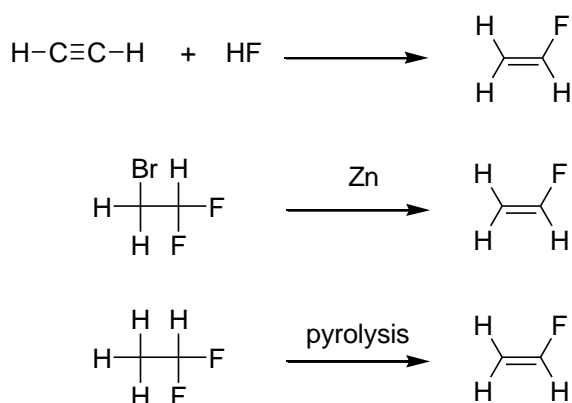


Scheme 3.3. Preparation of chlorotrifluoroethylene from 1,1,2-trichlorotrifluoroethane according to various strategies.

Thanks to its thermal properties and its chemical inertness PCTFE is a polymer of choice for military applications. PCTFE is resistant to radiations and it is regarded as the best polymer exhibits excellent thermal and gas barrier properties (especially against oxygen) and it is regarded as the polymer with the lowest permeability to gases and moisture. Its properties are assured in the temperature range $-240\text{ }^{\circ}\text{C}/+200\text{ }^{\circ}\text{C}$. Its glass transition and melting temperatures are $71\text{-}99\text{ }^{\circ}\text{C}$ and $211\text{-}216\text{ }^{\circ}\text{C}$ respectively. PCTFE homopolymers are currently produced by Honeywell and Daikin companies under Aclon[®] and Neoflon[®] tradenames.

3.1.4 Vinyl fluoride⁸

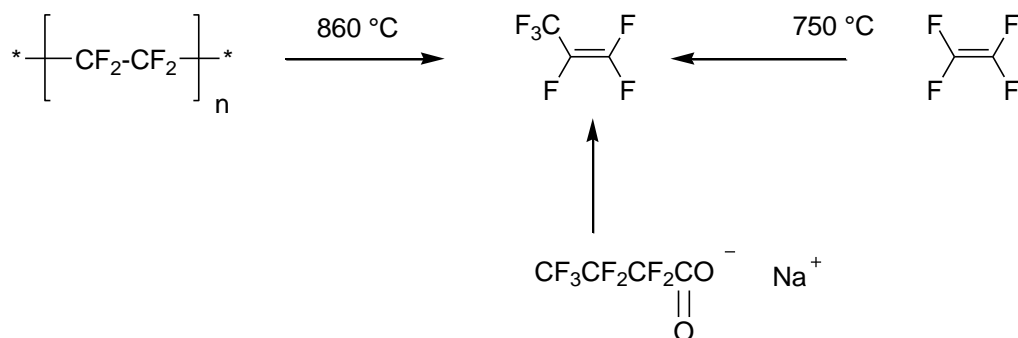
Vinyl fluoride (VF) (b.p. = $-72\text{ }^{\circ}\text{C}$) is obtained by several methods: (a) fluorination of acetylene in HF medium, (b) elimination of HBr from 1,1-difluoro-2-bromoethane in the presence of zinc, (3) by pyrolysis of 1,1-difluoroethane (Scheme 3.4).



Scheme 3.4. Examples of synthesis of vinyl fluoride.

3.1.5 Hexafluoropropylene⁹

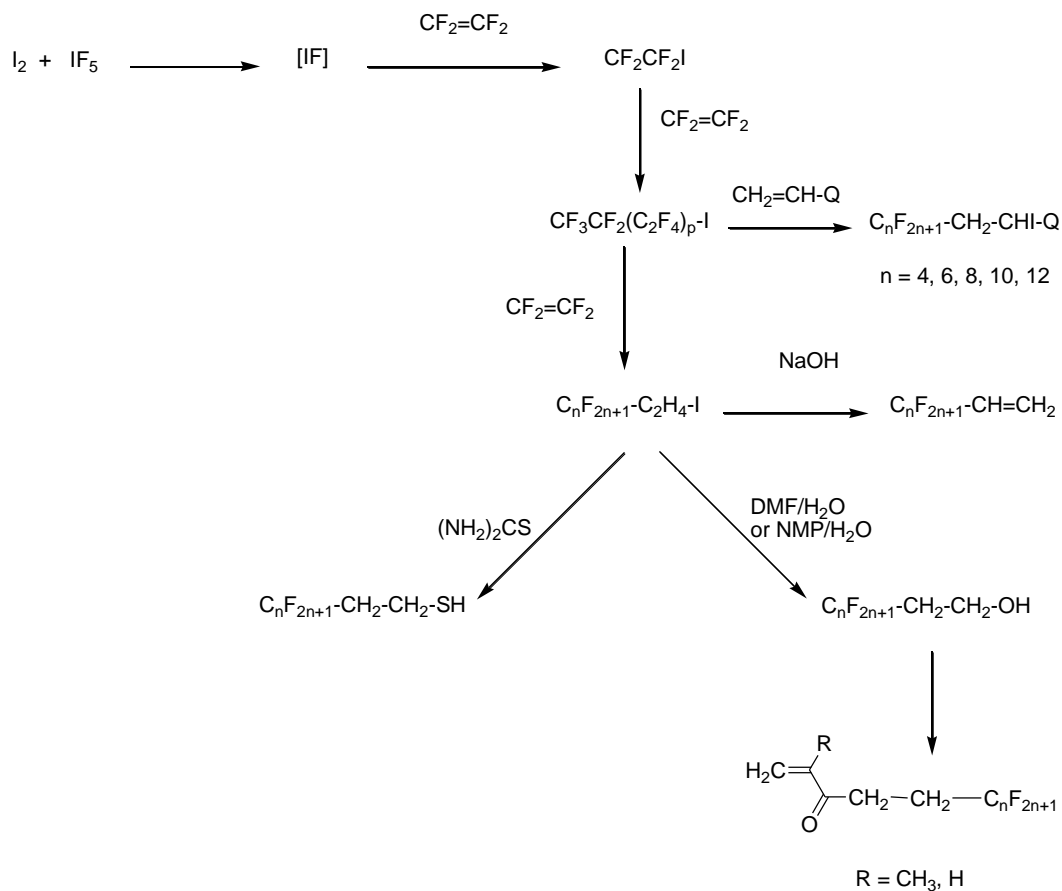
Hexafluoropropylene (HFPE) (b.p. = $-29\text{ }^{\circ}\text{C}$) is obtained by several methods: (a) pyrolysis of PTFE (at $860\text{ }^{\circ}\text{C}$, 58% yield), (b) pyrolysis of TFE (at $750\text{ }^{\circ}\text{C}$, 82% yield), (c) starting from $\text{CF}_3\text{CF}_2\text{CF}_2\text{CO}_2\text{Na}$ (Scheme 3.5). Hexafluoropropylene do not homopolymerized, but it is commonly used in co-polymerizations.



Scheme 3.5. Examples of synthesis of hexafluoropropylene.

3.1.6 Fluorinated (meth)acrylic monomers⁸

This kind of monomers is usually identified with the acronym FA (perFluoroAlkyl) and their general formula is $\text{CH}_2=\text{C}(\text{R})\text{CO}_2\text{C}_2\text{H}_4\text{C}_n\text{F}_{2n+1}$. Polyfluoro(meth)acrylates are synthesized by chemical functionalization of short perfluorinated oligomers obtained by telomerization of TFE.



Scheme 3.6. Step of industrial synthesis of fluorinated (meth)acrylates and other intermediates.

These polymers do not display the chemical and thermal properties of polymers with an highly fluorinated backbone but they are characterized by outstanding surface properties. These polymers find application in order to obtain hydrophobic and oleophobic coatings for surface protections (stain resistance finishes). Actually, fabric treatment used in the textile industry are one of the main applications of these products.

On the market there are several examples of stain resistant finishes used for the protection of different materials such as: textiles, paper, wood, metals, stone 3M (Schotchgard[®]), Atochem (Foraperle[®]), by Daikin (Lezanova[®]) or by Asahi Glass (Asahiguard[®]) to name a few.

Fluorinated copolymers

Fluorinated homopolymers are synthesized by radical polymerization of fluoroolefins. They exhibit a crystalline structure, which induces a poor solubility in common organic solvents and are not easily cured or cross-linked³.

The copolymerization of fluoroolefines with other monomers allows to obtain copolyemrs with many favourable features:

- (a) amorphous perfluoroplastics, which combine the outstanding properties of crystalline perfluoropolymers, while adding high optical clarity, improved mechanical properties and a certain solubility in perfluoropolyether solvents.
- (b) Perfluoroelastomers, which combine the outstanding properties of crystalline perfluoropolymers and the elasticity typical of natural rubber, silicones, nitril-butadiene polymers giving the possibility to obtain sealing materials for harsh conditions.
- (c) Polymers with reactive side chains such as bromine, epoxide, nitrile, cyanate useful for cross-linking, ion-exchange, hydrophilization.

Fluorinated copolymers can be classified in three categories: (i) copolymers consisting of ethylenic fluorinated monomers, (ii) copolymers obtaining by the polymerization of fluorinated monomers and non-fluorinated monomers, and (iii) copolymers containing heteroatoms in the chains. In the next paragraph several examples of fluorinated elastomers belonging to the first two categories indicated above are examined. Also, a brief description of the heteroatoms copolymers are provided in paragraph 3.3.2.

3.1.7 Fluorinated elastomers

The synthesis of elastomers requires a mixture of monomers having bulky side chains in order to insert disorder within the chains. Examples of fluorinated elastomers^{6,7,12-14} are reported in Table 3.2 in which TFE and VDF are the basis monomers. Fluoroelastomers must display high chemical and thermal resistance assuring suitable mechanical properties even in harsh

conditions. At 150 °C while most of conventional elastomers lose their elasticity, fluoroelastomers maintain their elongation properties.

In the same way, the stress resistance is improved (50% of the initial value for one year at 201 °C). Fluoroelastomers resist both to polar and apolar solvents. The resistance to acids and alkalis varies depending on monomers present in the perfluoroelastomer backbone. Poly(TFE-*co*-F₂C=CFOR_F) copolymers are resistant to alkaline media (contrarily to elastomers based on VDF that undergo a dehydrofluorination). Finally, fluorocarbon elastomers exhibit an extreme resistance to compression set. In order to increase mechanical, thermal and chemical properties (mainly swelling), pefluoroelastomers must be crosslinked. Crosslinking is usually carried out in the presence of peroxides or with hexamethylene diamine carbonate.

	HFP	PMVE	CTFE	P
VDF	Daiel [®] G801 ^(a)		Dyneon [®]	
	Dyneon [®] Elastomers ^(b)		Elastomer ^(b)	
	Tecnoflon [®] N/FOR ^(c)		SKF [®] -32 ^(d)	
	SKF [®] -26 ^(d)		Voltalef ^{®(f)}	
	Viton [®] A ^(e)			
TFE		Daiel [®] Perfluoro ^(a)		Aflas ^{®(f)}
		Dyneon [®] Elastomer ^(b)		Viton [®] Extreme TBR ^(e)
		Kalrez ^{®(e)}		
		Tecnoflon [®] PFR ^(c)		
VDF+TFE	Daiel [®] G 901 ^(a)	Daiel [®] LT ^(a)		Aflas ^{®(f)}
	Dyneon [®] Elastomer ^(b)	Dyneon [®] Elastomer ^(b)		
	Tecnoflon [®] P/T/TN/FOR ^(c)	Tecnoflon PL ^(c)		
	Viton [®] B/F/GF/GBL ^(e)	Viton [®] GLT/GFLT ^(e)		

Table 3.2. Main commercial available elastomers.

HFP = hexafluoropropylene (CF₂=CFCF₃)

PMVE = perfluoromethyl vinyl ether (CF₂=CFOCF₃)

CTFE = chlorotrifluoroethylene (CF₂=CFCl)

P = propylene (CH₂=CHCH₃)

VDF = vinylidene fluoride (CF₂=CH₂)

TFE = tetrafluoroethylene (CF₂=CF₂)

(a) Daikin

(b) 3M/Dungeo

(c) Solvay Specialty Polymers

(d) HaloPolymers

(e) DuPont Performance Elastomers

(f) Asahi Glass

(g) Arkema North America

The second series of elastomers is obtained by radical copolymerization of one fluorinated monomer with one or several non-fluorinated monomers. The most relevant example is

Aflas[®] produced by the Asahi Glass Co. This poly(TFE-*alt*-propylene) copolymer has a alternated structure and its T_g value worths $-2\text{ }^\circ\text{C}$ ^{6,7,12-14}. This copolymer is crosslinkable in many ways and its mechanical properties are excellent. However, and as expected, its thermal resistance is slightly lower than those of copolymers of fluorinated monomers (Table 3.3).

	T_u [$^\circ\text{C}$]	T_g [$^\circ\text{C}$]	% F	Trade name
$\text{CH}_2=\text{CF}_2/\text{C}_3\text{F}_6$	$-18 \div 210$	-18	66	^(a) Viton [®]
$\text{C}_2\text{H}_4/\text{C}_3\text{F}_6$	$0 \div 200$	0	54	^(b) Aflas [®]
$\text{C}_2\text{F}_4/\text{CF}_2=\text{CFOCF}_3$	$0 \div 280$	-2	73	^(a) Kalrez [®]
$\text{CH}_2=\text{CF}_2/\text{C}_3\text{F}_6/\text{C}_2\text{H}_4$	$-12 \div 230$	-16	67	^(c) Daief [®]
fluorosilicon	$-65 \div 175$	-68	37	^(d) Silastic [®]
fluorophosphazene	$-65 \div 175$	-65	55	^(e) NPF [®]

Table 3.3. Thermal properties of fluorinated elastomers.

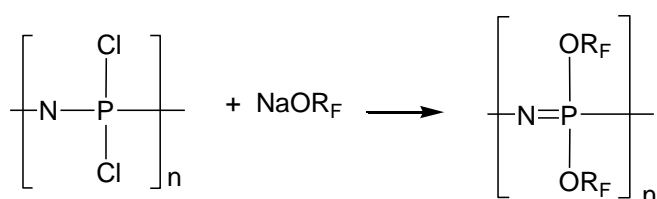
T_u = temperature of continuous use.

T_g = temperature of glass transition.

- (a) DuPont Performance Elastomers
- (b) Asahi
- (c) Daikin
- (d) Dow Corning
- (e) Firestone.

3.1.8 Copolymers containing heteroatoms in the chain

The addition of nitrogen, phosphorus or silicon atoms in the fluorinated back-bone improve typical properties. An example of such materials are the fluorinated poly(phosphazene)s (Figure 3.7).



Scheme 3.7. Synthesis of fluorinated poly(phosphazenes).

Their T_g values are $-70\text{ }^\circ\text{C}$ and their properties are satisfactory up to $175\text{ }^\circ\text{C}$, whereas their average molecular weights are high (M_n are higher than $10^6\text{ g}\cdot\text{mol}^{-1}$). Their chemical resistance are excellent and the presence of phosphorous atom impart to the resulting poly(phosphazene)s flame retardancy-properties.

Another example of fluorinated copolymers containing heteroatoms in the main backbone are the fluorinated silicones. The most conventional fluorinated polysiloxane and commercialized

mainly by Dow Corning Company and recently by Momentive company, is synthesized from D₃ cyclosiloxane (Figure 3.2).

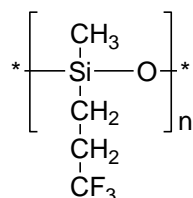


Figure 3.2. Example of commercial available fluorinated polysiloxane.

T_g value of this polymer is -68 °C and it is possible to cross-link it by various classical processes related to the silicone chemistry (e.g. peroxide or by SiH/Si-vinyl systems).

Fluorosilicones are used for their swelling resistance in non-polar medium (e.g. in Skydrol Fluid[®]) even at 100 °C but they are mainly used to replace copolymers (based on fluoromonomers) when a good resistance at low temperature is required.

Thermal depolymerization limits their stability at high temperature and this drawback led to extensive research on fluorinated silicones called “*hybrid*”¹⁵⁻¹⁷ (Figure 3.3).

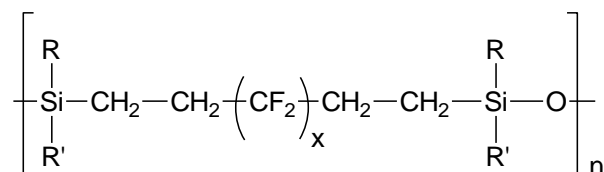


Figure 3.3. Structure of “*hybrid*” fluorinated silicones.

Improvement on the thermostability of the hybrid silicones was obtained introducing VDF, TFE and HFP units. Though the T_g values were acceptable (ranging from -50 to -20 °C), their thermostability was much higher (of ca. 200 °C) than that of commercially available fluorinated silicones mentioned above¹⁵⁻¹⁷.

Polymerization of fluoromonomers

Except for a few monomers such as fluorinated oxetanes, oxazonolines^{19,20}, vinyl ethers with fluorinated side group^{18,19}, hexafluoropropylene oxide^{20,21} and α-trifluoromethacrylic acids²² most fluoropolymers are synthesized by conventional radical polymerization. Radical polymerization is easy and straightforward, usually it does not requires extreme reaction conditions, reactants do not need high purity. For these reasons more than 95% of fluoropolymers are prepared in this way².

3.1.9 Telomerization

The processing of fluoropolymers is still difficult because several of them are not soluble and exhibit very high melting points. One of the most interesting strategies used in order to limit these drawbacks of fluoropolymers is the telomerization reaction. Telomerization, in contrast with polymerization usually leads to low molecular weight polymers, called telomers, or even to monoadducts with well-defined end groups. Such products are obtained from the reaction between a telogen or chain transfer agent (X-Y), and one or more (n) molecules of a polymerizable compound M called taxogen or monomer. Telogen X-Y should be easily cleavable by free radicals leading to an X· radical which will be able to react further with monomer. After the propagation of monomer, the final step consists of the transfer of the telogen to the growing telomeric chain. Telomers are intermediate products between organic compounds (e.g., n = 1) and macromolecular species (n >100).

Other differences between telomerization and polymerization are the following: (i) in telomerization, fragments of the initiator mainly induce the rupture of the telogen, whereas in polymerization, they add onto the monomer, (ii) the groups at the ends of the chain are significant from a chemical point of view because the molecular weights are low.

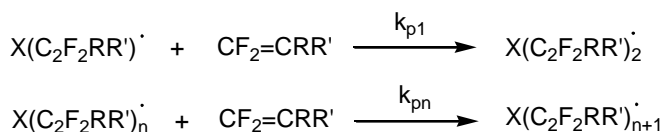
A telomerization reaction is the result of four step: initiation, propagation, termination and transfer. Telomerization can be initiated from various processes: photochemical (in presence of the UV rays), in presence of radical initiator or redox catalysts, thermally, or initiated by X- or γ -rays. Depending on the process different mechanism are involved.

The general mechanism of telomerization is reported in Scheme 3.8, where XY, $CF_2=CRR'$, k_i , k_{p1} , k_{Te} , and k_{tr} represent the telogen, the monomer, the rate constant of initiation, the rate constant of propagation, termination, and transfer respectively²³.

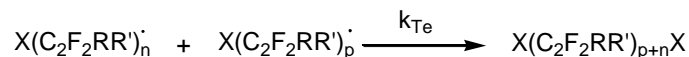
INITIATION



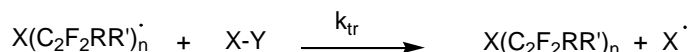
PROPAGATION



TERMINATION



TRANSFER



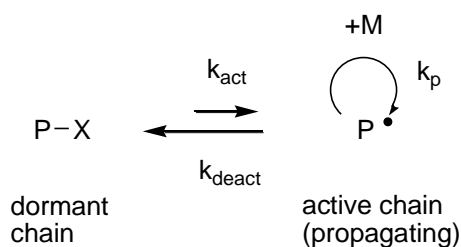
Scheme 3.8. General mechanism of telomerization.

Example of fluorinated fluoroalkenes used in telomerization are VDF, TFE, CTFE, and HFP.

3.1.10 Controlled Radical Polymerization

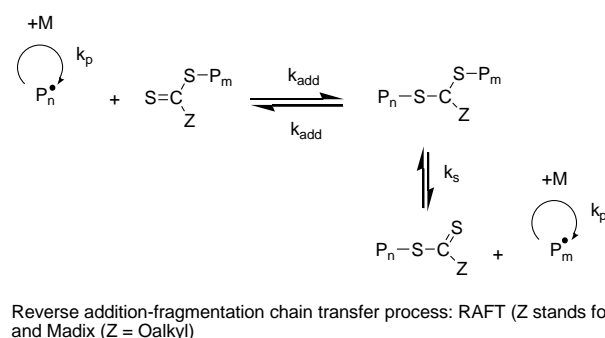
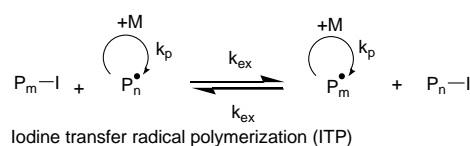
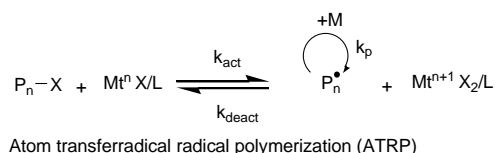
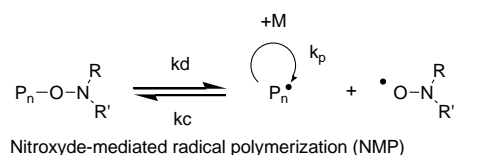
Studies on telomerization helped researchers to synthesize polymers with controlled architecture and properties. Several teams have taken part in the evolution of radical telomerization toward controlled radical polymerization²⁴.

Since the mid-90s, controlled radical polymerization has drawn much interest from both academic and industrial researchers. In the years new techniques have been proposed and developed in order to control the reactivity of free radicals. Such a control gives a “living” character to the radical polymerization. However, for radical polymerization the truly living character is far from being attained and it seem preferable to use the term “controlled” process, rather than “living” process. The general principle of the methods is based on a reversible activation-deactivation process (Scheme 3.9) between dormant chains (or capped chains) and active chains (or propagating radicals).



Scheme 3.9. Reversible activation in controlled radical polymerization (CRP).

Actually, controlled radical polymerization (CRP) has attracted a growing interest due to the ability of this process to control the polymeric structures and architectures^{2,25}. Controlled free-



Scheme 3.10. Various reversible activation processes of CRP.

(MADIX)⁴⁴ vi) organo-heteroatom radical polymerization^{45,46}, and CRP controlled by boron derivatives⁴⁷⁻⁵³, vii) organo-cobalt mediated radical polymerization, OCRP, based on (Co(acac)₂)⁵⁴. Schemes of the activation-deactivation process of CRPs are reported in Scheme 3.10.

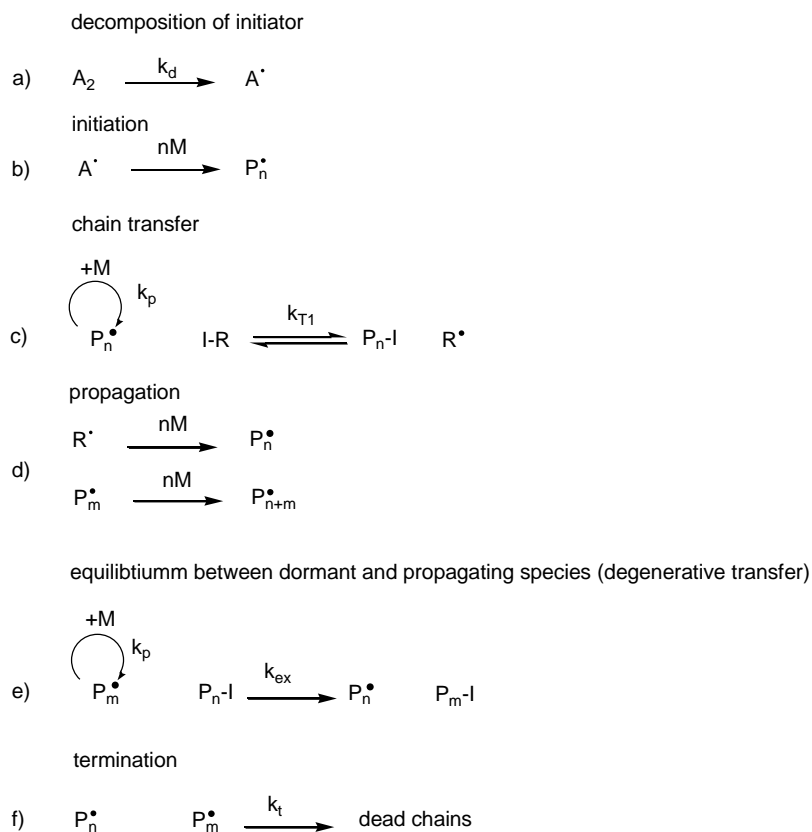
Iodine transfer polymerization

Iodine transfer polymerization was one of the radical living process developed in the late 1970s by Tatemoto at the Daikin company^{32,33,37}. In this polymerization perfluoroalkyl iodides are used as chain transfer. The highly electron withdrawing of perfluorinated group (R_F) allow the lowest level of the CF₂-I bond-dissociation energy (BDE). Various fluorinated monomers have been used in ITP²³. Basic similarities in these living polymerization systems are found in the stepwise growth of polymeric chains at each active species. The active living centre, generally located at the end-groups of the growing polymer, has the same reactivity at

radical polymerization enables to apply free-radical polymerization to the synthesis of well-defined polymers with predictable molar masses and narrow polydispersities²⁶. Example of different methods that lead the controlled free-radical polymerization are: i) nitroxide-mediated radical polymerization (NMP)^{27,28}, ii) atom transfer radical polymerization (ATRP)²⁹⁻³¹, iii) iodine transfer polymerization (ITP)^{23,32-41}, iv) reversed addition-fragmentation chain transfer (RAFT)^{42,43}, v)

macromolecular design by interchange of xanthate

any time during polymerization, even when the reaction is stopped. In the case of ITP of fluoroolefins, the thermal active bond is always the C-I bond originated from the initial iodine containing both chain transfer agent and monomer. The mechanism (Scheme 3.11) can be described as follows. The initiating radical $A\cdot$ generated by thermal decomposition of a conventional radical initiator (such as AIBN) in step a), adds onto M monomer and the



Scheme 3.11. General mechanism of iodine transfer polymerization (ITP).

resulting radical propagates (step b)). The exchange of iodine from the transfer agent, R-I, to the propagating radical, $P_n\cdot$, results in the formation of the polymer alkyl iodide, P_n-I , and a new initiating radical, $R\cdot$ (step c)). In step d), $R\cdot$, generated from the alkyl iodide or the $P_n\cdot$, adds onto a monomeric unit and propagates. As in any radical process, the termination occurs in ITP polymerization (step f)). Minimizing the termination step remains essential to keep a good control of the polymerization. Ideally in

ITP, to obtain polymer with a narrow molar mass distribution, the rate of exchange should be higher than that of the propagation.

As for telomerisation, also iodine transfer polymerization can be easily applied to fluorinated alkenes: ITP make it possible to control the polymerization of monomers such as VDF or TFE. This is observed by the linear increase in the mean degree of polymerization (DP_n) with VDF conversion. This behavior is observed when a R-CF-I transfer agent is used and evidenced the controlled character of the polymerization of VDF. Conversely the use of R- CH_2 -I chain transfer agent evidenced a poor control of the polymerization. These results suggested that when a chain transfer with a structure close to that of the dormant polymer is used the controlled behavior is improved.

Bibliography

- (1) Banks, R.E.; Smart, B.E.; Tatlow, J.C., *Organofluorine Chemistry, Principles and Commercial Applications*. 1994, New York: Plenum Press.
- (2) Ameduri, B. *Macromolecules* **2010**, 43, 10163-10184.
- (3) Taguet, A.; Ameduri, B.; Boutevin, B. *Adv. Polym. Sci.* **2005**, 184, 127-211.
- (4) Hougham, G; Cassidy, P.E.; Johns, K.; Davidson, T., *Fluoropolymers 2, Properties*. 1999, Plenum Publisher: New York.
- (5) Banks, R.E.; Smart, B.E.; Tatlow, J.C., *Organofluorine Chemistry: Principles and Commercial Applications*. 1994, Plenum Press: New York. pp. 339-372.
- (6) Ameduri, B.; Boutevin, B.; Kostov, C. *Prog. Polym. Sci.* **2001**, 26, 105-187.
- (7) Ameduri, B.; Boutevin, B. *J. Fluorine Chem.* **2005**, 126, 221-229.
- (8) Ameduri, B.; Boutevin, B., *Well Architected Fluoropolymers: Synthesis, Properties and Applications*. 2004, Elsevier: Amsterdam.
- (9) Ebnesajjad, S., *Fluoroplastics*. Plastic Design Lybrary Series 2003: New York.
- (10) Ebnesajjad, S., *Fluoroplastics, Volume 2: Melt Processible Fluoropolymers; The Definitive User's Guide and Databook*. 2003, William Andrew Publishing: New York.
- (11) Ameduri, B. *Chem. Rev.* **2009**, 109, 6632-6686.
- (12) Uschold, R.E. *Polym. J.* **1985**, 17, 253-263.
- (13) Logothetis, A. *Prog. Polym. Sci.* **1989**, 14, 251-296.
- (14) Scheirs, J., *Modern Fluoropolymers*. 1997, Wiley: New York.
- (15) Ameduri, B.; Boutevin, B.; Guida-Pietrasanta, F.; Manseri, A.; Ratsimihéty, A.; Caporiccio, G., *Use of Fluorinated Telomers for the Obtaining of Hybrid Fluorosilicones*. Vol. 2 1999. pp. 67-79.
- (16) Guida-Pietrasanta, F.; Boutevin, B.; *Adv. Polym. Sci.* **2005**, 179, 1-27.
- (17) Pasquet, C.; Longuet, C.; Hamdani-Devarenes, S.; Ameduri, B.; Ganachaud, F., *Silicone Surface Science*. ed. Owen M. and Dvornic P. 2012, Springer. pp. 115-178.
- (18) Lobert, M.; Kohn, U.; Hoogenboom, R.; Shubert U.S. *Chem. Commun.* **2008**, 1458-1460.
- (19) Hoogenboom, R.; Shubert, U.S. *Angew. Chem., Int. Ed.* **2009**, 48, 2-19.
- (20) Howell, J.L.; Lu, N.; Friesen, C.M. *J. Fluorine Chem.* **2005**, 126, 281-288.
- (21) Kostjuk, S.V.; Ortega E.; Ganachaud, F.; Ameduri, B.; Boutevin, B. *Macromolecules* **2009**, 42, 612-619.
- (22) Narita, T. *J. Fluorine Chem.* **2010**, 131, 812-828.
- (23) David, G.; Boyer, C.; Tonnar, J.; Ameduri, B.; Lacroix Desmazes, P.; Boutevin, B. *Chem. Rev.* **2006**, 106, 3936-3962.
- (24) Boutevin, B. *J. Polym. Sci.: Part A: Polym. Chem.* **2000**, 38, 3235-3243.

- (25) Matyjaszewski, K.; Gnanou, Y.; Leibler, L., *Macromolecular Engineering*. 2007, Wiley-VHC.
- (26) Jankova, K.; Bednarek, M.; Hvilsted, S. *J. Polym. Sci., Part A: Polym. Chem.* **2005**, 43, 3748-3759.
- (27) Hawker, C.J.; Bosman, A.W.; Harth, E. *Chem. Rev.* **2001**, 101, 3661-3688.
- (28) Sciannamea, V.; Jérôme, V.; Detrembleur, C. *Chem. Rev.* **2008**, 108, 1104-1126.
- (29) Kamigaito, M.; Ando, T.; Sawamoto, M. *Chem. Rev.* **2001**, 101, 3689-3746.
- (30) Matyjaszewsky, K.; Xia, J. *Chem. Rev.* **2001**, 101, 2921-2990.
- (31) Tsarevsky, N.V.; Matyjaszewski, K. *Chem. Rev.* **2007**, 107, 2270-2299.
- (32) Tatemoto, M.; Suzuki, T.; Tomoda, M.; Furukawa, Y.; Ueta, Y.; De. Patent 2,815,187, **1978**,
- (33) Tatemoto, M.; Morita, S. US Patent 4,361,678, **1982**, Daikin.
- (34) Oka, M.; Tatemoto, M., *Vinylidene fluoride-hexafluoropropylene copolymer having terminal iodines*. Contemporary Topics in Polymer Science, ed. W.J.; Tsuruta Bailey, T. 1984, Plenum Press: New York. pp. pp. 763-781.
- (35) Tatemoto, M. *Int. Poly. Sc. Tech.* **1985**, 12, 85-98.
- (36) Tatemoto, M.; Nakagawa, T. Japanese Patent 61,049,327, **1986**,
- (37) Tatemoto, M., *Polymeric Materials Encyclopedia*. CRC Boca Raton, ed. J.C. Salamone. Vol. 5 1996: FL.
- (38) Tatemoto, M.; Shimizu, T., *Thermoplastic Elastomers*. Modern Fluoropolymers, ed. J. Scheirs 1997, Wiley: New York. pp. Chapt. 30, pp 565-576.
- (39) Beuermann, S.; Imran-Ul-haq, M. *Macromol. Symp.* **2007**, 259, 210-217.
- (40) Imran-Ul-Haq, M.; Förster, N.; Vukićević, R.; Herrmann, K.; Siegmann, R.; Beuermann, S. , ed. ACS Symposium. Vol. 1024 2009. pp. 210-236.
- (41) Vukićević, R.; Beuermann, S. *Macromolecules* **2011**, 44, 2597-2603.
- (42) Perrier, S.; Takolpuckdee, P. *Polym. Sci., Part A: Polym. Chem.* **2005**, 43, 5347-5393.
- (43) Boyer, C.; Bulmus, V.; Davis, T.P.; Ladmiral, V.; Liu, J.; Perrier, S. *Chem. Rev.* **2009**, 109, 5402-5436.
- (44) Destarac, M.; Kalai, C.; Wilczewska, A.; Petit, L.; Van Gramberen, E.; Zard, S.Z., *Controlled/Living Radical Polymerization: From Synthesis to Materials*. ACS Symposium, ed. K. Matyjaszewski 2006: Washington D.C. pp. 564-571.
- (45) Yamago, S. *Chem. Rev.* **2009**, 109, 5051-5068.
- (46) Asandei, D.A.; Adebolu, I.O.; Simpson, P.C. *J. Amer. Chem. Soc.* **2012**, 134, 6080-6083.
- (47) Chung, T. C.; Petchsuk, A. US Patent 6,355,749 **2002**, (assigned to Dai-Act).
- (48) Chung, T. C.; Petchsuk, A. *Macromolecules* **2002**, 35, 7678-7683.
- (49) Chung, T. C.; Hong, H.; Oka, M.; Kubo, K. US Patent 6,911,509, **2005**, (assigned to Penn State Research Foundation/Dai-Act).

- (50) Chung, M.; Zhang, Z.; Chalkova, E.; Wang, C.; Fedkin, M.; Komarneni, S.; Sharma, S.; Lvov, S. *Electr. Chem. Soc. Trans.* **2007**, 11, 35-45. Proceedings of the 212th Meeting of the Electr. Chem. Soc., Washington, Oct. 7-12 2007.
- (51) Zhang, Z.C.; Chung, T.C. *Macromolecules* **2007**, 40, 783-790.
- (52) Zhang, Z.-C.; Wang, Z.; Chung, T.C. *Macromolecules* **2007**, 40, 5325-5243.
- (53) Zhang, Z.C.; Wang, Z.; Chung, T.C. *Macromolecules* **2007**, 40, 5235-5240.
- (54) Bunck, D. N.; Sorenson, G. P.; Mahanthappa, M. K. *J. Polym. Sci. Part A: Polym. Chem.* **2011**, 49, 242-249.

Chapter 4. Synthesis of 4'-nonafluorobutyl styrene

Monomers and polymers containing telomeric fluorinated moieties have been used for long time because of their unique combination of useful surface properties such as: hydrophobicity, lyophobicity, oleophobicity, resistance to ageing and oxidation, chemical inertness, low gas permeability. They have found many applications in surface coating in metal, stone, plastic, paper, textiles, leather, automotive and petrochemical industries¹. In this chapter the synthesis of a fluorinated monomer bearing a 'short-chain' fluorinated moiety, 4'-nonafluorobutyl styrene is investigated. The aim of this Chapter is the investigation of many crucial parameters of this three-steps synthesis such as the optimization of the synthesis of the first intermediate, the evaluation of the role of chemical variables such as reactants, solvents, ligands and physical parameters such as temperature. For each step the synthesis procedure is described and the products obtained are characterized by IR, ¹H NMR, ¹⁹F NMR, GC-MS analysis.

Introduction

Shafrin and Zisman² formulated the Constitutive Law of Wettability in which they affirmed that *"the wettability of organic surfaces is determined by the nature and packing of the surface atoms or exposed groups of atoms of the solid and is otherwise independent of the nature and arrangements of the underlying atoms and molecules"*. For understanding this statement it is important to underline that the surface atoms attract each other by highly localized attractive force fields, such as London dispersion forces, which decrease in intensity with the sixth power of distance. The influence of such a field of force become unimportant at a distance of only a few atoms diameters. For this reason, surface properties are localized only in the first ten angstrom of the surface, and they can be deeply modified by coating.

The Constitutive Law of Wettability emphasizes not only the crucial role of the nature of the surface atoms, but also the effect of their structural organization on the surface itself. Molecules having long fluorinated moieties (at least 8 to 12 completely fluorinated carbon atoms) show highly ordinate structures due to the liquid crystal behavior of the rigid fluorinated side groups³⁻¹².

Wang et al.⁷ studied the semifluorinated side-chain end-structures of crystalline semifluorinated block copolymers. On the basis of structural analysis, at room temperature, semifluorinated side chains with less than six -CF₂- segments form a disordered isotropic phase with both -CF₃ and -CF₂- groups exposed to the surface. In contrast, semifluorinated side chains with more than six -CF₂ units form higher ordered phases, with only -CF₃ groups exposed to the surface. In particular, with more than ten fluorinated carbon atoms a crystalline

phase with a uniform hexagonal close packed array of perfluorinated side chains is formed. The resulting surface morphology consists of a regular and smooth surface covered with $-CF_3$ groups (Fig. 4.1). This behavior is due to the superficial rearrangements of the long fluorinated chains. In the case of long fluorinated chains the exposition of the $-CF_3$ groups on the surface is more favored than in short ones; this results in a marked decrease of the surface energy due to the lower surface energy of the close-packed $-CF_3$ structure compared to $-CF_2$ system (Table 4.1).

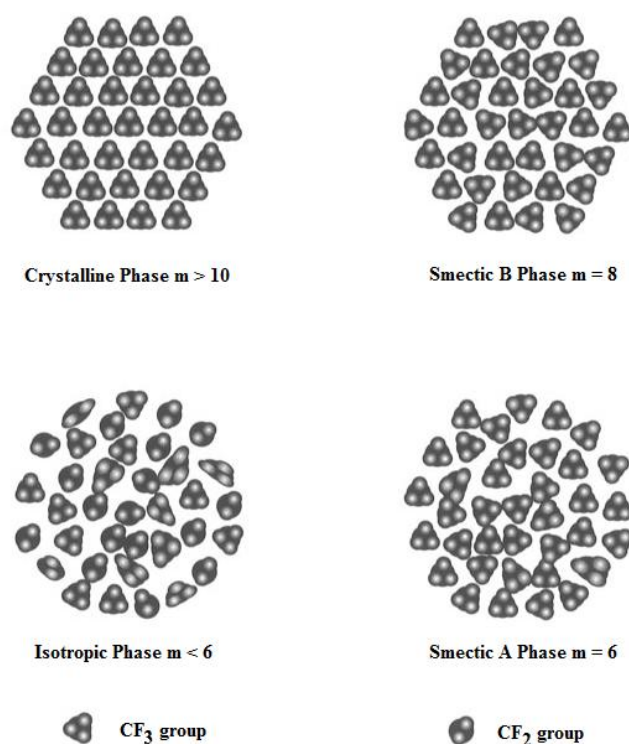


Figure 4.1. Schematic representation of the semifluorinated side chain end structures of semifluorinated copolymers with different fluorinated chain length $F(CF_2)_m$ [7].

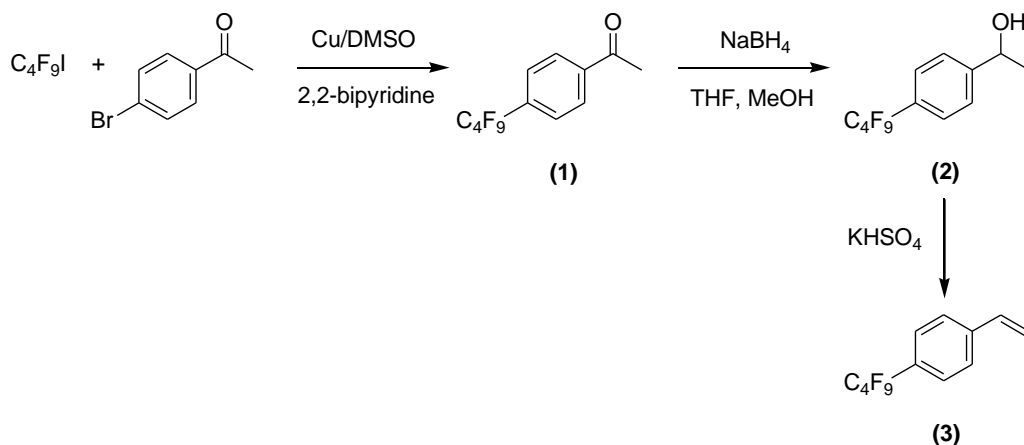
Hare et al.¹³ measured surface tensions of perfluorinated carboxylic acids, showing a decrease of the critical surface tension as the length of the fluorocarbon chain increased. This implies that long fluorinated chains have better surface properties than short ones. As explained in Chapter 2, long perfluorinated chains are persistent in the environment and have strong bioaccumulative effects¹⁴⁻²⁵ and they will be banned as stated by the *PFOA Stewardship Program* launched by U.S. EPA in 2006. The use of shorter chain is detrimental to surface properties because of the partial or complete loss of highly structuring liquid-crystal properties. One of the strategies adopted to increase the molecular rigidity of short chain fluorinated telomers is the introduction of a phenyl or biphenyl group as molecular spacer.

	<i>surface structure</i>	γ_c [mN · m ⁻¹]
a)		6
b)		15
c)		24

Table 4.1. Critical surface tension of a) perfluoro carbon chain, b) semifluorinated carbon chain, c) hydrocarbon chain.

The introduction of the phenyl ring

The introduction of phenyl rings impart to side chains less flexibility enhancing the self-assembling tendency of pendant chains. The intermolecular interaction between aromatic rings in the side chains induces an high level of lateral order of side chains increasing the packing of superficial -CF₃ groups¹².

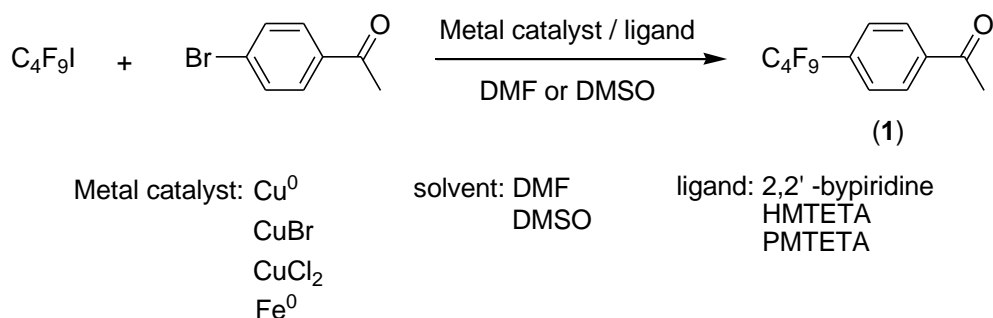


Scheme 4.1. Synthetic route for the preparation of 4'-nonafluorobutyl styrene (3).

The synthesis of 4'-nonafluorobutyl styrene was achieved in three steps (Scheme 4.1): (1) reduction of 4'-nonafluorobutyl acetophenone, (2) reduction in the presence of NaBH₄ leading to the formation of alcohol, (3) dehydration in the presence of KHSO₄ leading to the desired monomer (3). The synthesis of 4'-nonafluorobutyl acetophenone is a cross coupling reaction and it is described in the next paragraph. In order to optimize the global yield of the synthesis a series of changes of the experimental conditions were carried out.

Cross-coupling reaction in presence of perfluoroalkyl iodide.

The synthesis of fluorinated organic compounds that bear an aromatic ring directly linked to a fluorinated alkyl group *via* copper catalysis cross-coupling reaction was first discovered by McLoughlin and Thrower^{26,27} and revisited and improved by Chen and Tamborsky who used this reaction pathway for the introduction of trifluoromethyl groups in bromoaromatics^{28,29} and bromoheterocyclic³⁰⁻³². α -Fluoroalkyl-substituted aromatic compounds are used as pharmaceuticals and agrochemicals intermediates³³⁻³⁶, liquid crystals^{37,38}, and precursors for hydrophilic and hydrophobic silane coupling agents^{39,40}. Many different routes have been reported for the synthesis of fluoroalkyl-substituted aromatics. Bravo et al.⁴¹ reported the free-radical perfluoroalkylation of aromatics with 1-iodo-perfluorobutane in presence of benzoyl peroxide and Cu(II). Huang et al.⁴² reported the fluoroalkylation of aromatics with per(poly)fluoroalkyl chlorides initiated by sodium dithionite in dimethylsulfoxide and Knauber et al.⁴³ reported the copper catalyzed trifluoromethylation of aryl iodides employing potassium (trifluoromethyl)trimethoxyborate. Recently,⁴⁴ a copper-catalytic method in which the copper complex is reusable was discovered. Among all the methods proposed that of McLoughlin and Thrower proved to be the most efficient and regiospecific for the perfluoroalkylation of 4'-bromoacetophenone because the introduction of perfluoroalkyl chains in the aromatic ring occurs exclusively at the halogen site and the formation of biaryls is excluded. This work deals with the synthesis of 4'-nonafluorobutylacetophenone by the reaction between 1-iodo-perfluorobutane and 4'-bromoacetophenone in the presence of N,N dimethylformamide or dimethylsulfoxide as the solvent, catalysed by different transition metals such as Fe⁰, Cu⁰, or metal salts CuBr, CuCl₂ (Scheme 4.1). The effects of ligands, solvents, temperature and metal catalysts were investigated to optimize the reaction by finding the best experimental conditions.



Scheme 4.2. Synthesis of 4'-nonafluorobutylacetophenone from the metal-assisted cross-coupling of 1-iodo-perfluorobutane (1) with 4'-bromoacetophenone.

Synthesis of 4'-nonafluorobutyl acetophenone (1)

4.1.1 Materials and Methods

Iron, copper, copper(I) bromide, copper(II) chloride, 2,2 bipyridine, N,N,N',N'',N''',N''''-hexamethyltriethylenetetramine (HMTETA), N,N,N',N'',N'''-pentamethyldiethylenetriamine (PMTETA), 4'-bromoacetophenone, N,N dimethyl-formamide (DMF) and dimethylsulfoxide (DMSO) were purchased from the Aldrich Chemical Company. 1-Iodo-perfluorobutane was purchased by Maflon s.p.a.. The solvents were used as received. All the reactions were conducted under nitrogen atmosphere.

The conversion (χ , Eq. 4.1) was assessed by the sum of the values of the integrals ($\sum I$, Eq. 4.2) of the signals relative to 4'-bromoacetophenone measured by ^1H NMR spectroscopy at initial time (0) and at the end (f) of the reaction.

$$\chi = \frac{[\sum I]_0 - [\sum I]_f}{[\sum I]_0} \quad \text{Eq. 4.1}$$

$$\sum I = \int \frac{CH_2^{7.69ppm}}{2} + \int \frac{CH_2^{8.07ppm}}{2} + \int CH^{2.64ppm} \quad \text{Eq. 4.2}$$

Where $\int CH_x^{i ppm}$ represents the integral of the signal assigned to CH_x centered at i ppm.

4.1.2 General procedure for the synthesis of 4'-nonafluorobutylacetophenone, C₄F₉C₆H₄COCH₃ (1).

In a 100 mL round bottom flask, equipped with a magnetic stirrer and a reflux condenser, a mixture composed of 1.0 mol of 4'-bromoacetophenone, 4.0 mol of N,N dimethylformamide, 1.0 mol of 1-iodoperfluorobutane, 4.6 mol of copper and 0.1 mol of 2,2-bipyridine were heated under stirring for 20 hours at 60 °C. After the reaction, the copper powder was removed by filtration and the liquid layer was washed three times with 30 mL of water and 30 mL of diethyl ether, separating each time the ether layer. The ether was removed under reduced pressure and the 4'-nonafluorobutylacetophenone (b.p. 66-69 °C/0.2 mmHg) was distilled as a colorless liquid.

4.1.3 Chemical characterization of 4'-nonafluorobutylacetophenone

Hereafter are reported the chemical characterization of 4'-nonafluorobutylacetophenone: IR (Figure 4.2), ^1H NMR (Figure 4.3), ^{13}C NMR (Figure 4.4-4.5), ^{19}F NMR (Figure 4.6), , and GC-MS spectroscopy (Figure 4.7).

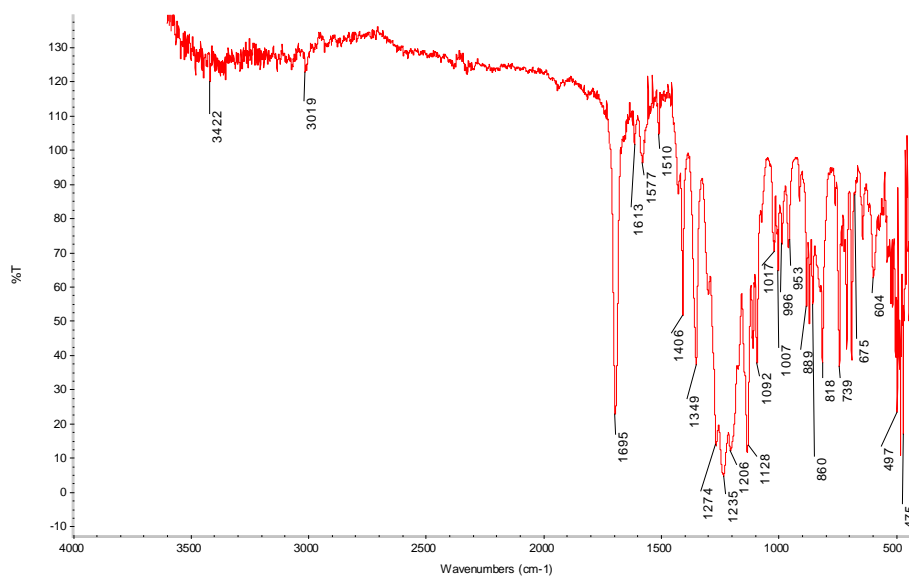


Figure 4.2. IR spectrum of 4'-nonafluorobutyl acetophenone.

IR (cm^{-1}): 3422 (ν_{as} , C=O), 1695 (ν_{s} , C=O), 1613-1577 (ν_{s} , phenyl ring), 1202-1274 (δ_{s} , CF_2, CF_3), 1349 (τ , CH_3).

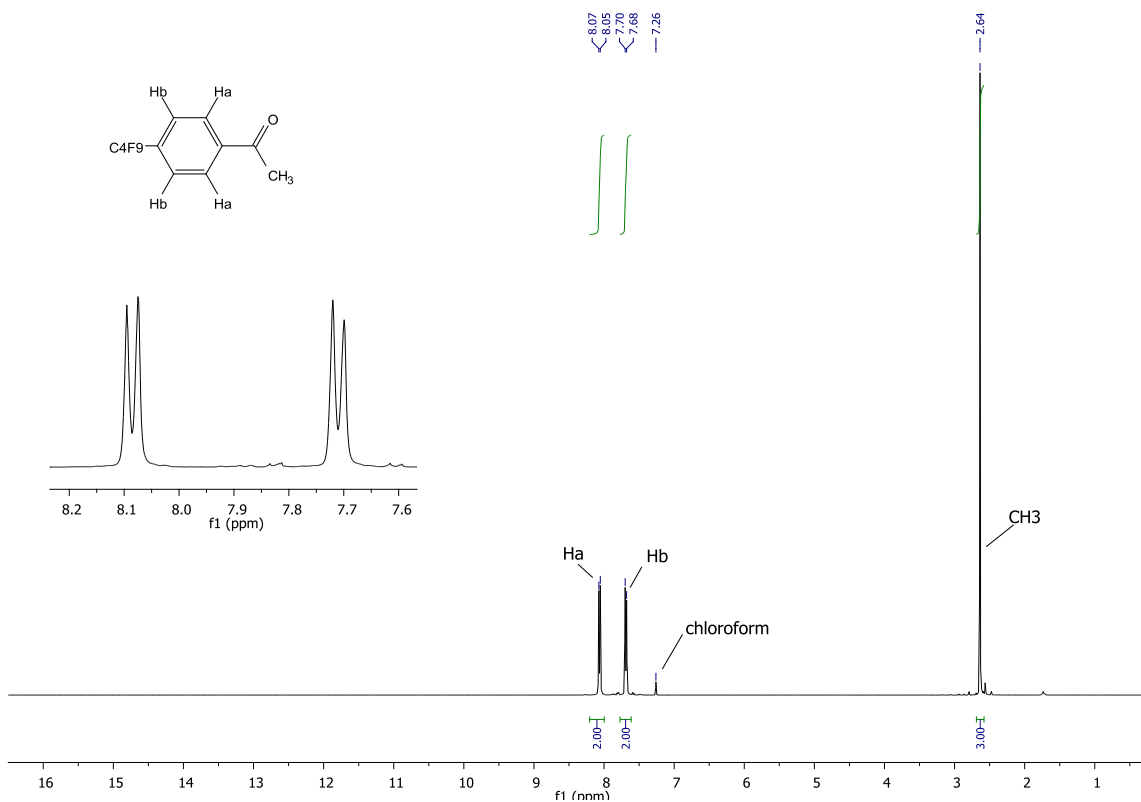


Figure 4.3. ^1H NMR spectrum of 4'-nonafluorobutyl acetophenone in CDCl_3 .

^1H NMR (CDCl_3) δ : 2.64 ppm (3H, s, CH_3); 7.69 ppm (2H, d, $J = 8.5$ Hz, m -protons from $\text{C}=\text{O}$); 8.07 ppm (2H, d, $J = 8.5$ Hz, o -protons from $\text{C}=\text{O}$).

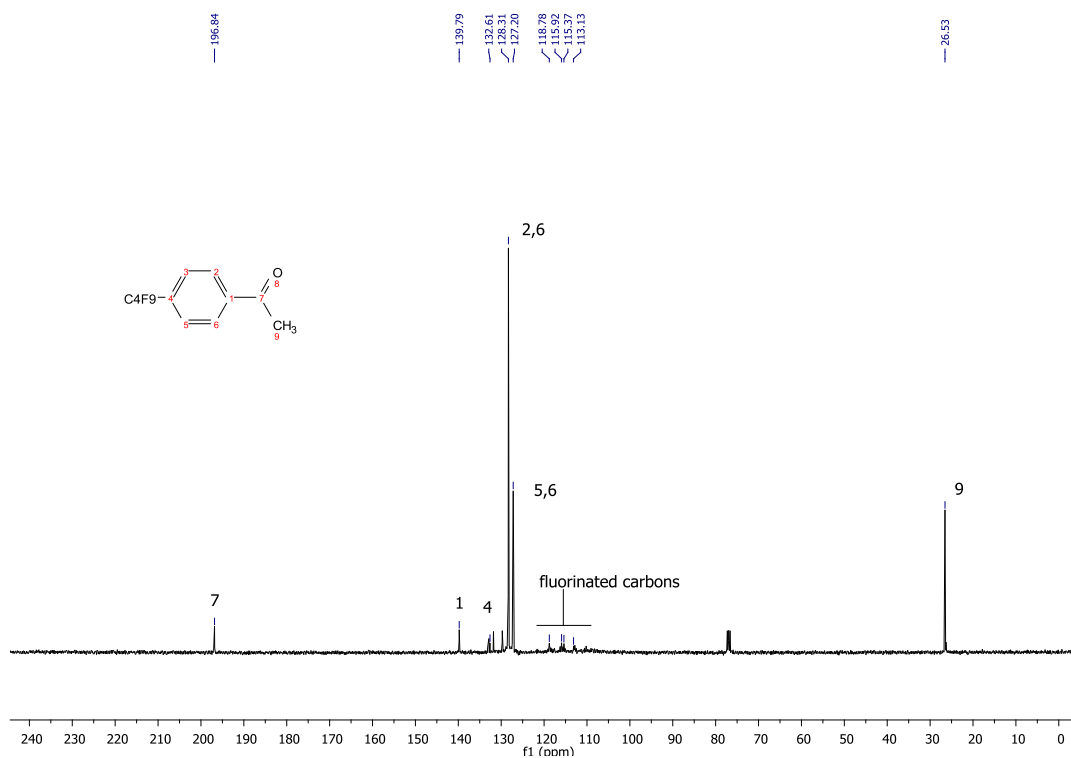


Figure 4.4. ^{13}C NMR of 4'-nonafluorobutyl acetophenone in CDCl_3 .

^{13}C NMR (CDCl_3) δ : 196.8 ppm (s, $\underline{\text{C}}=\text{O}$); 139.8 ppm (s, *p*-carbon from CF_2); 132.8 ppm (t, $^2\text{J}_{\text{C-F}} = 24$ Hz, *p*-carbon from $\text{C}=\text{O}$); 128.3 ppm (s, *o*-carbons from $\text{C}=\text{O}$); 127.2 ppm (t, $^2\text{J}_{\text{C-F}} = 6$ Hz, *m*-carbons from $\text{C}=\text{O}$); 118.8 ppm (t, $^2\text{J}_{\text{C-F}} = 33$ Hz, $\text{CF}_3\text{-CF}_2\text{-}\underline{\text{CF}}_2\text{-CF}_2\text{-Ph}$); 115.9 ppm (t, $^2\text{J}_{\text{C-F}} = 33$ Hz, $\underline{\text{CF}}_3\text{-CF}_2\text{-CF}_2\text{-CF}_2\text{-Ph}$); 115.4 ppm (t, $^2\text{J}_{\text{C-F}} = 33$ Hz, $\text{CF}_3\text{-}\underline{\text{CF}}_2\text{-CF}_2\text{-CF}_2\text{-Ph}$); 113.1 ppm (m, $^2\text{J}_{\text{C-F}} = 33$ Hz, $\text{CF}_3\text{-CF}_2\text{-CF}_2\text{-}\underline{\text{CF}}_2\text{-Ph}$); 26.5 ppm (s, $\underline{\text{C}}\text{H}_3$).

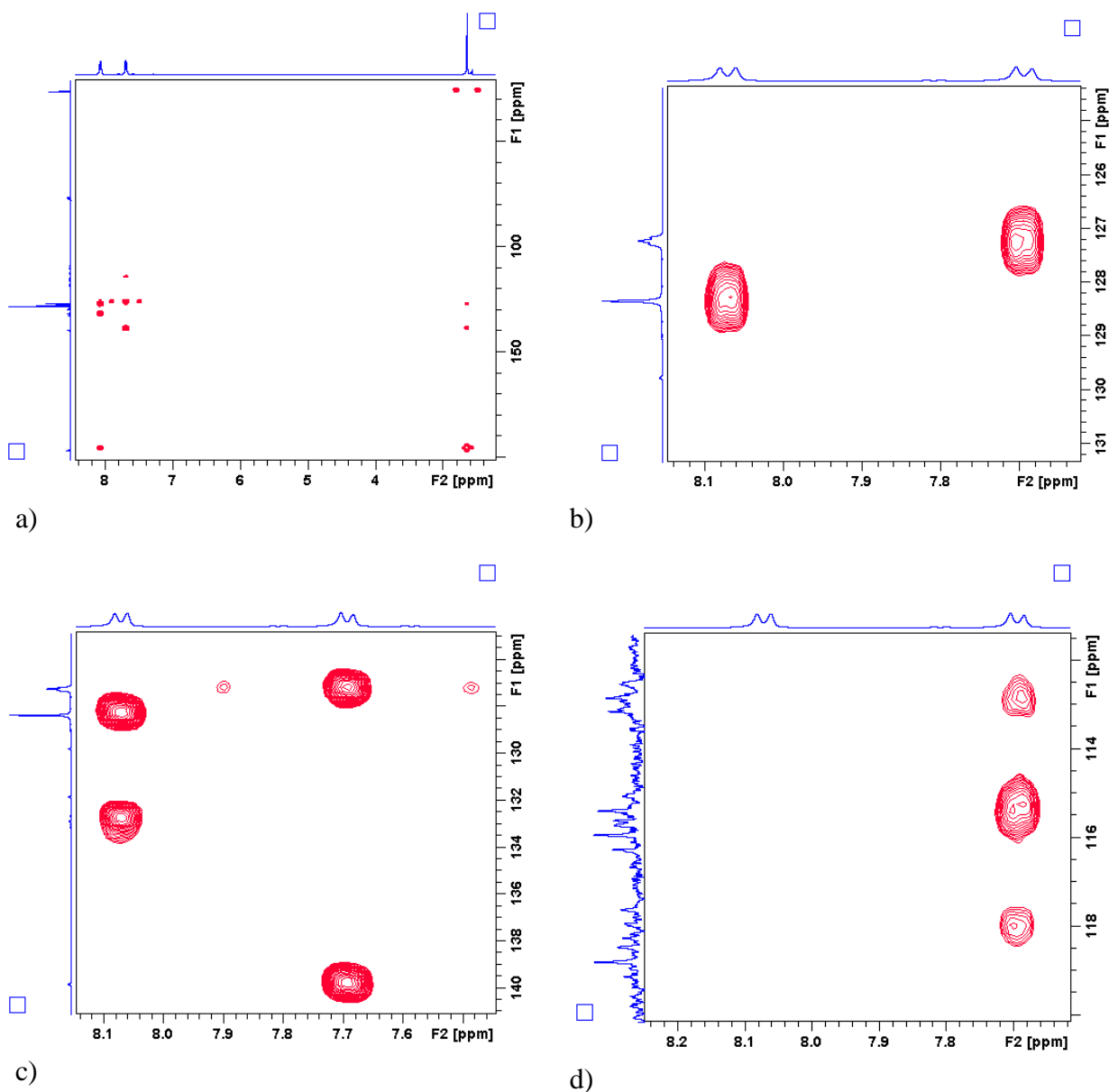


Figure 4.5. $^1\text{H},^{13}\text{C}$ -HMQC of 4'-nonafluorobutyl acetophenone, a) full scale, b) and c) aromatic carbons, d) fluorinated carbons moieties.

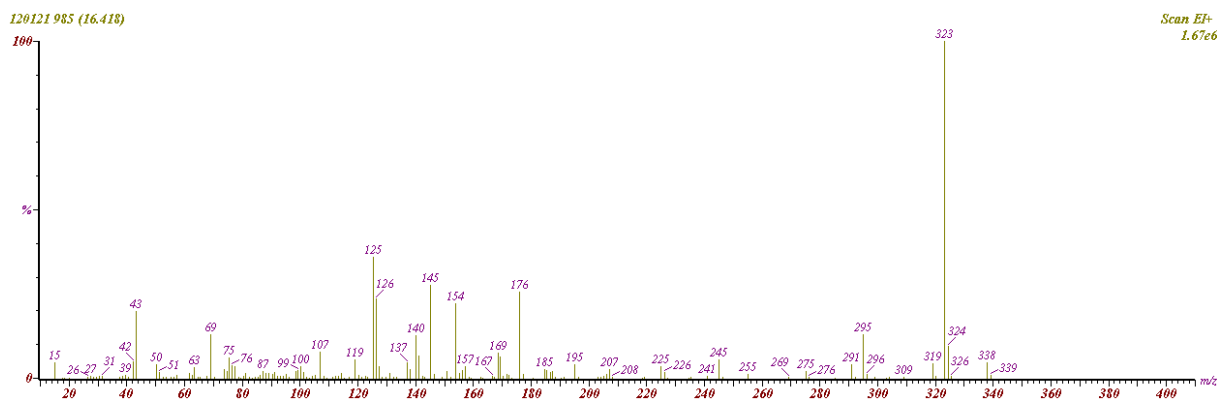


Figure 4.7. . GC-MS spectrum of 4'-nonafluorobutyl acetophenone (1).

Spectral data: MS m/z (rel. ab. %): 338 ($[M]^+$, 10%); 323 ($[M-CH_3]^+$, 100%); 295 ($[M-COCH_3]^+$, 20%); 119 ($[M-C_4F_9]^+$, 5%).

Anal. Calcd for $C_{12}F_9H_7O$: C, 42.6 % ; F, 50.6 % ; H, 2.1 %. Found: C, 41.9 % ; F, 50.9 % ; H, 2.0 %.

Results and discussion

4'-Nonafluorobutylacetophenone was synthesised by varying one or more experimental parameters for each run. All the reactions were carried out for a fixed time of 20 hours to compare the results obtained. The development of the optimum conditions is discussed below, taking into account various factors.

4.1.4 Effect of the metal catalyst

Transition metal-catalyzed cross coupling reactions of organic halides containing a C-X bond (X = I, Br, Cl, OTf, OTs, etc..) with organometallic reagents are among the most important transformations for carbon-carbon bond formation.

Exp	metal	ligand	solvent	$[R_F I]_0/[ligand]_0/[metal]_0/[solvent]$	T [°C]	η^{**} %	χ^* %
1	Fe ⁰	-	DMF ^a	1/0/4.6/4	130	-	-
2	Fe ⁰	-	DMSO ^b	1/0/4.6/4	130	-	-
3	Fe ⁰	2,2-bipyridine	DMF	1/0.1/4.6/4	100	-	-
4	CuBr	-	DMF	1/0/4.6/4	130	-	-
5	CuBr	-	DMSO	1/0/4.6/4	130	-	-
6	CuBr	HMTETA ^c	DMF	1/0.1/4.6/4	80	-	-
7	CuCl ₂	-	DMF	1/0/4.6/4	130	-	-
8	CuCl ₂	-	DMSO	1/0/4.6/4	130	-	-
9	CuCl ₂	2,2-bipyridine	DMF	1/0.1/4.6/4	80	-	-
10	Cu ⁰	-	DMF	1/0/4.6/1	130	50	70

Table 4.2. Series of reactions of synthesis of 4'-nonafluorobutylacetophenone from cross-coupling of 1-perfluorobutyl iodide with 4'-bromoacetophenone (reaction time of all runs: 20 hrs).

*Conversion calculated by ¹H NMR spectroscopy as reported in the material and methods part.

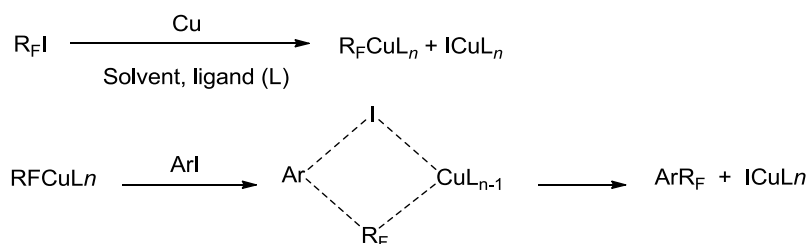
**Yield.

a) DMF = N,N-dimethylformamide

b) DMSO = dimethyl sulfoxide

c) HMTETA = N,N,N',N'',N''',N''''-hexamethyltriethylenetetramine

For constructing new alkyl chains several transition metals could be used. In the synthesis of 4'-nonafluorobutylacetophenone by cross-coupling reactions copper metal only was efficiently used as the catalyst. Different kinds of transition metals and metal salts were tested as potential catalysts: Fe⁰, CuBr, CuCl₂ (entries 1-9, Table 4.2), but these attempts to get the desired product systematically failed. For the effectiveness of the synthesis, the [metal]₀ / [1-iodo-perfluorobutane]₀ molar ratio must be at least 2 / 1. The high amount of required copper could be explained by the reaction mechanism proposed by McLaughlin and Thrower^{45,46} (Scheme 4.4).



Scheme 4.4. General mechanism of the synthesis of perfluoroalkyl aromatic compounds *via* copper-assisted cross-coupling reaction^{26,27}.

The mechanism of copper-assisted cross-coupling reaction must be similar to that involved in the reaction between halogenoaromatic compounds and cuprous acetylides⁴⁷. The mechanism is composed of two steps: first, in the metallation stage, the fluoroalkylcopper compound is formed as a solvated complex, then it interacts with the aromatic halide which is followed by an exchange between the halogen and the perfluoroalkyl chain on the aromatic derivative. To

stabilize the fluoroalkylcopper complex formed in the former stage the solvent must also induced a ligand effect onto copper.

4.1.5 Effect of the solvent

For the success of the cross-coupling reaction with perfluoroalkyl iodides a polar aprotic solvent must be used. For this purpose, N,N-dimethylformamide (DMF) and dimethylsulfoxide (DMSO) were both used as solvents. The comparison on the effect of both these solvents is shown in Table 4.3. Changing the solvent while keeping all the reaction conditions unmodified does not affect the yield and conversion. Conversely, the quantity of both solvents have a remarkable effect on the reaction yields (Exp. 11-15 for DMF, and Exp. 16-20 for DMSO).

Exp	metal	solvent	$[R_F I]_0/[metal]_0/[solvent]$	T [°C]	$\eta^{**}\%$	$\chi^*\%$
11	Cu ⁰	DMF	1/4.6/1	130	50	70
12	Cu ⁰	DMF	1/4.6/2	130	54	72
13	Cu ⁰	DMF	1/4.6/3	130	54	73
14	Cu ⁰	DMF	1/4.6/4	130	58	75
15	Cu ⁰	DMF	1/4.6/5	130	58	75
16	Cu ⁰	DMSO	1/4.6/1	130	51	70
17	Cu ⁰	DMSO	1/4.6/2	130	53	72
18	Cu ⁰	DMSO	1/4.6/3	130	54	72
19	Cu ⁰	DMSO	1/4.6/4	130	58	75
20	Cu ⁰	DMSO	1/4.6/5	130	58	75

Table 4.3. . Series of reactions of synthesis of 4'-nonafluorobutylacetophenone from cross-coupling of 1-perfluorobutyl iodide with 4'-bromoacetophenone (reaction time of all runs: 20 hrs).

*Calculated by ¹H NMR spectroscopy as reported in the material and methods part.

.....**Yield.

a) DMF = N,N-dimethylformamide

b) DMSO = dimethyl sulfoxide

Furthermore, an increase in the initial $[solvent]_0/[1\text{-iodo-perfluorobutane}]_0$ molar ratio from 1 to 4 induced a 8% yield increase while a further increase from 4 to 5 was not beneficial (as noted in Figure 4.1). These results confirm previous studies and revealed that the optimized solvent / 1-iodo-perfluorobutane molar ratio is 4 / 1.

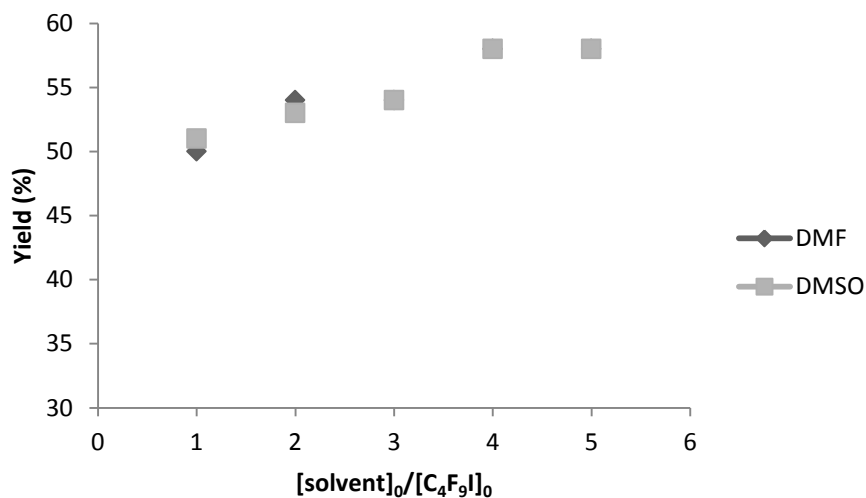


Figure 4.8. Effect of the $[\text{solvent}]_0 / [\text{C}_4\text{F}_9\text{I}]_0$ initial molar ratio in the yield in the copper-assisted cross-coupling reaction of 1-iodoperfluorobutane with 4'-bromoacetophenone using DMF or DMSO as the solvent (Table 4.3).

4.1.6 Effect of the ligand

The important effect of the ligand on the copper mediated cross-coupling reaction can be explained by examining the mechanism proposed in the paragraph above. For the synthesis of 4'-nonafluorobutylacetophenone, 2,2'-bipyridine, HMTETA, PMTETA were used as complexing ligands (Figure 4.8). It has been shown that a catalytic amount of these compounds was particularly beneficial to the reaction yield. Using DMSO and DMF as solvents, without ligands, the reaction conversion was limited to 75% and the yield did not exceeded 58% in 20 hours (Exp. 21-22, Table 4.4).

Exp.	metal	ligand	solvent	$[\text{R}_f\text{I}]_0 / [\text{ligand}]_0 / [\text{metal}]_0 / [\text{solvent}]$	T [°C]	η^{**} %	χ^* %
21	Cu ⁰	-	DMSO	1/0/4.6/4	130	58	75
22	Cu ⁰	-	DMF	1/0/4.6/4	130	58	75
23	Cu ⁰	HMTETA	DMF	1/0.1/4.6/4	80	60	88
24	Cu ⁰	2.2-bipyridine	DMF	1/0.1/4.6/4	60	62	88
25	Cu ⁰	2.2-bipyridine	DMSO	1/0.1/4.6/4	60	62	88
26	Cu ⁰	PMDETA	DMF	1/0.1/4.6/4	100	69	90
27	Cu ⁰	2.2-bipyridine	DMF	1/0.1/4.6/4	80	73	93
28	Cu ⁰	2.2-bipyridine	DMF	1/0.1/4.6/4	100	73	99

Table 4.4. Series of reactions of synthesis of 4'-nonafluorobutylacetophenone from cross-coupling of 1-perfluorobutyl iodide with 4'-bromoacetophenone (reaction time of all runs: 20 hrs).

*Calculated by ¹H NMR spectroscopy as reported in the material and methods part.

.....**Yield.

a) DMF = N,N-dimethylformamide

b) DMSO = dimethyl sulfoxide

c) HMTETA = N,N,N',N'',N''',N''''-hexamethyltriethylenetetramine.

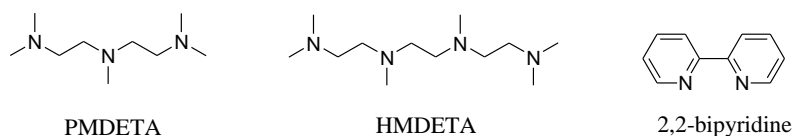


Figure 4.9. Ligands used in the synthesis of 4'-nonafluorobutyl acetophenone.

A presence of catalytic amount of an amino ligand induced an increase of both conversion and yield (entries 20-25, Table 4.4). From these results, 2,2-bipyridine is regarded as the best ligand that led to conversion higher than 90% and yield higher than 70% depending on the temperature.

4.1.7 Effect of temperature

For the copper-mediated cross-coupling reaction of 1-iodo-perfluorobutane and 4'-bromoacetophenone, the effect of temperature is noted by comparison of entries 21, 24, 25 (Table 4.5) in which three different temperatures were used, 60, 80 and 100 °C.

Exp.	metal	ligand	solvent	$[R_F I]_0/[ligand]_0/[metal]_0/[solvent]$	T [°C]	η^{**} %	χ^* %
29	Cu ⁰	2,2-bipyridine	DMF	1/0.1/4.6/4	60	62	88
30	Cu ⁰	2,2-bipyridine	DMF	1/0.1/4.6/4	80	73	93
31	Cu ⁰	2,2-bipyridine	DMF	1/0.1/4.6/4	100	73	99

Table 4.5. Series of reactions of synthesis of 4'-nonafluorobutylacetophenone from cross-coupling of 1-perfluorobutyl iodide with 4'-bromoacetophenone (reaction time of all runs: 20 hrs).

*Conversion calculated by ¹H NMR spectroscopy as reported in the material and methods part.

.....**Yield.

a) DMF = N,N-dimethylformamide

As displayed in Figure 4.9 when the temperature increases, a linear increase in conversion was observed. Conversely, the yield increases almost linearly from 60 to 80 °C and then it reached a plateau to 73% indicating that a further temperature increase was not necessary.

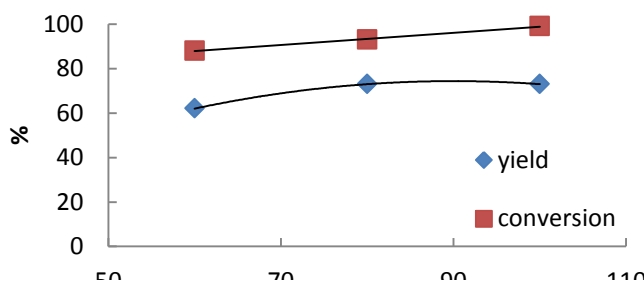


Figure 4.10. Effect of the temperature on the yield and conversion for the reaction between Cu⁰, N,N-dimethylformamide, in the presence of 2,2-bipyridine (entries 21, 24 and 25, Table 1).

Conclusion

The aim of this first part of this chapter is the optimization the synthesis of 4'-nonafluorobutylacetophenone by the copper-assisted cross-coupling reaction, by changing the experimental conditions. The use of an aprotic polar solvent is compulsory for the success of the reaction as shown by the mechanism (Scheme 3.2), but changing N,N dimethylformamide or dimethylsulfoxide does not seem to have any significant effect on yield and conversion. Therefore, in view of a possible industrial application, DMSO should be preferred to DMF because the former is less toxic.

The study conducted on the quantity of solvent required for the reaction showed that the optimum [solvent]₀ / [1-iodo-perfluorobutane]₀ molar ratio is 4. Different experiments were attempted to assess the role of the metal catalyst in the cross-coupling reaction. McLoughlin and Thrower showed that mercury and zinc were ineffective catalysts. The use of metallic iron and cupric and cuprous salts as potential metal catalysts was investigated, but the desired product was not obtained, and only copper metal led to obtain a significant yield. Among the complexing ligands used (2,2'-bipyridine, HMTETA, PMTETA), 2,2'-bipyridine gave the best results both for conversion and yield. Further, using 2,2'-bipyridine when the temperature increased from 60 to 100 °C showed a positive effect on reaction yield and conversion.

Synthesis of 4'-nonafluorobutyl ethanol (2)

The synthesis of 4'-nonafluorobutyl-styrene was achieved into two steps (Scheme 3.1), in which a reduction of 4'-nonafluorobutyl acetophenone (**1**, obtained in a previous paragraph), in the presence of NaBH₄ as reducing agent, led to the formation of the alcohol (**2**), the dehydration of the latter, in the presence of KHSO₄, conducted to synthesize the desired monomer (**3**).

4.1.8 Materials

2,2' Azobisisobutyronitrile (AIBN), tetrahydrofuran (THF), methanol, acetonitrile (CH₃CN), potassium hydrogen sulfate (KHSO₄), sodium borohydride (NaBH₄), diiodomethane (CH₂I₂) and toluene were purchased from the Aldrich Chemical Company. 1-Iodo-perfluorohexane was a gift from Elf Atochem. All the solvents and reagents were used with a purity of 98-99%. AIBN was purified by recrystallization from methanol and dried under vacuum prior to use.

4.1.9 General procedure for the synthesis of 4'-nonafluorobutyl phenylethanol C₄F₉C₆H₄CH(OH)CH₃

4'-Nonafluorobutylacetophenone (**1**) (15.5 g, 45.8 mmol), sodium borohydride (1.8 g, 47.7mmol), and THF (50 mL) as the solvent were stirring into a 100 mL round bottom flask in an ice bath. Methanol (50 mL) was slowly added drop-wise into the flask and the mixture was refluxed for 2 hours under heating after being stirred for 30 minutes at room temperature. Methanol was removed by distillation. Water was added to the ether solution and the ether layer was taken out. The ether was removed by rotavapor and 14.4 g of colorless oil (b.p. 60-65 °C/0.2 mmHg) were obtained (yield: 90%).

4.1.10 Chemical characterization of 4'-nonafluorobutyl phenylethanol

Hereafter are reported the chemical characterization of 4'-nonafluorobutyl phenylethanol: IR (Figure 4.10), ¹H NMR (Figure 4.11), ¹⁹F NMR (Figure 4.12), and GC-MS spectroscopy (Figure 4.13).

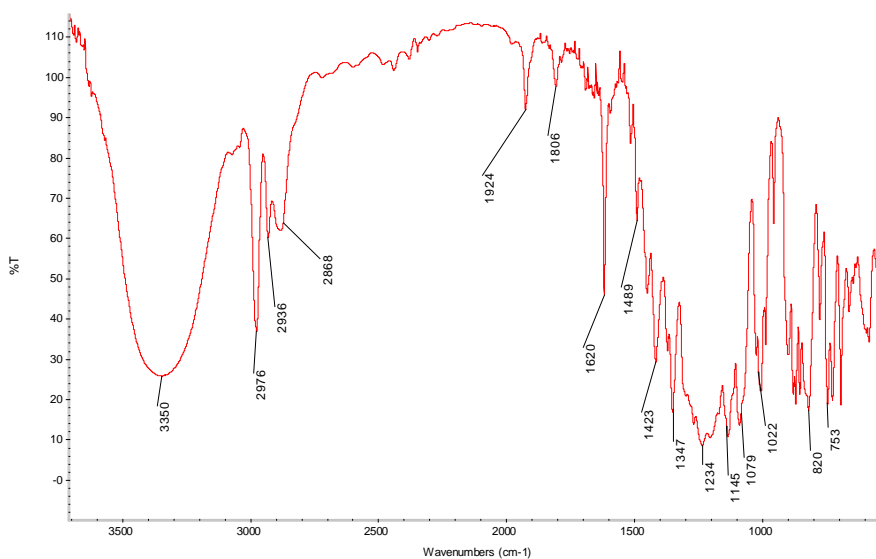


Figure 4.11. IR spectrum of 4'-nonafluorobutyl phenylethanol.

IR (cm⁻¹): 3350 (ν_{as}, -OH), 1347 (δ_s CH₃), 1606 (ν_s, phenyl ring), 1145-1234 (δ_s, CF₂, CF₃), 1079 (δ_{as}, CH), 753 (ρ, CH₃).

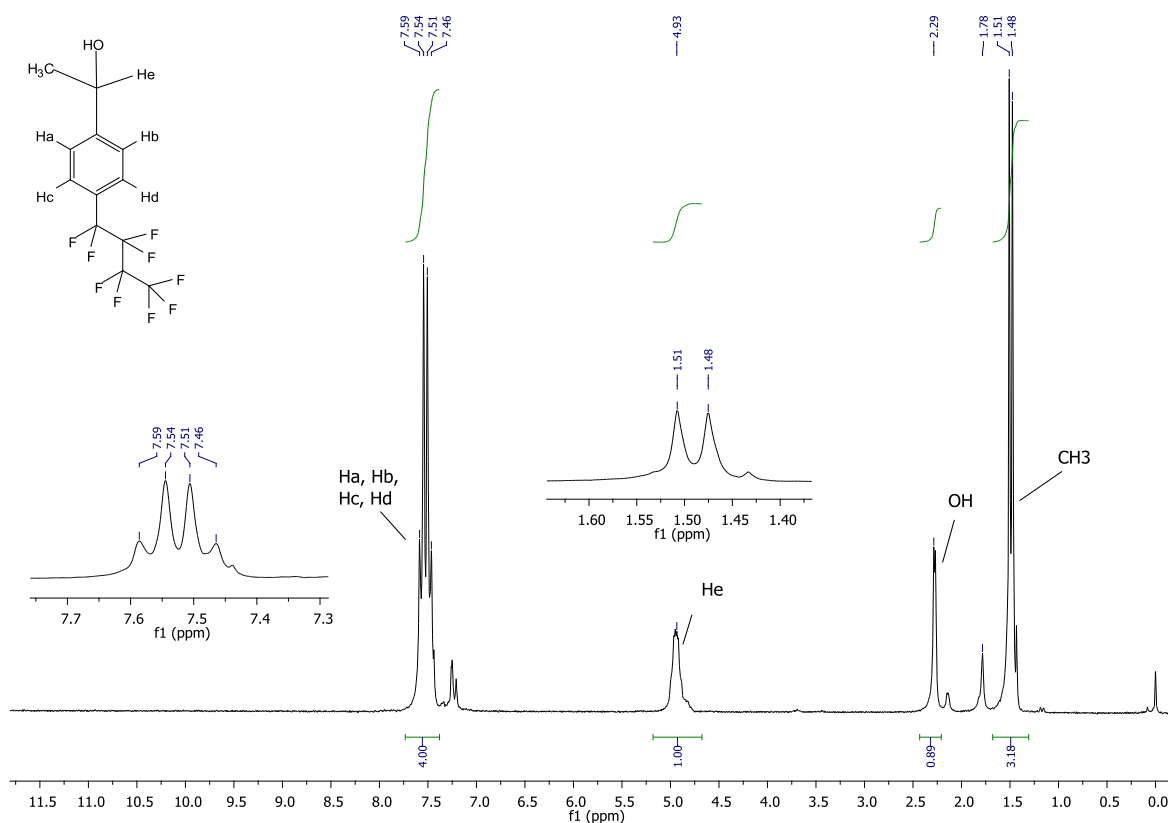


Figure 4.12. ^1H NMR spectrum of 4'-nonafluorobutyl acetophenone (2) (recorded in CDCl_3).

^1H NMR of 4'-nonafluorobutyl phenylethanol (2), δ (in CDCl_3): 1.48 ppm (3H, d, $^3J_{\text{HH}} = 6.0$ Hz, CH_3); 2.29 ppm (1H, s, -OH); 4.93 ppm (1H, m, CH); 7.50 ppm (2H, dd, $^3J_{\text{HH}} = 16$ Hz; 8 Hz, protons form phenyl ring).

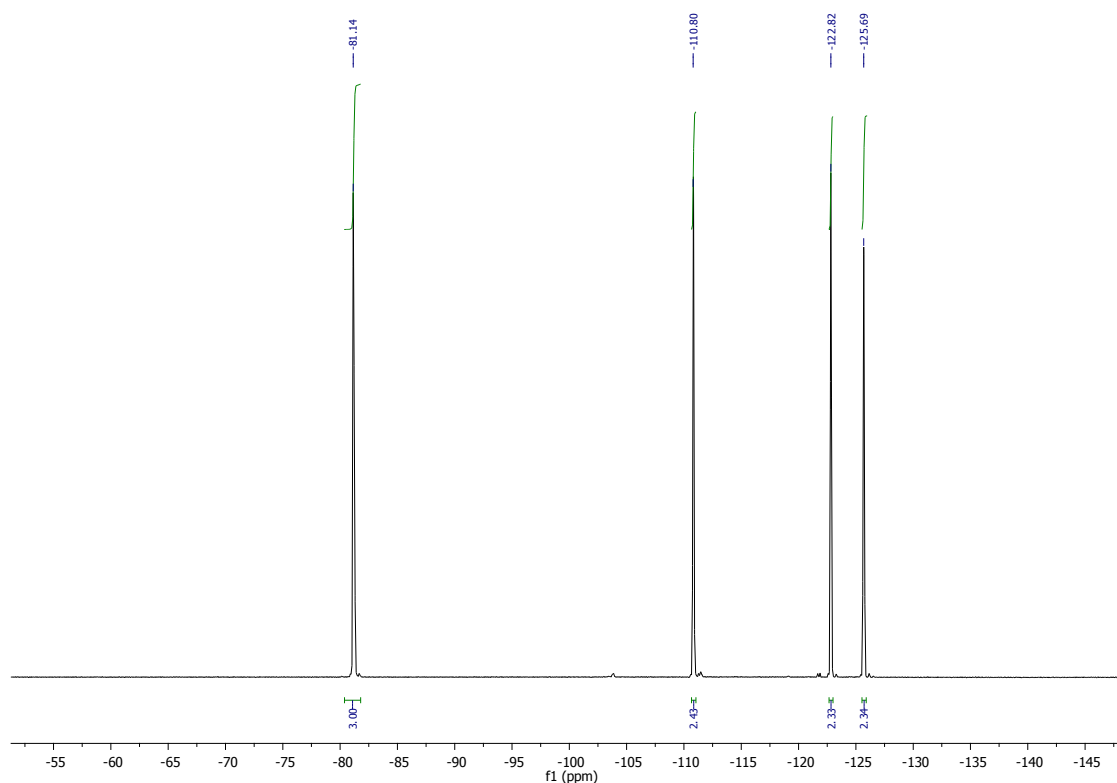
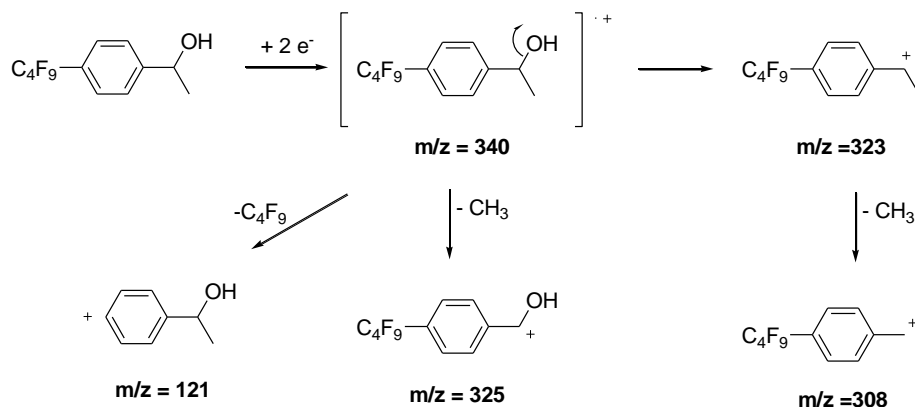


Figure 4.13. ^{19}F NMR 4'-nonafluorobutyl phenylethanol (2) (recorded in CDCl_3).

^{19}F NMR spectrum of 4'-nonafluorobutyl phenylethanol δ : -81.1 ppm ($\text{CF}_3\text{-CF}_2\text{-CF}_2\text{-CF}_2\text{-Ph}$); -125.7 ppm ($\text{CF}_3\text{-CF}_2\text{-CF}_2\text{-CF}_2\text{-Ph}$); -122.8 ppm ($\text{CF}_3\text{-CF}_2\text{-CF}_2\text{-CF}_2\text{-Ph}$); -110.8 ppm ($\text{CF}_3\text{-CF}_2\text{-CF}_2\text{-CF}_2\text{-Ph}$).



Scheme 4.5. Possible fragmentation of 4'-nonafluorobutyl phenylethanol (2).

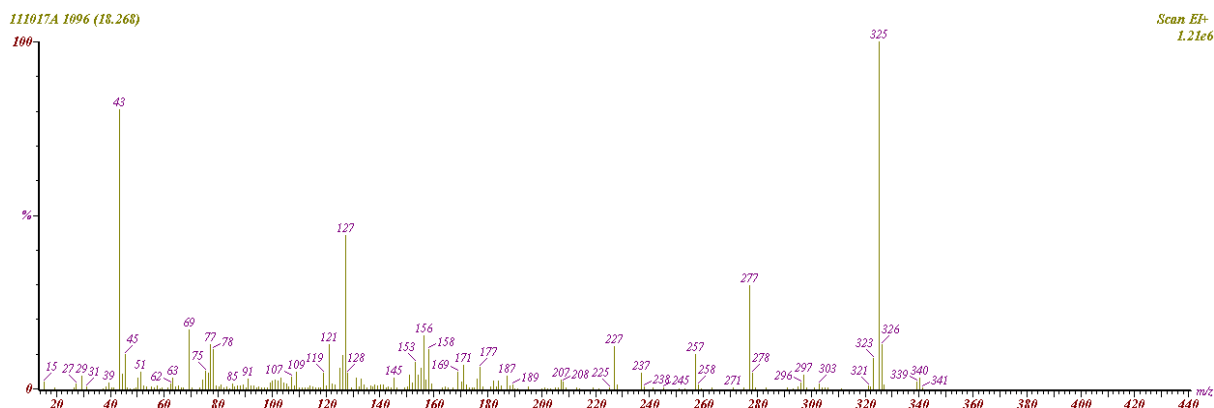


Figure 4.14. GC-MS spectrum of 4'-nonafluorobutyl phenylethanol (**2**).

GC-MS (rel. ab. %): 340 ($[M]^+$, 5%); 325 ($[M-CH_3]^+$, 100%); 121 ($[M-C_4F_9]^+$, 20%).

4.1.11 General procedure for the synthesis of 4'-nonafluorobutyl styrene $C_4F_9C_6H_4CHCH_2$

A mixture composed of 4'-nonafluorobutyl phenylethanol (**2**) (14.41 g, 42.3 mmol), toluene (50 mL) and potassium hydrogen sulfate (4.02 g, 29.5 mmol) was heated under stirring at 100 °C for 48 hours in a 100 mL round flask connected to a reflux condenser. The reaction was monitored by gas-chromatography. After reaction, the mixture was distilled under vacuum and a colorless liquid was obtained (9.35 g, b.p. 66-69 °C/0.39 mmHg, yield 77%).

4.1.12 Chemical characterization of 4'-nonafluorobutyl styrene

Hereafter are reported the chemical characterization of 4'-nonafluorobutyl styrene (**3**): IR (Figure 4.14), 1H NMR (Figure 4.15), ^{19}F NMR (Figure 4.16), and GC-MS spectroscopy (figure 4.17).

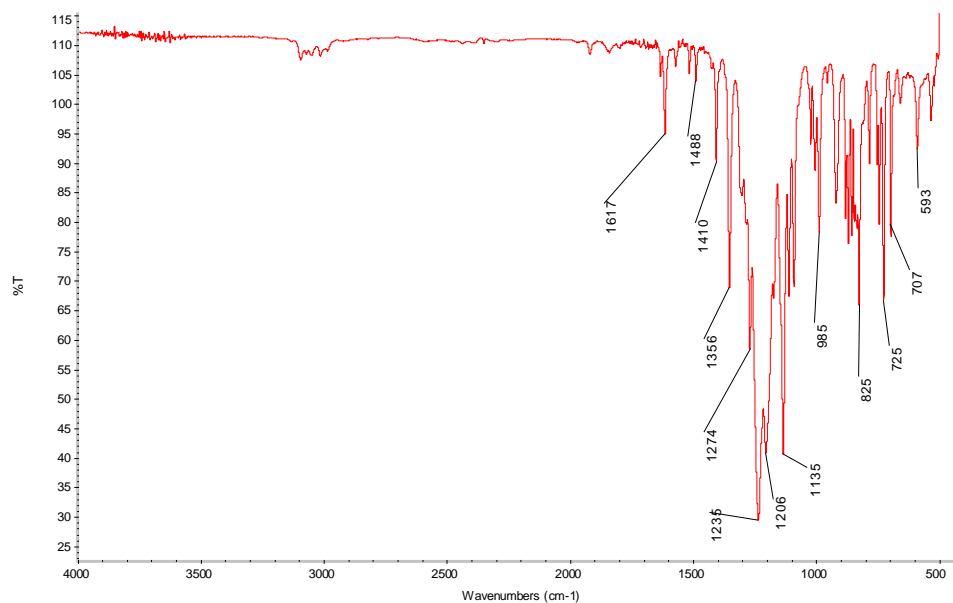


Figure 4.15. IR spectrum of 4'-nonafluorobutyl styrene (3).

IR (cm⁻¹): 1617 (v_s, phenyl ring), 1206-1274 (δ_s, CF₂, CF₃), 825 (ρ, C=C).

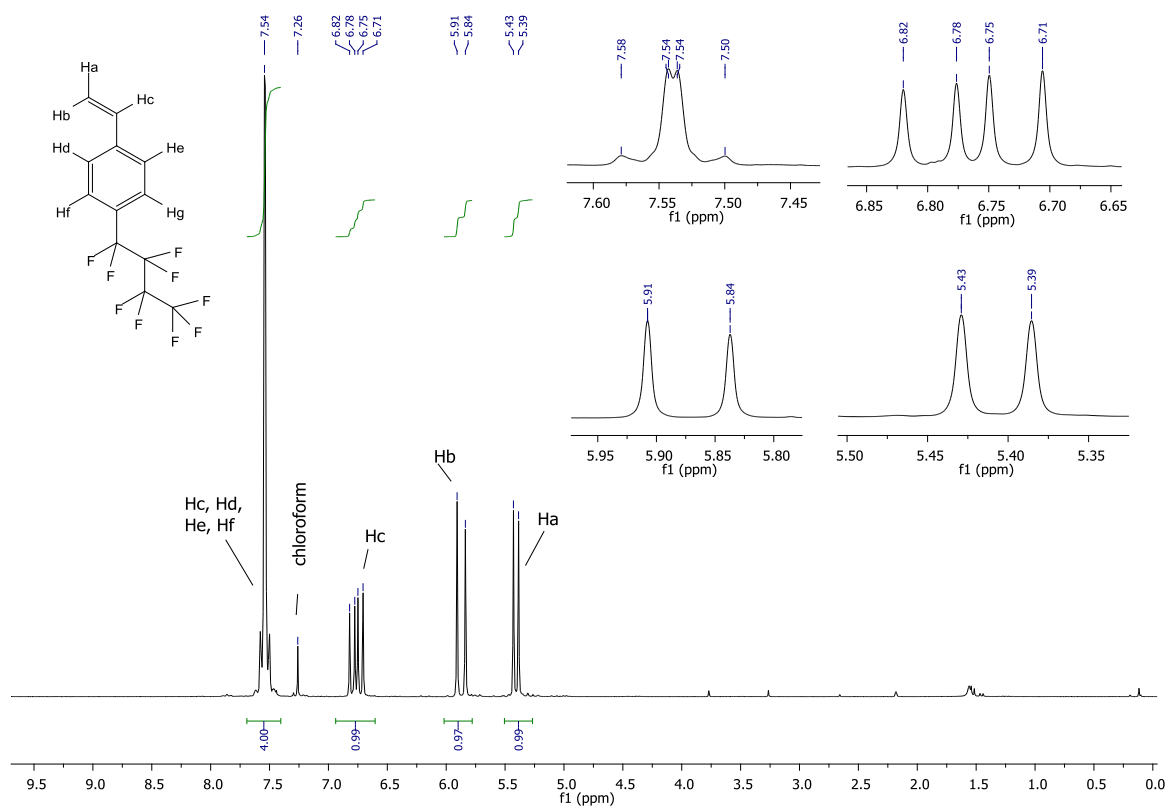


Figure 4.16. ¹H NMR spectrum of 4'-nonafluorobutyl styrene (3) (recorded in CDCl₃).

^1H NMR of 4'-nonafluorobutyl styrene, δ (in CDCl_3): 5.41 ppm (1H, d, cis = CH_2 , $^3J_{\text{HH}} = 10.0$ Hz); 5.87 ppm (1H, trans = CH_2 , $^3J_{\text{HH}} = 17.5$ Hz), 6.71-6.82 ppm (1H, doublet of doublets, $^3J_{\text{HH}} = 17.5$ Hz; 10 Hz, = CH); 7.52 ppm (2H, d, $^3J_{\text{HH}} = 10.0$ Hz, *m*- protons from C_4F_9), 7.56 ppm (2H, d, $^3J_{\text{HH}} = 10.0$ Hz, *o*- protons from C_4F_9).

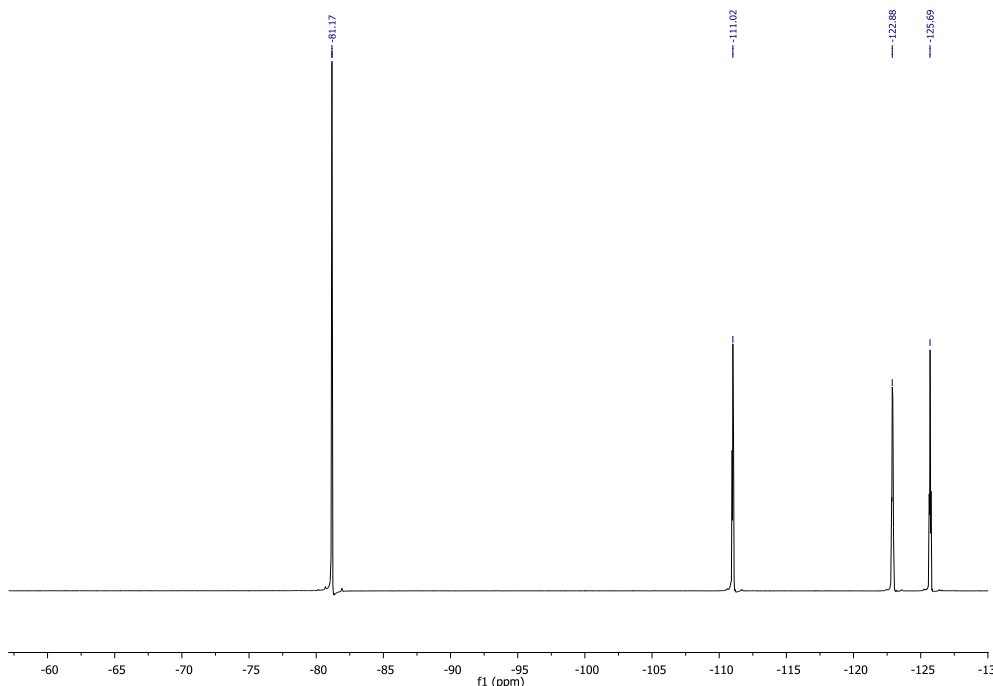
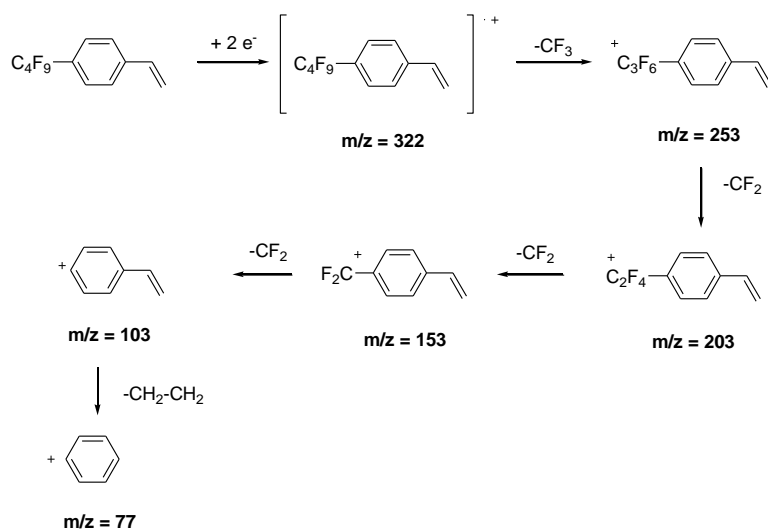


Figure 4.17. ^{19}F NMR 4'-nonafluorobutyl styrene (3) (in CDCl_3).

^{19}F NMR, δ (in CDCl_3): -81.1 ppm ($\text{CF}_3\text{-CF}_2\text{-CF}_2\text{-CF}_2\text{-Ph}$); -125.7 ppm ($\text{CF}_3\text{-CF}_2\text{-CF}_2\text{-CF}_2\text{-Ph}$); -122.9 ppm ($\text{CF}_3\text{-CF}_2\text{-CF}_2\text{-CF}_2\text{-Ph}$); -111.0 ppm ($\text{CF}_3\text{-CF}_2\text{-CF}_2\text{-CF}_2\text{-Ph}$).



Scheme 4.6. Possible fragmentation of 4'-nonafluorobutyl styrene (3).

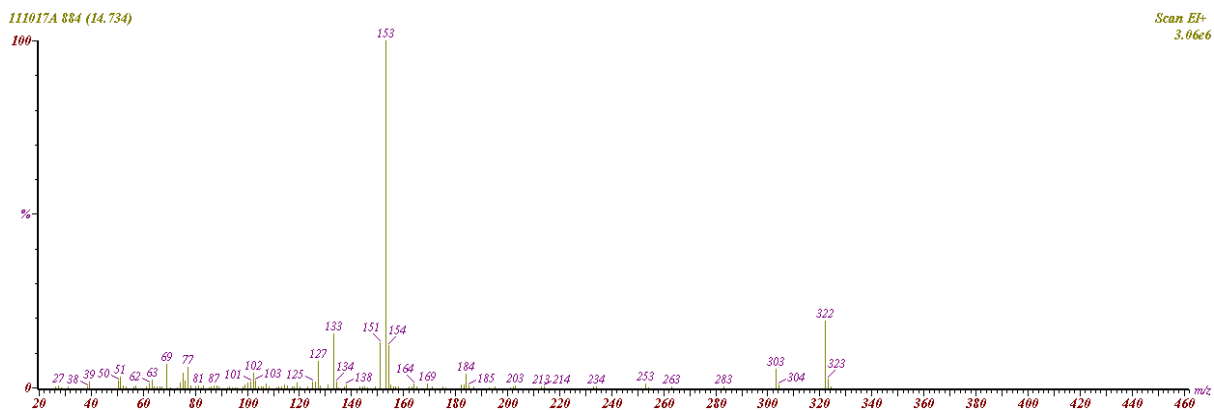


Figure 4.18. GC-MS spectrum of 4'-nonafluorobutylstyrene (3).

GC-MS measurement m/z (rel. ab. %): 322 ([M]⁺, 20%); 253 ([M-CF₃]⁺, 5%); 153 ([M-C₃F₇]⁺, 100%, 103 ([M-C₄F₉]⁺, 5%, 77 ([Ph]⁺, 15%).

Bibliography

- (1) Ameduri, B.; Boutevin B., *Telomerization of Fluoroalkenes*, in *Well-Architected Fluoropolymers: Synthesis and Applications*. 2004, Elsevier: Amsterdam. Chap. 1, p. 1-99.
- (2) Shafrin, E.G.; Zisman, W.A. *J. Phys. Chem.* **1960**, 64, 519-524.
- (3) Mahler, W.; Guillon, D.; Skoulios A. *Mol. Cryst. Liq. Cryst. Lett.* **1985**, 2, 111-119.
- (4) Russell, T.P.; Rabolt, J.F.; Twieg, R.J.; Siemens R.L. *Macromolecules* **1986**, 19, 1135-1143.
- (5) Viney, C.; Russell, T.P.; Depero, L.E.; Twieg R.J. *Liq. Cryst.* **1989**, 168, 63-82.
- (6) Iyengar, D.R.; Perutz, S.M.; Dai, C.A.; Ober, C.K.; Kramer E.J. *Macromolecules* **1996**, 29, 1229-1234.
- (7) Wang, J.; Mao, G.; Ober, C.K.; Kramer E.J. *Macromolecules* **1997**, 30, 1906-1914.
- (8) Mao, G.; Wang, J.; Clingman, S.R.; Ober, C.K.; Chen, J.T.; Thomas E.L. *Macromolecules* **1997**, 30, 2556-2557.
- (9) Genzer, J.; Sivaniah, E.; Kramer, E.J.; Wang, J.; Körner, H.; Xiang, M.; Yang, S.; Ober, C.K.; Char, K.; Chaudhury, M.K.; Dekoven, M.; Bubeck, R.A.; Fischer, D.A.; Sambavisan S. *Mater. Res. Soc. Symp. Proc.* **1998**, 524, 356-370.
- (10) Genzer, J.; Sivaniah, E.; Kramer, E.J.; Wang, J.; Körner, H.; Xiang, M.; Char, K.; Ober, C.K.; DeKoven, B.M.; Bubeck, R.A.; Chaudhury, M.K.; Sambavisan, S.; Fischer D.A. *Macromolecules* **2000**, 33, 1882-1887.
- (11) Genzer, J.; Sivaniah, E.; Kramer, E.J.; Wang, J.; Körner, H.; Char, K.; Ober, C.K.; DeKoven, B.M.; Bubeck, R.A.; Fischer, D.A.; Sambavisan S. *Langmuir* **2000**, 16, 1993-1997.
- (12) Li, X.; Andruzzi, L.; Chiellini, E.; Galli, G.; Ober, C.K.; Hexemer, A.; Kramer, E.J.; Fischer, D.A. *Macromolecules* **2002**, 35, 8078-8087.
- (13) Hare, E.F.; Shafrin, E.G.; Zisman, W.A. *J. Physic. Chem.* **1954**, 58, 236-239.
- (14) Key, B.D.; Howell, R.D.; Criddle, C.S. *Environ. Sci. Technol* **1997**, 31, 2445-2454.
- (15) Giesy, J.P.; Kannan, K. *Environ. Sci. Technol* **2002**, 36, 146-152.
- (16) Hansen, K.J.; Johnson, H.O.; Eldridge, J.S.; Butenhoff, J.L.; Dick, L.A. *Environ. Sci. Technol.* **2002**, 1681-1685.
- (17) Kannan, K.; Corsolini, S.; Falandysz, J.; Oehme, G.; Focardi, S.; Giesy J.P. *Environ. Sci. Technol* **2002**, 36, 3210-3216.
- (18) Butenhoff, J.L.; Kennedy, G.L.; Frame, S.R.; O'Connor, J.C.; York, R.G. *Toxicology* **2004**, 196, 95-116.
- (19) Kennedy, G.L.; Butenhoff, J.L.; Olsen, G.W.; O'Connor, J.C.; Seacat, A.M.; Perkins, R.G.; Biegel, L.B.; Murphy, S.R.; Farrar, D.G. *Crit. Rev. Toxicol* **2004**, 34, 351-384.
- (20) Kubwabo, C.; Vais, N.; Benoit F.M. *J. Environ. Monit.* **2004**, 6, 540-545.

- (21) Harada, K.; Saito, N.; Inoue, K.; Yoshinaga, T.; Watanabe, T.; Sasaki, S.; Kamiyama, S.; Koizumi A. *J. Occup. Health* **2004**, 46, 141-147.
- (22) Kannan, K.; Tao, L.; Sinclair, E.; Pastva, S.D.; Jude, D.J. ; Giesy J.P. *Arch. Environ. Contam. Toxicol.* **2005**, 48, 559-566.
- (23) Hinderliter, P.M.; Mylchreest, E.; Gannon, S.A.; Butenhoff, J.F.; Kennedy G.L. *Toxicology* **2005**, 139-148.
- (24) Emmett, E.A.; Shofer, F.S.; Zhang, H.; Freeman, D.; Desai, C.; Shaw, L.M. *J. Occup. Environ. Med.* **2006**, 48, 759-770.
- (25) Kostov, G.; Boschet, F.; Ameduri, B. *J. Fluorine Chem.* **2009**, 130 1192-1199.
- (26) Mc Loughlin, V.C.R.; Thrower, J. **1965**, Minister of Technology.
- (27) Mc Loughlin, V.C.R.; Thrower, J. *Tetrahedron* **1969**, 25, 5921-5940.
- (28) Chen, G.J.; Tamborsky, C. *J. Fluorine Chem.* **1989**, 43, 207-228.
- (29) Chen, J.; Chen, L.S.; Eapen K.C. *J. Fluorine Chem.* **1993**, 63, 113-123.
- (30) Chen, G.J.; Chen, L.S.; Eapen, K.C. *J. Fluorine Chem.* **1993**, 65, 59-65.
- (31) Banks, R.E.; Smart, B.E.; Tatlow, J.C., *Organofluorine Chemistry, Principles and Commercial Applications*. 1994, New York: Plenum Press.
- (32) Purser, S.; Moore, P.R.; Swallow, S.;Gouverneur V. *Chem. Soc. Rev.* **2008**, 37, 320-330.
- (33) Jeschke, P. *ChemBioChem* **2004**, 5, 570-589.
- (34) Thayer, A.M. *Chem. Eng. News* **2006**, 84, 15-24.
- (35) Muller, K.; Faeh, C.; Diederich, F. *Science* **2007**, 317, 1881-1886.
- (36) Kirk, K.L. *Org. Process Res. Dev.* **2008**, 12, 305-321
- (37) Kirsch, P.; Bremer, M. *Angew. Chem. Int. Ed.* **2000**, 39, 4216-4235.
- (38) Reiffenrath, V.; Krause, J.; Plach, H. J.; Weber, G. *Liq. Cryst.* **1989**, 5, 159-170.
- (39) Yoshino, N.; Sasaki, A.; Seto, T. *J. Fluorine Chem.* **1995**, 71, 21-29.
- (40) Kondo, Y.; Miyao, K.; Aya, Y.; Yoshino, N. *J. Oleo Sci.* **2004**, 53, 143-151.
- (41) Bravo, A.; Bjørsvik, H.; Fontana, F.; Liguori, L.; Mele, A.; Minisci, F. *J. Org. Chem.* **1997**, 62, 7128-7136.
- (42) Huang, X.-T.; Long, Z.-Y.; Chen, Q.-Y. *J. Fluorine Chem.* **2001**, 111, 107-113.
- (43) Knauber, T.; Arikan, F.; Roschenthaler, G.-V.; Gooßen, L.-J. *Chem. Eur. J.* **2011**, 17, 2689-2697.
- (44) Oishi, M.; Kondo, H.; Amii, H. *Chem. Comm.* **2009**, 14, 1909-1911.
- (45) V.C.R. Mc Loughlin, J. Thrower **1965**, Minister of Technology.
- (46) V.C.R. Mc Loughlin, J. Thrower *Tetrahedron* **1969**, 25, 5921-5940.
- (47) Stephens, R.D.; Castro, C.E. *J. Org. Chem.* **1963**, 28, 3313-3315.

Chapter 5. Polymerization of 4'-nonafluorobutyl styrene: surface and thermal characterizations of the resulting polymer

4'-nonafluorobutyl styrene is polymerized both by conventional radical polymerization and by iodine transfer polymerization in presence of 1-iodoperfluorohexane as iodinated chain transfer. The polymer obtained is characterized by NMR, TGA, GPC, DSC and surface analysis. Furthermore, a kinetic study is performed for the ITP of 4'-nonafluorobutyl styrene.

Synthesis of poly(4'-nonafluorobutyl styrene)

Literature reports only few examples of fluoroalkyl substituted styrene monomers¹ and most of them were polymerized by conventional²⁻⁴ or controlled⁵⁻⁹ radical polymerization (Table 5.1).

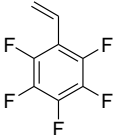
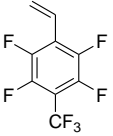
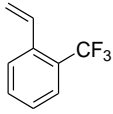
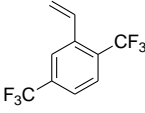
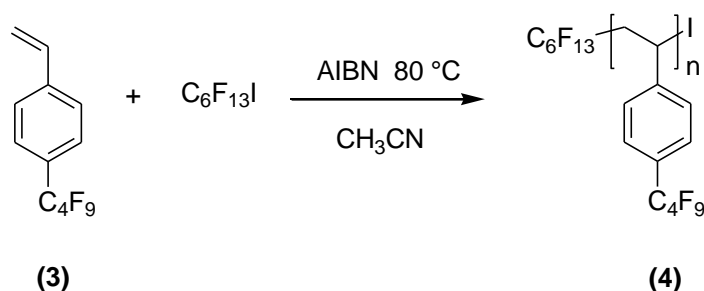
Monomer	polymerization	M _n	M _w /M _n	T _g [°C]	T _d [°C]	Ref.
	CONV.	470,000	1.83	107	420	3
	ATRP	11,400	1.21	95	436	5
	NMP	3,500	1.03	-	-	7
	CONV.	390,000	2.20	112	-	3
	CONV.	59,700	3.23	165	382	4
	CONV.	88,800	3.00	160	366	4

Table 5.1. Methods of radical polymerization (CONV. stands for conventional radical polymerization, ATRP stands for atom transfer radical polymerization, and NMP stands for nitroxy-mediated radical polymerization) and thermal properties and molecular weights of some fluorinated and fluoroalkyl styrene based-polymers.

To the best of our knowledge scarce fluorinated styrene monomers, e.g. 2,3,4,5,6-pentafluorostyrene, has been polymerized under ATRP^{5,10,11} or NMP⁷⁻⁹ only. However, no fluorinated styrene has been polymerized under degenerative transfer.

The conventional and controlled free-radical polymerizations of 4'-perfluorobutyl styrene have been investigated. First, the conventional radical polymerization was initiated by AIBN with an initial $[3]_0/[AIBN]_0$ molar ratio of 100, using acetonitrile as the solvent. Second, in iodine transfer polymerization of monomer (3), the initiator was required together with the iodine chain transfer agent (in the present case 1-iodoperfluorohexane was chosen) (Scheme 5.1).



Scheme 5.1. Iodine transfer polymerization of 4'-nonafluorobutyl styrene (3) in the presence of 1-iodoperfluorohexane as the chain transfer agent, initiated by AIBN.

That controlled radical polymerization was carried out in similar experimental conditions, but with the presence of 1-iodoperfluorohexane as the chain transfer, with $[3]_0/[AIBN]_0$ and $[3]_0/[C_6F_{13}I]_0$ initial molar ratios of 100 and 20, respectively. That reaction was simply carried out at atmospheric pressure and after purification the resulting poly(4'-nonafluorobutyl styrene) was characterized by spectroscopy and chromatography.

5.1.1 Materials

2,2' Azobisisobutyronitrile (AIBN), tetrahydrofuran (THF), methanol, acetonitrile (CH₃CN), diiodomethane (CH₂I₂) and toluene were purchased from the Aldrich Chemical Company. 1-Iodo-perfluorohexane was a gift from Elf Atochem. 4'-Nonafluorobutylacetophenone (1) was synthesized as in a previous chapter¹² from the cross coupling reaction of 1-iodoperfluorobutane with 4'-bromoacetophenone. All the solvents and reagents were used with a purity of 98-99%. AIBN was purified by recrystallization from methanol and dried under vacuum prior to use.

5.1.2 Radical polymerization of 4'-nonafluorobutyl styrene by conventional radical polymerization

The conventional radical polymerization of 4'-nonafluorobutyl styrene was carried out in a 50 mL two necked round flask equipped with a magnet bar, a rubber septum and a condenser

connected to argon source, and containing 10.1 mg ($1.02 \cdot 10^{-2}$ mol·L⁻¹) of AIBN, 2.00 g (1.03 mol·L⁻¹) of 4'-nonafluorobutyl styrene, and 4 mL of acetonitrile. The flask was evacuated and backfilled with argon for 20 minutes and 5 thaw-freeze cycles were applied prior to the polymerization. The reaction mixture was then placed in an oil bath, pre-heated at 80 °C for 270 minutes. Then, the solvent was removed by rotavapor, the residue was solubilized in minimum of THF and precipitated from a large excess of cold methanol. After filtration, the precipitated product was dried in a vacuum oven at 60 °C for 15 h and 1.00 g (yield 50%) of a white powder was obtained.

5.1.3 Radical polymerization of 4'-nonafluorobutyl styrene by iodine transfer polymerization

Iodine transfer polymerization of 4'-nonafluorobutyl styrene was carried out in the same conditions as above. The mixture was composed of 10.1 mg ($1.02 \cdot 10^{-2}$ mol·L⁻¹) of AIBN, 2.00 g (1.03 mol·L⁻¹) of 4'-nonafluorobutyl styrene, 138.0 mg ($5.15 \cdot 10^{-2}$ mol·L⁻¹) of 1-iodoperfluorohexane, 153.7 mg (0.26 mol·L⁻¹) of 1,2-dichloroethane and 4 mL of acetonitrile. After bubbling argon for 20 minutes, and 5 thaw-freeze cycles were applied, the reactant mixture was placed for 270 minutes in a oil bath pre-heated at 80 °C. The same purification procedure was adopted as above. Samples were periodically withdrawn from the medium during the polymerization to monitor the monomer conversion by ¹H and ¹⁹F NMR spectroscopy. The precipitated product was dried in vacuum oven at 60 °C for 15 h, 1.01 g (yield 50%) of white polymer was obtained.

Characterization

The average number of monomer units present in the final polymer was calculated by ¹⁹F NMR. In the case of iodine transfer polymerization (ITP), the ¹⁹F NMR spectrum (Figure 5.1), exhibits an overlapping between the signals assigned to CF₂ of the perfluorobutyl chain resulting from the monomer units and the signals of perfluorohexyl that belong to the chain transfer (C₆F₁₃I) moiety. However, the CF₃ end groups were the only ones to be distinguished by two different peaks: one centered at -82.14 ppm (signal *a*) assigned to the perfluorobutyl chain arising from the pendant styrene and that at -82.44 ppm (signal *m*) attributed to the CF₃ group resulting from the perfluorohexyl of the chain transfer agent. Hence, the integrals of these signals obtained from the ¹⁹F NMR spectrum enabled us to assess the average monomer units present in the polymer, as DP_n (Eq. 5.1).

$$DP_n = \frac{\left(\int_{Styrene} CF_3 - \int_{C_6F_{13}} CF_3 \right) + \sum \left(\int_{Styrene} CF_2 - \int_{C_6F_{13}} CF_2 \right)}{\text{number of fluorine atoms for each monomer unit (9)}} \quad \text{Eq. 5.1}$$

Where $\int_x CF_i$ stands for the integral of signal of CF_i in x unit (monomer or CTA).

Subtracting the values of the integrals assigned to the fluorinated moiety in the fluorinated pendant chains ($\int_{Styrene} CF_3$) from the integral of the peaks corresponding to the chain transfer agent ($\int_{C_6F_{13}} CF_3$) enabled us to obtain an average DP_n value of 8 monomeric units.

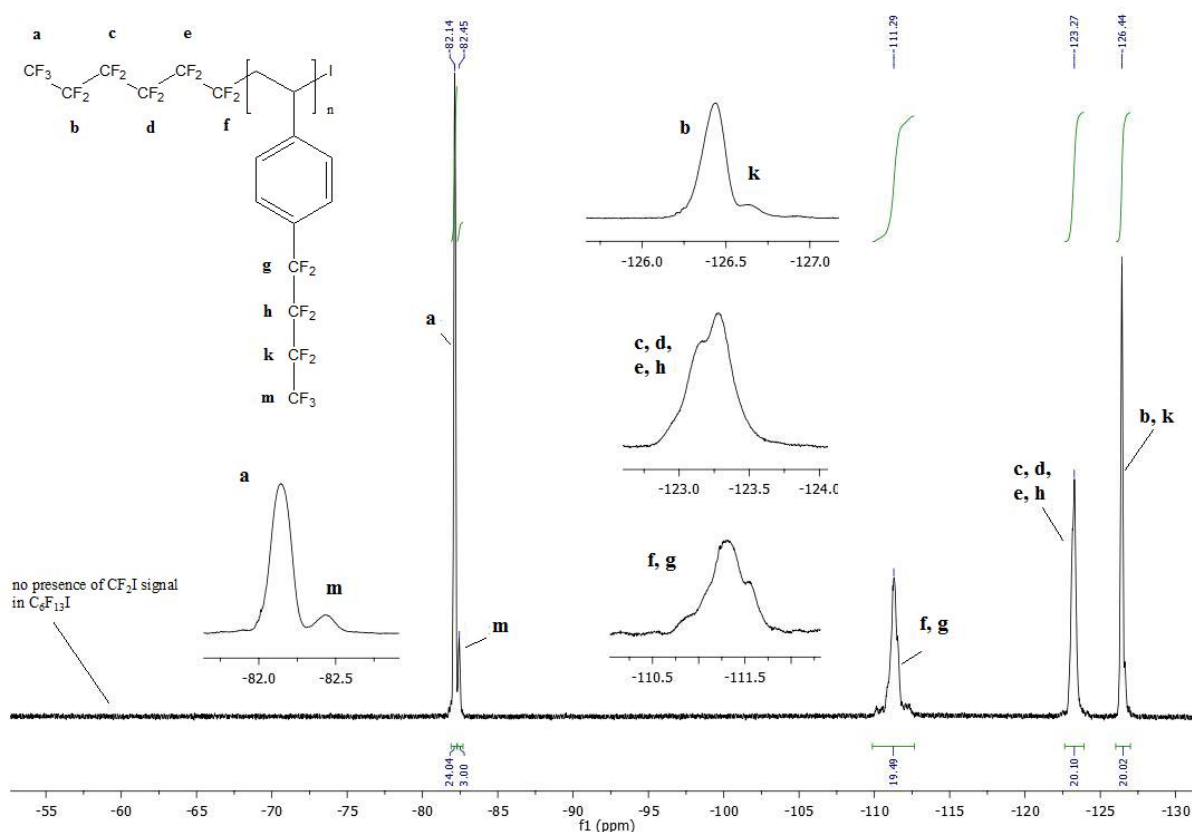


Figure 5.1. ^{19}F NMR spectrum of poly(4'-nonafluorobutyl styrene) synthesized by CRP (recorded in TDF), $[3]_0:[C_6F_{13}I]_0:[AIBN]_0=100:5:1$.

	M_n	PDI	T_d (10 %)
conventional	7400	1.30	305
controlled (ITP)	7500	1.15	305

Table 5.2. Values of the average molecular weight (M_n), polydispersity index (PDI) measured by GPC (gel permeation chromatography), and temperature of the thermal stability after 10% of the loss of the polymer (TGA), obtained by conventional and controlled radical polymerization of 4'-nonafluorobutyl styrene

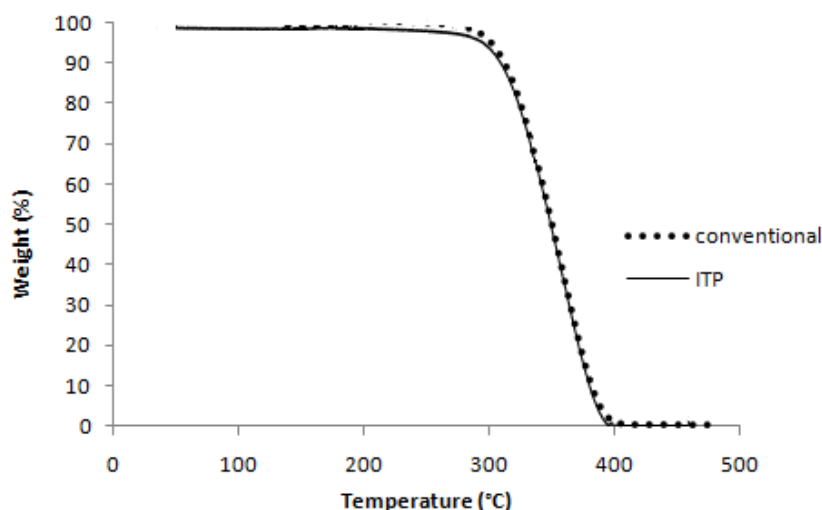


Figure 5.2. TGA thermograms of the polymer (under air) obtained by conventional and controlled radical polymerization of 4'-nonafluorobutyl styrene.

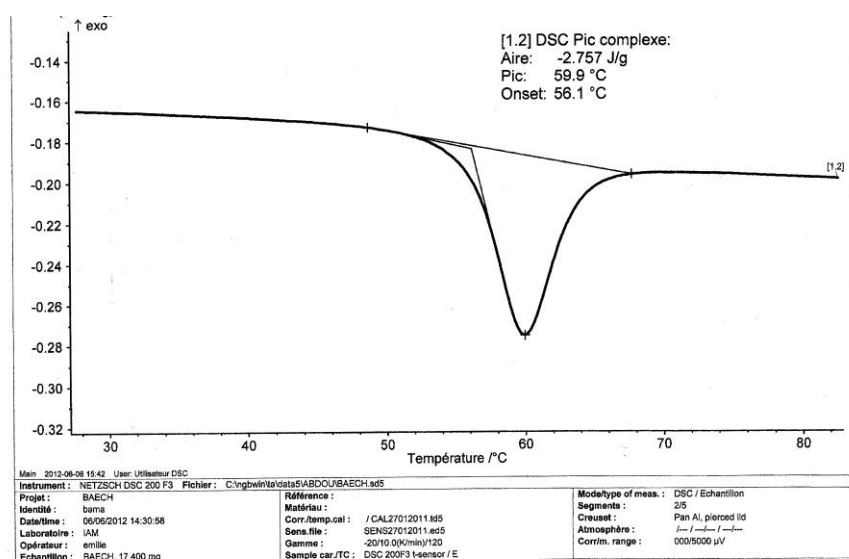


Figure 5.3. DSC spectrum of poly(4'-nonafluorobutyl styrene).

The values of polydispersity indices (PDI) are 1.30 for the conventional polymerization and 1.15 for the iodine transfer polymerization (ITP). The thermal stability (Figure 5.2) of the polymers was satisfactory (the 10% of the weight loss under air was achieved from 305 °C, Table 5.2) and the melting point (T_m) was 47 °C, as evidenced by the DSC chromatogram reported in Figure 5.3.

Kinetics of iodine transfer polymerization of 4'-nonafluorobutyl styrene (3)

The kinetics of radical homopolymerization of monomer (3) by ITP was monitored from the calculation of the integrals assessed from the ^1H NMR spectrum of 4'-nonafluorobutyl styrene. ^1H NMR spectroscopy was used to monitor the conversion (χ) using 1,2-dichloroethane as the internal standard. In fact, 1,2-dichloroethane was added to the reaction mixture as it exhibits a singlet at 3.66 ppm assigned to four equivalent protons (Figure 5.4).

When the polymerization reaction was carried out in the presence of acetonitrile as the solvent, the NMR spectrum does not exhibit the signals characteristic of the polymer but only those of the monomer, because the polymer precipitates when it is formed. However, these NMR spectra (Figure 5.4) enabled to monitor the fluorostyrene conversion *versus* time during ITP of 4'-nonafluorobutyl styrene.

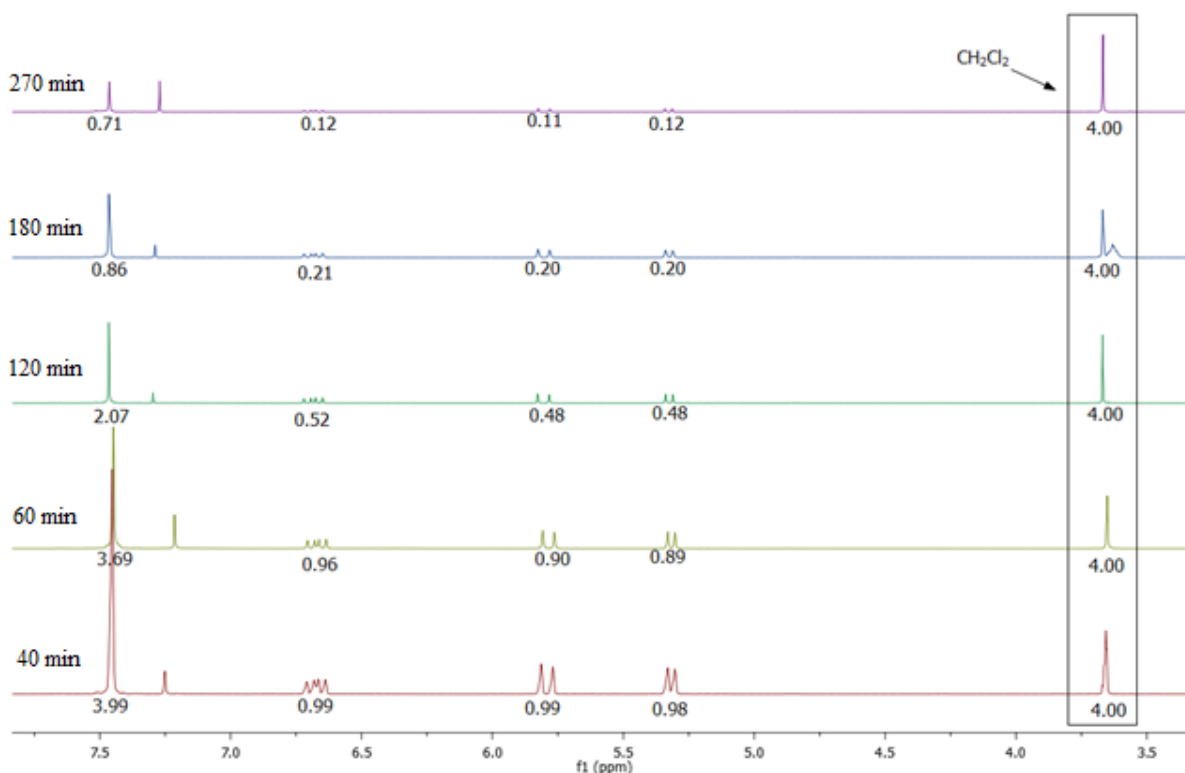


Figure 5.4. ^1H NMR spectra of samples from the controlled radical polymerization of 4'-nonafluorobutyl styrene in presence of $\text{C}_6\text{F}_{13}\text{I}$ after 40 min (bottom), 60 min, 90 min, 180 min and 270 min (top) of reaction (recorded in CDCl_3).

4'-Nonafluorobutyl styrene conversion (χ) was calculated according to Eq. 5.2.

$$\chi = \frac{[M]_0 - [M]}{[M]_0} * 100 \quad \text{Eq. 5.2}$$

Where $[M]_0$ and $[M]$ represent the initial concentration of (3) monomer and the concentration of the monomer at time t, respectively. Values of χ were assessed from the integrals of the signals of 4'-nonafluorobutyl styrene deduced from the ^1H NMR measurements (Eq. 5.3).

$$\chi = \frac{\left(\int_{7.3 \text{ ppm}}^{7.4 \text{ ppm}} C_6H_4 + \int_{6.6 \text{ ppm}}^{6.7 \text{ ppm}} CH + \int_{5.3 \text{ ppm}}^{5.8 \text{ ppm}} CH_2 \right)_{t=0} - \left(\int_{7.3 \text{ ppm}}^{7.4 \text{ ppm}} C_6H_4 + \int_{6.6 \text{ ppm}}^{6.7 \text{ ppm}} CH + \int_{5.3 \text{ ppm}}^{5.8 \text{ ppm}} CH_2 \right)_t}{\left(\int_{7.3 \text{ ppm}}^{7.4 \text{ ppm}} C_6H_4 + \int_{6.6 \text{ ppm}}^{6.7 \text{ ppm}} CH + \int_{5.3 \text{ ppm}}^{5.8 \text{ ppm}} CH_2 \right)_{t=0}} \quad \text{Eq. 5.3}$$

The results of the calculation of χ are reported in Table 5.3. The maximum of 4'-nonafluorobutyl styrene conversion was reached at 84.9 % after 270 minutes.

Time (min)	$[M]/[M]_0$	$([M]_0 - [M])/[M]_0$	$\ln ([M]_0/[M])$	$1 - \exp(-k_d * t/2)$	χ (%)
0	1	0	0	0	0.0
40	0.9929	0.0071	0.0072	0.1393	0.7
60	0.9200	0.0800	0.0834	0.2015	8.0
120	0.5071	0.4929	0.6790	0.3624	49.3
180	0.2100	0.7900	1.5606	0.4908	79.0
270	0.1514	0.8486	1.8876	0.6367	84.9

Table 5.3. Evolution of the 4'-nonafluorobutyl styrene conversion monitored by ^1H NMR spectroscopy ($[\text{monomer}]_0 : [\text{AIBN}]_0 : [\text{C}_6\text{F}_{13}\text{I}] = 100 : 1 : 5$ at 80°C).

Values of fractional conversion *versus* time are plotted in Figure 5.4, and showed no evidence of the Trommsdorf's effect.

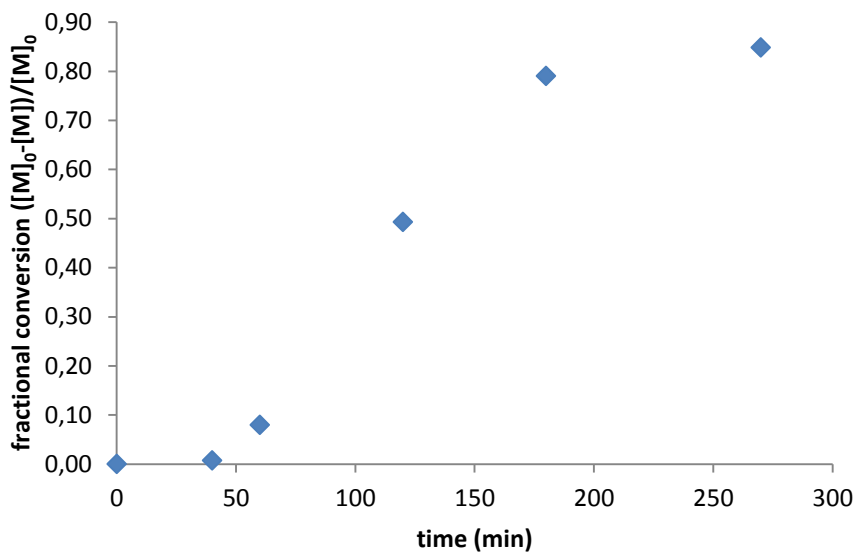


Figure 5.5. Fractional conversion of 4'-nonafluorobutyl styrene ($([M]_0/[M])/ [M]_0$) versus time for the controlled radical polymerization of 4'-nonafluorobutylstyrene (3) in the presence of 1-iodoperfluorohexane as the chain transfer agent ($[\text{monomer}]_0 : [\text{C}_6\text{F}_{13}\text{I}]_0 : [\text{AIBN}]_0 = 100: 5 :1$) at 80 °C.

The mechanism of free-radical polymerization^{13,14} requires that the polymerization rate be of first order with respect to the monomer and of half-order with respect to initiator concentration. Using the Tobolsky's equation¹⁵ (see appendix B):

$$\ln\left(\frac{[M]_0}{[M]}\right) = 2k_p \sqrt{\frac{f[I]_0}{k_d k_t}} \left(1 - e^{-\frac{k_d t}{2}}\right) \quad \text{Eq. 5.4}$$

and plotting the experimental values of $\ln\left(\frac{[M]_0}{[M]}\right)$ versus $\left(1 - e^{-\frac{k_d t}{2}}\right)$ enabled us to assess the value of the square of the propagation rate to the termination rate, k_p^2/k_t , (Figure 5.6) from the slope of the straight line¹⁶. For the determination of the value of k_p^2/k_t , considering the rate of decomposition of the initiator¹⁷, k_d (AIBN in acetonitrile at 80 °C) as $1.25 \cdot 10^{-4} \text{ s}^{-1}$ and the efficiency of the initiator¹⁵ (f) as 0.6.

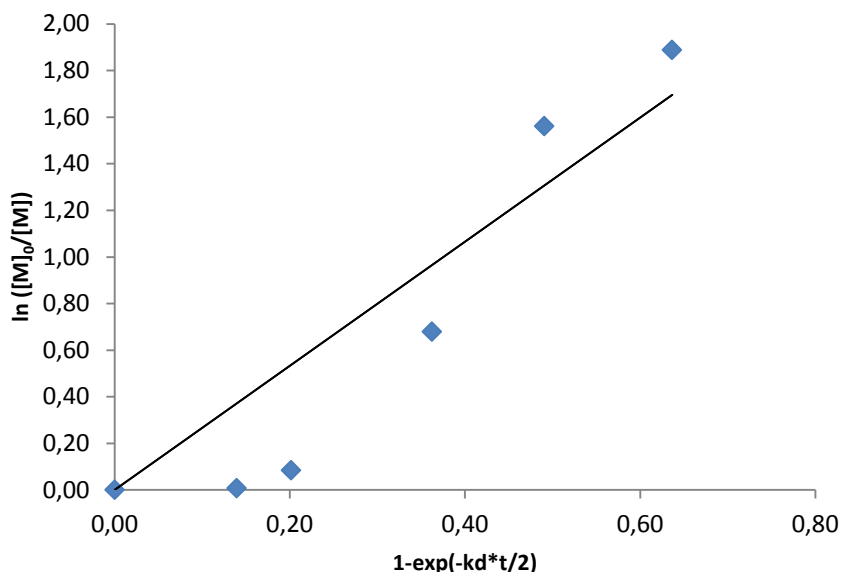


Figure 5.6. $\ln([M]_0/[M])$ versus $1-\exp(-k_d*t/2)$ for the controlled radical polymerization of 4'-nonafluorobutyl styrene initiated by AIBN at 80 °C, in the presence of $C_6F_{13}I$ as chain transfer agent. Slope = 2.6644.

The k_p^2/k_t value of 4'-nonafluorobutyl styrene obtained is $3.62 \cdot 10^{-2}$ ($L \text{ mol}^{-1} \text{ s}^{-1}$) at 80 °C. Table 5.4 lists k_p^2/k_t values for different styrenic monomers. Considering that is difficult to compare k_p^2/k_t values calculated from different surveys because the results can be influenced by temperature, the solvent and the initiator (as evidenced by the first three values obtained by the polymerization of styrene), it is found a higher k_p^2/k_t values respect to that of the others monomers.

Monomer	k_p^2/k_t ($L \text{ mol}^{-1} \text{ s}^{-1}$)	T(°C)	initiator	Ref.
Styrene	$8.37 \cdot 10^{-3}$	100	AIBN	15
Styrene	$3.84 \cdot 10^{-3}$	80	DTBP*	18
Styrene	$1.11 \cdot 10^{-3}$	60	DTBP*	18
Pentafluorostyrene	$2.96 \cdot 10^{-3}$	60	AIBN	19
4'-nonafluorobutyl styrene (3)	$3.62 \cdot 10^{-2}$	80	AIBN	This work
Vinylbenzyl chloride	$3.40 \cdot 10^{-3}$	80	AIBN	20
p-chlorostyrene	$2.92 \cdot 10^{-4}$	30	AIBN	21
p-methylstyrene	$1.70 \cdot 10^{-4}$	30	AIBN	21

Table 5.4. Values of k_p^2/k_t for different styrenic and fluorinated styrenic monomers.

*DTBP stands for di *t*-butyl peroxide.

Contact angle assessment

Polymers surface morphology affects their surface properties²²⁻²⁵. One of the most important property of fluoropolymers is the hydro- and oleophobicity^{26,27} which can be assessed by contact angle measurements between solid and liquid interfaces. Spontaneous spreading of a solvent (water or diiodomethane) onto the surface of a polymer film has been studied with the sessile drop method (see Chapter 1, appendix A). Three different types of contact angles can be measured: i) static contact angle, θ_s (a drop is produced before the measurements and has a constant volume during the experiment), ii) advancing contact angle, θ_a (the mean of the contact angle measurements during the advancing of the liquid boundary over a dry clean surface), and iii) receding contact angle, θ_r (the mean of the contact angle values measured during the retreating of the liquid boundary over a previously wetted surface). The contact angle hysteresis is defined as the difference between the advancing and the receding angles ($\Delta\theta = \theta_a - \theta_r$)²⁸.

Advancing and receding contact angles are determined by the needle-syringe method using a stainless steel needle connected with an automatically microliter syringe (diameter of the needle 0.5 mm). Solvent introduction and withdrawal are monitored by a video camera that recorded the profile during the process. All calculation methods are based on the sessile drop method, while the surface energies calculation are assessed by the Owens-Wendt method²⁹.

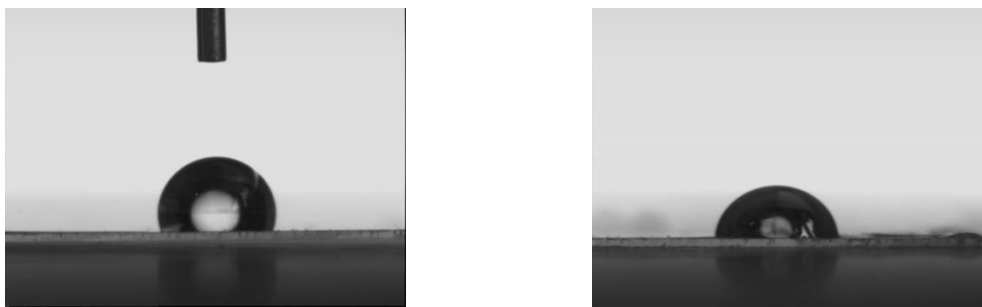


Figure 5.7. Drops of water (left, $\theta = 110^\circ \pm 1^\circ$) and diiodomethane (right, $\theta = 85^\circ \pm 1^\circ$) deposited on a surface treated with a poly (4'-nonafluorobutyl styrene) polymerized by ITP.

Values of static contact angles are calculated for water and diiodomethane drops on the surface of a glass spin-coated with poly(4'-nonafluorobutyl styrene) (Figure 5.7), to calculate the surface tension of the solid. Measurements were achieved onto coatings of polymers obtained both by conventional and controlled radical polymerization of 4'-nonafluorobutyl styrene. A comparison between them is reported in Table 5.5. Polymers achieved by controlled radical polymerization showed a water and diiodomethane static contact angle of $110^\circ \pm 1^\circ$ and $85^\circ \pm 1^\circ$ respectively, while for that obtained by conventional method, the static contact angles were $103^\circ \pm 1^\circ$ and $84^\circ \pm 1^\circ$, respectively.

Static contact angles of a surface spin-coated with poly(4'-nonafluorobutyl styrene) are comparable with those obtained by Takahara's team with *poly(2-perfluorooctyl-ethyl acrylate)*³⁰. It is important to underline that poly(2-perfluorooctyl-ethyl-acrylate) have four -CF₂- units more than poly(4'-nonafluorobutyl) styrene. The total surface energy of poly(4'-nonafluorobutyl styrene) synthesized by conventional radical polymerization calculated by the Owens and Wendt equation²⁹ is $18 \pm 2 \text{ mN}\cdot\text{m}^{-1}$. The polymer obtained by ITP, has a value of the surface energy of $15 \pm 2 \text{ mN}\cdot\text{m}^{-1}$.

	PDI	water contact angle (degree)	CH ₂ I ₂ contact angle (degree)	polar part (mN/m)	disperse part (mN/m)	surface tension (mN/m)
poly(4'-nonafluorobutyl styrene)	1.30	103 ± 1	84 ± 1	3 ± 1	15 ± 1	18 ± 2
	1.15	110 ± 1	85 ± 1	1 ± 1	14 ± 1	15 ± 2
poly(2-perfluorooctyl-ethyl acrylate) ³⁰	1.86	122	99	-	-	7.7
	1.05	115	103	-	-	9.4

Table 5.5. Comparison between the static contact angle measurements and surface tension of poly(4'-nonafluorobutylstyrene) and poly(2-perfluorooctyl-ethyl acrylate)³⁰ with broad and narrow PDI, achieved by conventional and controlled radical polymerization, respectively.

These results underline that ITP process improves not only the PDI but also the hydro- and oleophobicity of the polymer. Yamaguchi et al.³⁰ compared the surface properties of poly(2-perfluorooctyl-ethyl acrylate) with broad ($M_w/M_n = 1.86$) and narrow ($M_w/M_n = 1.05$) polydispersity indices synthesized by surface-initiated ATRP on a flat silicon substrate. These authors found that contact angle hysteresis strongly depended on the PDI of such fluoropolymers. Conversely, no significant differences were noted between static contact angles assessed on poly(2-perfluorooctyl-ethyl acrylate) with broad and narrow PDI. The relationship between PDI values and surface free energy for poly(4'-nonafluorobutyl styrene) is in agreement with that obtained by Takahara's group for poly(2-perfluorooctyl-ethyl acrylate) (Table 5.6).

	PDI	θ_a^a (degree)	θ_r^b (degree)	hysteresis ^c (degree)
poly(4'-nonafluorobutyl styrene)	1.30	102 ± 1	84 ± 1	18° ± 2
	1.15	113 ± 1	66 ± 1	47° ± 2
poly(2-perfluorooctyl-ethyl acrylate) ³⁰	1.86	128	105	23
	1.05	115	80	35

Table 5.6. Comparison between the dynamic water contact angle measurements of poly(4'-nonafluorobutylstyrene) and poly(FA-C8) with narrow and broad PDI.

^a θ_a = advancing contact angle, ^b θ_r = receding contact angle, ^c hysteresis = $\theta_a - \theta_r$.

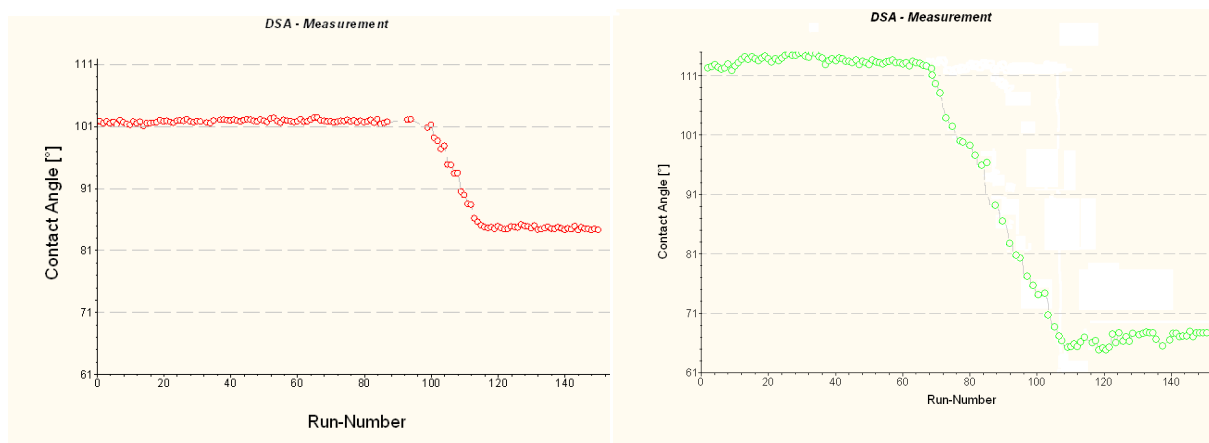


Figure 5.8. Advancing and receding water contact angle values assessed with water drop on surface spin-coated with poly(4'-nonafluorobutyl styrene) surface synthesized by conventional radical (left) and iodine transfer polymerization (right).

Values of advancing and receding water contact angles are reported in Figure 5.8. In the case of broad PDI of poly(4'-nonafluorobutyl styrene), the mean advancing contact angle (θ_a) was $102^\circ \pm 1^\circ$, while the average receding contact angle (θ_r) was $84^\circ \pm 1^\circ$ with a hysteresis of $18^\circ \pm 2^\circ$. Instead, in the case of narrow PDI the poly(4'-nonafluorobutyl styrene) mean advancing contact angle (θ_a) reached $113^\circ \pm 1^\circ$, while mean receding contact angle (θ_r) was $66^\circ \pm 1^\circ$ with an hysteresis of $47^\circ \pm 2^\circ$. In conclusion, water repellency of poly(4'-nonafluorobutyl styrene) is strongly influenced by the PDI value. In analogy with the work reported by other authors^{30,31}, the relationship between the aggregation state of the fluorinated chains and PDI should deserve to be further investigated.

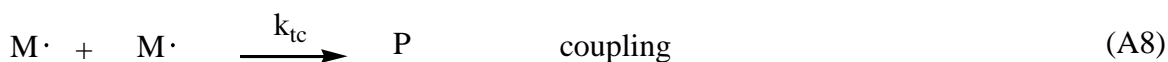
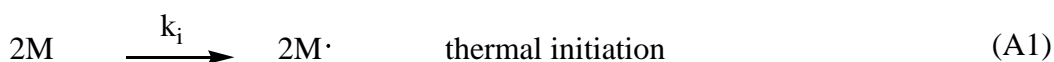
Conclusion

For the first time, the iodine transfer polymerization (ITP) of 4'-nonafluorobutyl styrene controlled by 1-iodoperfluorohexane has been reported and compared to the conventional radical one. As expected, polymers obtained by ITP displayed more narrow polydispersity index (PDI = 1.13) than those achieved from the conventional radical polymerization (PDI = 1.30). The thermal stability of the polymers was satisfactory, and the 10% of the weight loss under air was achieved from 305 °C. The kinetic of radical homopolymerization enabled us to assess the k_p^2/k_t value ($3.62 \cdot 10^{-2} \text{ L} \cdot \text{mol}^{-1} \cdot \text{sec}^{-1}$ at 80 °C). Measurements of the static contact angles in the presence of water and diiodomethane, and dynamic contact angles, in the presence of water were performed on spin-coated surfaces with poly(4'-nonafluorobutyl styrene) achieved from both strategies. Values of contact angles evidenced the satisfactory hydro- and oleophobicity of the polymers synthesized, and no significant differences were

detected by the static contact angles between the polymer synthesized by ITP and that obtained by conventional radical polymerization with a surface tension of $15 \pm 2 \text{ mN}\cdot\text{m}^{-1}$ and $18 \pm 2 \text{ mN}\cdot\text{m}^{-1}$, respectively. Conversely, an increase of hysteresis in polymer with lower polydispersity index ($47^\circ \pm 2^\circ$) compared to those with higher PDI ($18^\circ \pm 2^\circ$) was observed. The results obtained suggest a strong correlation between PDI values and surface properties of poly(4'-nonafluorobutyl styrene). The influence of the PDI onto the molecular aggregation state and the fluorinated groups should be further investigated. However, the hydro- and oleophobicity of poly(4'-nonafluorobutyl styrene) are comparable with those of polyperfluoroacrylate with longer perfluorinated chains. This comparison evidenced the ability of the phenyl rings to form an efficient structure and candidate the poly(4'-nonafluorobutyl styrene) as an alternative to long perfluorinated coatings.

Appendix B: the Tobolsky's equation

The general mechanism of the free radical polymerization is reported in Scheme 5.2¹³. The monomer is indicated as (M). The monomer radical (M·) could be formed by thermal initiation (A1) or, in a second way by addition of radicals. In the former case, the radicals (2R·) are originated by the decomposition of the initiator (I) (A2).



Scheme 5.2. General mechanism of free radical polymerization.

The radicals formed can recombine by a first order reaction (A3) or react with the monomer and initiate the polymer chains (A4). The initiator efficiency factor (f) is determined by the fraction of radical produced by the primary cleavage of the initiator that start the polymer chains (Eq. 5.5).

$$f = \frac{k_a[2R\cdot][M]}{k_r[2R\cdot] + k_a[2R\cdot][M]} = \frac{1}{\frac{k_r}{k_a[M]} + 1} \quad \text{Eq. 5.5}$$

Once the radical monomer (M·) is formed it can react with a monomer (M) starting the propagation reaction (A5). The termination reaction can occur by disproportionation (A7) or by coupling reaction (A8). The mechanism of free-radical polymerization requires that the polymerization rate be first order with respect to monomer and half-order with respect to

initiator concentration¹⁴. A6 and A9 represents the chain transfer reaction with the monomer and with the initiator respectively.

Assuming steady state assumption:

$$[M \cdot] = \sqrt{\frac{k_i[M]^2 + k_d f[I]}{k_{td} + k_{tc}}} \quad \text{Eq. 5.6}$$

The rate of polymerization is:

$$-\frac{d[M]}{dt} = k_p[M \cdot][M] = k_p[M \cdot] \sqrt{\frac{k_i[M]^2 + k_d f[I]}{k_{td} + k_{tc}}} \quad \text{Eq. 5.7}$$

If we are disregarding the polymer produced by thermal polymerization, Eq. 5.7 can be rewritten as:

$$-\frac{d[M]}{dt} = k_p[M \cdot] \sqrt{\frac{k_d f[I]}{k_{td} + k_{tc}}} \quad \text{Eq. 5.8}$$

If we put the sum of the specific rates of combination and diproportionation as:

$$k_t = k_{td} + k_{tc} \quad \text{Eq. 5.9}$$

and the rate of disappearance of the initiator:

$$-\frac{d[I]}{dt} = k_d[I] \quad \text{Eq. 5.10}$$

Integrating from the initial concentration of the initiator $[I]_0$ and if the initiator is all added at the beginning of the polymerization, one obtains:

$$[I] = [I]_0 e^{-k_d t} \quad \text{Eq. 5.11}$$

Substituting Eq. 5.11 into Eq. 5.8 and integrating we obtain the Tobolsky's equation¹⁵:

$$\ln\left(\frac{[M]_0}{[M]}\right) = 2k_p \sqrt{\frac{f[I]_0}{k_d k_t}} \left(1 - e^{-\frac{k_d t}{2}}\right) \quad \text{Eq. 5.12}$$

Plotting the experimental values of $\ln\left(\frac{[M]_0}{[M]}\right)$ versus $\left(1 - e^{-\frac{k_d t}{2}}\right)$ is possible to extrapolate the value of k_p^2/k_t from the slope of the straight line.

Bibliography

- (1) Wadekar, M.N.; Jager, F.J.; Sudholter, E.J.R.; Picken, S.J. *J. Org. Chem.* **2010**, *75*, 6814-6819.
- (2) Bachman, G.B.; Lewis, L.L. *J. Am. Chem. Soc.* **1947**, *69*, 2022-2025.
- (3) Lou, L.; Koike, Y.; Okamoto, Y. *J. Polym. Sci. Part A Polym. Chem.* **2010**, *48*, 4938-4932.
- (4) Teng, H.; Lou, L.; Koike, K.; Koike, Y.; Okamoto Y. *Polymer* **2011**, *52*, 949-953.
- (5) Jankova, K.; Hvilsted, S. *Macromolecules* **2003**, *36*, 1753-1758.
- (6) Hansen, N.M.L.; Jankova, K.; Hvilsted, S. *Eur. Polym. J.* **2007**, *43*, 255-293.
- (7) Remzi, B.C.; Babiuch, K.; Pilz, D.; Hornig, S.; Heinze, T.; Gottschaldt, M.; Schubert U.S. *Macromolecules* **2009**, *42*, 2387-2394.
- (8) Remzi, B.C.; Hoogenboom, R.; Schubert, U.S. *Angew. Chem. Int. Ed.* **2009**, *48*, 4900-4908.
- (9) Riedel, M.; Stadermann, J.; Komber, H.; Voit, B. *Polymer Preprints* **2011**, *52*, 642-643.
- (10) Suzuki, S.; Whittaker, M.R.; Wentrup-Byrne, E.; Monteiro, M.J.; Grondahl, L. *Langmuir* **2008**, *24*, 13075-13083.
- (11) Gudipati, C.S.; Tan, M.B.H.; Hussain, H.; Liu, Y.; He, C.; Davis, T.P. *Macromol. Rapid Commun.* **2008**, *29*, 1902-1907.
- (12) Ceretta, F.; Zaggia, A.; Conte, L.; Ameduri, B. *J. Fluorine Chem.* **2012**, *135*, 220-224.
- (13) Mayo, F. R.; Gregg, R. A.; Matheson, M. S. *J. Am. Chem. Soc.* **1951**, *73*, 1691-1700.
- (14) Senogles, E.; Woolf, L. A. *J. Chem. Educ.* **1967**, *44*, 157-159.
- (15) Tobolsky, A. V. *J. Am. Chem. Soc.* **1958**, *80*, 5927-5929.
- (16) Guyot, B.; Ameduri, B.; Boutevin, B.; Melas, M.; Viguier, M.; Collet, A. *Macromol. Chem. Phys.* **1998**, *199*, 1879-1885.
- (17) Kochi, J.K.; Mog, D.M. *J. Am. Chem. Soc.* **1965**, *87*, 522-528.
- (18) Pryor, W.A.; Lee, A.; Witt, C.E. *J. Amer. Chem. Soc.* **1964**, *86*, 4229-4234.
- (19) Pryor, W.A.; Huang, T.-L. *Macromolecules* **1969**, *2*, 70-77.
- (20) Couture, G.; Ameduri, B. *Eur. Polym. J.* **2012**, *48*, 1348-1356.
- (21) Boyer, C.; Bousquet, A.; Rondolo, J.; Whittacker, M.R.; Stenzel, M.H.; Davis, T.P. *Macromolecules* **2010**, *43*, 3775-3784.
- (22) Schonhorn, H. *Macromolecules* **1968**, *1*, 145-151.
- (23) Katano, Y.; Tomono, H.; Nakajima, T. *Macromolecules* **1994**, *27*, 2342-2344.
- (24) Hikita, M.; Tanaka, K.; Nakamura, T.; Kajiyama, T.; Takahara, A. *Langmuir* **2004**, *20*, 5304-5310.

- (25) Yokohama, H.; Tanaka, K.; Takahara, A.; Kajiyama, T.; Sugiyama, K.; Hyrao, A. *Macromolecules* **2004**, 37, 939-945.
- (26) Ameduri, B.; Boutevin, B., *Well Architected Fluoropolymers: Synthesis, Properties and Applications*. 2004, Elsevier: Amsterdam.
- (27) Banks, R.E.; Smart, B.E.; Tatlow, J.C., *Organofluorine Chemistry: Principles and Commercial Applications*. 1994, Plenum Press: New York. pp. 339-372.
- (28) Erbil, H. Y.; McHale, G.; Rowan, S. M.; Newton, M. I. *Langmuir* **1999**, 15, 7378-7385.
- (29) D.K. Owens, R.C. Wendt *J. Appl. Polym. Sci.* **1969**, 13, 1741-1747.
- (30) Yamaguchi, H.; Kikuchi, M.; Kobayashi, M.; Ogawa, H.; Masunaga, H.; Sakata, O.; Takahara, A. *Macromolecules* **2012**, 45, 1509-1516.
- (31) Honda, K.; Morita, M.; Otsuka, H.; Takahara, A. *Macromolecules* **2005**, 38, 5699-5705.

Chapter 6. Telomerization of VDF in presence of CF₃I and C₄F₉I as chain transfer agents

Polyvinylidene fluoride (PVDF) exhibits various interesting properties¹⁻⁵ such as chemical inertness, resistance to acids, piezo- and pyroelectrical properties. Further, PVDF has found applications in the semiconductor industry^{6,7}, nuclear industry⁸, in paints and coatings⁹, mechanical substrates for fuel cells membranes^{4,10}, elastomers for gaskets in space shuttles¹⁰. VDF-containing telomers are valuable products as perfluorooctanoate surfactant substituents, precursors of hybrid silicones¹¹, and original thermoplastic elastomers^{4,10}. In literature there are several examples of radical telomerisation of VDF by different chain transfer agents (CTA)⁴. In particular, the use of perfluoroalkyl iodides (C_nF_{2n+1}I)¹²⁻¹⁶ exhibit high transfer constants and produce VDF telomers with the iodine as terminal group that can be used for further functionalizations¹⁷.

In this chapter the telomerisation of VDF by Iodine Transfer Polymerization (ITP) in presence of CF₃I as chain transfer is presented. *Tert*-butyl peroxyvalate (TBPP) is used as initiator, that is commonly used in this kind of reactions. *Bis*(4-*tert*-butylcyclohexyl)peroxydicarbonate (Perkadox[®] 16s) as alternative initiator is also tested.

Furthermore, telomerisation of VDF in presence of C₄F₉I as chain transfer agent and TBPP as initiator is carried out. The telomer C₄F₉-(VDF)₂-I was used to synthesize the alcohol C₄F₉-CH₂CF₂-CH₂CF₂-CH₂-CH₂-CH₂-OH, an important intermediate for the synthesis of fluorinated acrylates.

Introduction

There are many examples of the reactivity of radicals with olefins reported in literature. According to Tedder and Walton^{18,19}, “*no simple property can be used to determine the orientation of addition of radicals*”, which depends on polar and steric parameters and on bond strengths. The efficiency of the telomerisation process is influenced by the cleavage of a specie bearing a weak X-Y bond, called telogen. The bond dissociation energy (BDE) of the telogen X-Y (yielding X· and Y· radicals) has to be taken in account as an indicator of its intrinsic reactivity. The C-F bond is the most difficult to cleave whereas -CF₂-I group has a better chance to be cleaved²⁰ (Table 6.1). Considering the ability of telogens to initiate the telomerisation, the reactivity and the regioselectivity of the telogen radical X· toward the olefin is driven by precise rules. Usually, fluoroalkenes are regarded as electron poor olefins, and thus they easily react with nucleophilic radicals⁴. Walton *et al.* studied the kinetics of several radicals such as ·CH₃²¹, Br₃C²², CH₂I²³, CFHI²⁴, C₂F₅, CF₃(CF₂)_n (n = 6,7)²⁵, to specific site of unsymmetrical fluoroalkenes.

R_FI	BDE [kJ · mol⁻¹]
CF ₃ I	220
C ₂ F ₅ I	212
n-C ₃ F ₇ I	206
i-C ₃ F ₇ I	206
n-C ₄ F ₉ I	202

Table 6.1. Bond dissociation energies (BDE) of some R_FI.

They determined the rate constants of these radicals to both sites of these olefins and the corresponding Arrhenius parameters. Results were mainly correlated to the electrophilicity of radicals which add more easily to nucleophilic alkenes: more electrophilic the radical (i.e. the more branched the perfluoroalkyl radical), the more selective the addition to the -CH₂- site (Table 6.2).

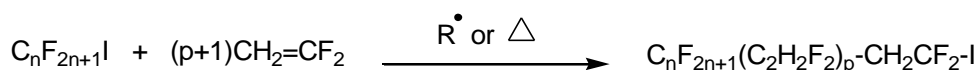
Radicals	CH₂=CF₂	
CH ₂ F	1	0.440
CHF ₂	1	0.150
CF ₃	1	0.032
CF ₂ CF ₃	1	0.011
CF ₂ CF ₂ CF ₃	1	0.009
CF(CF ₃) ₂	1	0.001

Table 6.2. Probabilities of addition of chloro- and fluororadicals to both sites of VDF.

Chambers et al.²⁶ suggested the following reactivity series about VDF: CF₃I < C₂F₅I < n-C₃F₇-I < i-C₃F₇-I mainly linked to the decrease of strength of the C-I bond.

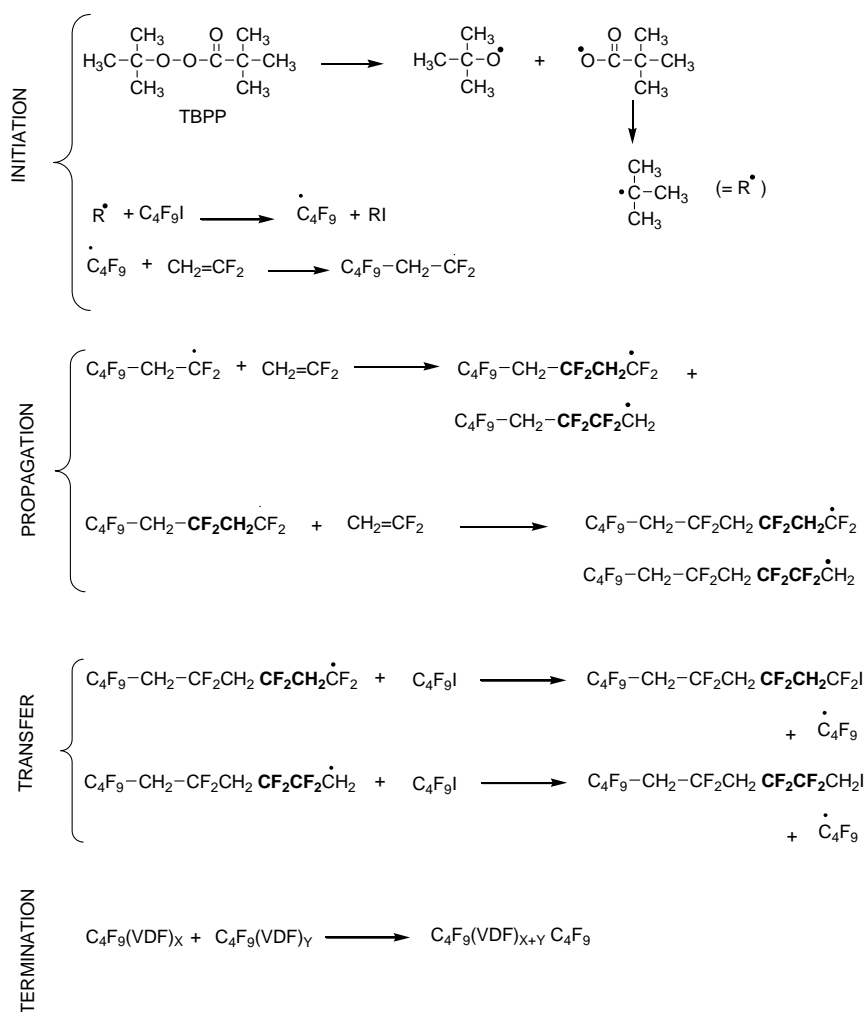
The mechanism of the telomerisation of VDF

In Scheme 6.1 the iodine transfer polymerization of VDF, in presence of 1-perfluoroalkyl iodide as chain transfer is presented.



Scheme 6.1. Iodine transfer polymerization of vinylidene fluoride in the presence of 1-iodoperfluoroalkane

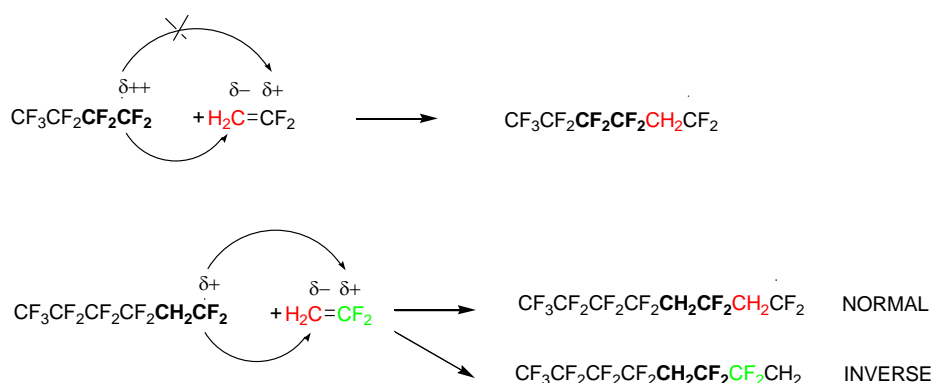
The mechanism of the telomerisation of VDF in presence of C_4F_9I as chain transfer agent, and TBPP as initiator is reported in Scheme 6.2 and it is chosen as example to explain the evolution of the reaction.



Scheme 6.2. Mechanism of telomerisation of VDF in presence of C_4F_9I as chain transfer agent and TBPP as initiator.

In the initiation step the initiator, in this case TBPP, is thermally decomposed and it forms the radical specie $R\cdot$ which reacts with the chain transfer agent (C_4F_9I), breaking the C-I bond to form the perfluoroalkyl radical $C_4F_9\cdot$. The latter attacks the double bond of the VDF monomer to give the $C_4F_9-CH_2-CF_2\cdot$ radical.

Chambers^{26,27} confirmed that the monoadduct coming from the radical addition of $R_F\cdot$ to VDF is composed of two isomers $R_F-CH_2CF_2I$ (95 %) and $R_F-CF_2CH_2I$ (5 %). However, recent 1H NMR and ^{19}F NMR investigation demonstrate that $C_4F_9-CH_2-CF_2-I$ is the only isomer produced by thermal telomerization of the VDF from the corresponding transfer agent^{4,28} (Scheme 6.3) and the radical (called head-to-head) $C_4F_9-CF_2-CH_2\cdot$ in this case is not detected.



Scheme 6.3. Electrophilic attack of the $C_4F_9\cdot$ and $C_4F_9CH_2CF_2\cdot$ radicals onto VDF monomer.

Conversely, when in the propagation step the radical $C_4F_9-CH_2-CF_2\cdot$ reacts again with the VDF monomer, both the head-to-head and head-to-tail species are formed. This behavior could be explained considering the effect of the electronegativity of the fluorinated groups, that in the case of two or more consecutives CF_2 groups is greater than in the case of alternate CH_2-CF_2- groups and oriented the attack on the hydrocarbon moiety of the VDF monomer. In conclusion, in this kind of reaction, the absence of head-to-head species (also called defects) in the chain, is possible only with one unit of monomer inside the telomer chain ($C_4F_9-(CH_2CF_2)-I$). The termination of the chain can be accomplished into two ways: by coupling two radicals, or by a transfer process in which the growing radicals react with the chain transfer agent in order to form a new radical $C_4F_9\cdot$ and the telomer $C_4F_9-(VDF)_n-I$. Furthermore, the higher the temperature, the higher the $[R_F I]/[VDF]$ initial molar ratio, the more selective the telomerization²⁸⁻³¹ is.

The telomerization of vinylidene fluoride with iodinated telogens has been carried out with two initiators: *tert*-butyl peroxyvalate (TBPP) and *bis*(4-*tert*-butylcyclohexyl)peroxydicarbonate (Perkadox[®] 16s).

The physical properties of the initiators are summarized in Table 6.3.

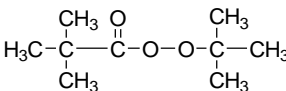
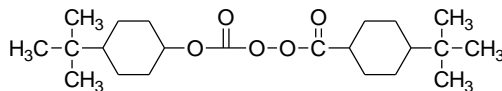
	 TBPP	 Perkadox[®] 16s
molecular weight [g·mol⁻¹]	174.2	398.5
appearance	solution of isodecane	white powder
density [g·cm⁻³]	0.875	0.113
half-life [°C] (0.1 hour)	94	82
half-life [°C] (1.0 hour)	75	64
half-life [°C] (10 hour)	57	48

Table 6.3. TBPP and Perkadox[®] 16s properties.

Telomerization of VDF with R_{FI} as chain transfer

6.1.1 Materials and methods

Vinylidene fluoride (VDF), and CF₃I were kindly donated by Solvay, acetonitrile and n-pentane were supplied by Aldrich. Acetonitrile was distilled over calcium hydride and then degassed from an argon flow for 10-15 minutes, prior to use. The initiators *tert*-butyl peroxyvalate (TBPP) and *bis*(4-*tert*-butylcyclohexyl)peroxydicarbonate (Perkadox[®] 16s) were purchased by Aldrich and Akzo Nobel respectively.

The conversion χ of VDF was calculated as:

$$\chi = \frac{m_{VDF}^0 - \Delta m}{m_{VDF}^0} \quad \text{Eq. 6.1}$$

Where m_{VDF}^0 is the quantity of VDF (and CF₃I in the case it is used as chain transfer) initially filled in the autoclave, and Δm is the quantity of the unreacted VDF (and CF₃I if used as chain transfer agent, because it is gaseous instead C₄F₉I).

The yield η of the telomer synthesized is calculated as:

$$\eta = \frac{m_{tot}}{m_{VDF}^0 + m_{RFI}^0} \quad \text{Eq. 6.2}$$

Where m_{tot} is the total amount of telomer synthesized and m_{RFI}^0 is the quantity of perfluorinated iodine initially introduced into the autoclave.

The characteristic properties of the telomers were calculated by the integrals of the signals measured by ^{19}F NMR spectroscopy. In particular, the mean degree of polymerization (DP_n) was calculated as:

$$DP_n = \frac{3}{2} \frac{\sum \int(CF_2)}{\sum \int(CF_3)} \quad \text{Eq. 6.3}$$

Where $\int(CF_2)$ and $\int(CF_3)$ represents the values of the integral corresponding to the signals of the fluorine in the CF_2 and CF_3 groups respectively.



Figure 6.1. The autoclave used for the telomerisation process.

6.1.2 Telomerization of VDF using TBPP as initiator

The reaction was carried out in 100 mL Hastelloy autoclave (Figure 6.1) equipped with inlet and outlet valves, a manometer, and a rupture disk, where were placed 1.30 g (7.5 mmol) of *tert*-butyl peroxyvalate (TBPP) and 20 mL of acetonitrile, and 20 mL of 1,1,1,3,3-pentafluorobutane as solvent. Then the autoclave was cooled, degassed, and pressurized with 10 bar of nitrogen to check the eventual leaks. Vacuum was performed to remove air. Then, the autoclave was left under vacuum for 15 minutes, after which, by double weighting, 11 g (56 mmol) of CF_3I was first introduced in the autoclave, followed by 27 g (422 mmol) of VDF. Then the autoclave was progressively heated to 75 °C, corresponding to the half life of the TBPP. After reaction the autoclave was placed in an ice bath for about 30 minutes, 11 g of unreacted VDF and CF_3I was released. After the opening of the autoclave a slurry composed of yellow solid and yellow liquid was obtained. The slurry, dissolved in acetone was precipitated in cold *n*-pentane. The solution was filtrated: the solid part, consisting of 11.2 g of a yellow powder (CF_3I -TBPP-VDF1) and a filtrated yellow liquid was obtained. The yellow filtrated liquid was distilled and 1.5 g of yellow solid (CF_3I -TBPP-VDF2) was obtained. ($\chi = 71 \%$, $\eta = 33 \%$).

6.1.3 Telomerization of VDF using (Perkadox[®] 16s) as initiator

The procedures and purification techniques employed were similar to those for telomerization in presence of TBPP as initiator, the only variation is the amount of the initiator Perkadox[®] 16s, which in this case was of 3.0 g (7.5 mmol) and the temperature of reaction that was fixed at 64 °C. After reaction the autoclave was placed in an ice bath for about 30 minutes, 2 g of unreacted VDF and CF₃I were released. After purification 19.1 g of yellow powder (CF₃I-Perkadox-VDF1) and 3.5 g of yellow solid (CF₃I-Perkadox-VDF2) were obtained. ($\chi = 95 \%$, $\eta = 60 \%$).

6.1.4 Characterization of the telomers

The ¹H and ¹⁹F NMR spectra of the telomers, exhibit similar signals that can be divide into two main groups: signals that come from the “normal” telomer, which present a regular alternation between CF₂ and CH₂ groups (and also terminated with CF₂I group), and signals originated by the fluorinated groups of the inverse monomer that present defect on the chain as head-to-head addition (-CH₂-CF₂-CF₂-CH₂-) or tail-to-tail addition (-CF₂-CH₂-CH₂-CF₂-), and terminated with CF₂-CH₂I group. In Figure 6.2 and 6.3 are reported two examples of CF₃-(VDF)_n-I spectra of ¹H NMR and ¹⁹F NMR respectively.

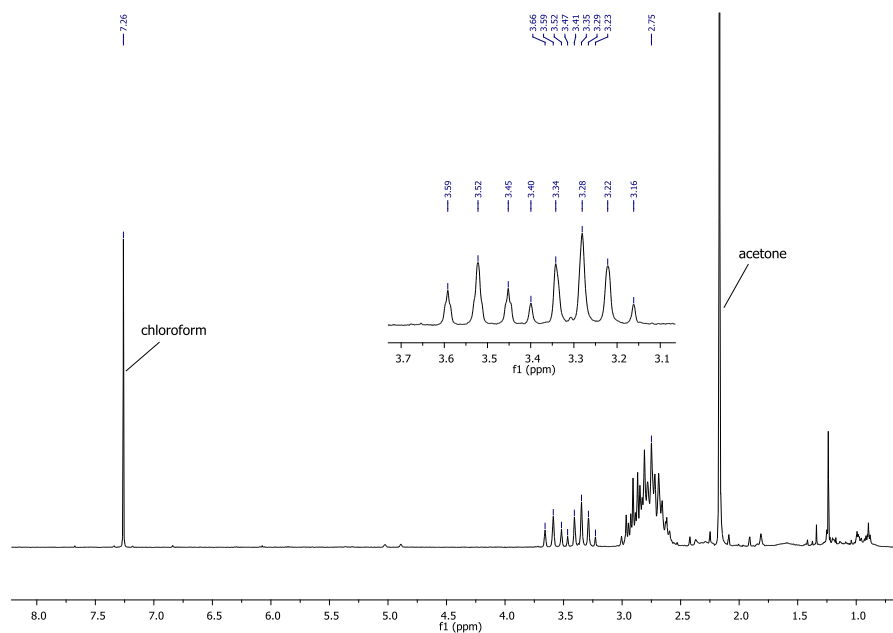


Figure 6.2. Example of ¹H NMR of CF₃-(VDF)_n-I (recorded in CDCl₃).

¹H NMR (CDCl₃) δ : 3.5 ppm (t, ³J_{HF} = 17.5 Hz, 2H, -CF₂-CH₂I); 3.3 ppm (m, 2H, CF₃-CH₂-CF₂-), 2.7 ppm (m, (n-2) H, -CF₂-CH₂-CF₂-).

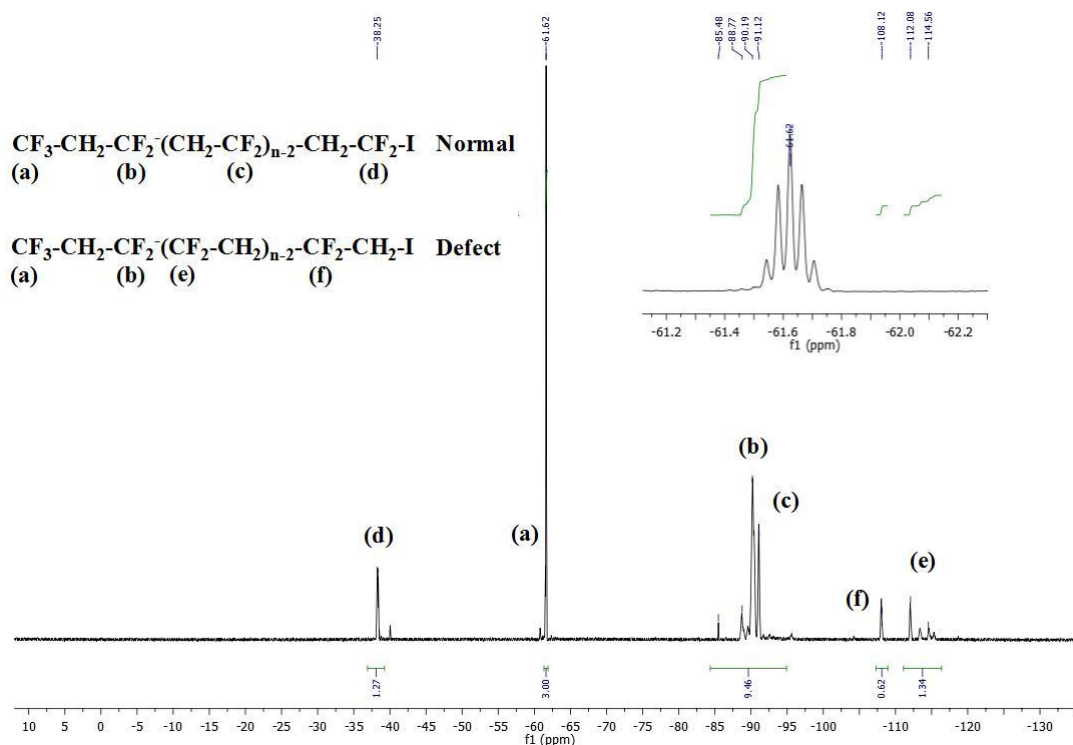


Figure 6.3. Example of ¹⁹F NMR of CF₃-(VDF)_n-I (recorded in CDCl₃).

¹⁹F NMR (CDCl₃) δ: -61.6 ppm (q, ³J_{FH} = ⁴J_{FF} = 10.0 Hz, 3F, CF₃-CH₂-CF₂-(C₂F₂H₂)_{n-2}); -88.3 ppm (m, 2F, CF₃-CH₂-CF₂-(C₂F₂H₂)_{n-2}); from -90 to -95 ppm (m, (n-2)F, CF₃-CH₂-CF₂-(CH₂-CF₂)_{n-2}, normal adduct); -38.2 ppm (m, 2F, -CH₂-CF₂I, normal adduct), from -112 to -115 ppm (m, (n-2)F, CF₃-CH₂-CF₂-(CF₂-CH₂)_{n-2}, inverse adduct), -108.1 ppm (m, 2F, -CF₂-CH₂I, inverse adduct).

Results and discussion

Two telomerization reactions of vinylidene fluoride (VDF) by ITP, in presence of CF₃I as chain transfer agent were carried out. In one was used *tert*-butyl peroxyvalate (TBPP) as initiator and in the other *bis*(4-*tert*-butylcyclohexyl)peroxydicarbonate (Perkadox[®] 16s). Each reaction produced two telomers, one with high mean molecular weight and one with lower. The two products obtained using TBPP as initiators were called CF₃I-TBPP-VDF1 and CF₃I-TBPP-VDF2, instead, using Perkadox[®] 16s as initiator the two fractions of telomers obtained were called CF₃I-Perkadox-VDF1 and CF₃I-Perkadox-VDF2.

Using the informations from the integrals of the signals obtained by ^{19}F NMR measured for each of the four products synthesized is possible to calculate the percentage of defects (U%) present in each telomer (Eq. 6.4-6.5).

$$U\% = 100 \frac{\sum \int (CF_2 \text{ defects})}{\sum \int (CF_2 \text{ defects} + CF_2 \text{ normal})} \quad \text{Eq. 6.4}$$

$$U\% = 100 \frac{\int_{-109 \text{ ppm}} CF_2 + \int_{-113 \text{ ppm}}^{-116 \text{ ppm}} CF_2}{\int_{-109 \text{ ppm}} CF_2 + \int_{-113 \text{ ppm}}^{-116 \text{ ppm}} CF_2 + \int_{-90 \text{ ppm}}^{-95 \text{ ppm}} CF_2 + \int_{-40 \text{ ppm}} CF_2} \quad \text{Eq. 6.5}$$

Also, the with the integrals of the signals of the ^{19}F NMR is possible to calculate the mean degree of polymerization DP_n (Eq. 6.6).

$$DP_n = \frac{\int_{-109 \text{ ppm}} CF_2 + \int_{-113 \text{ ppm}}^{-116 \text{ ppm}} CF_2 + \int_{-90 \text{ ppm}}^{-95 \text{ ppm}} CF_2 + \int_{-40 \text{ ppm}} CF_2}{2} \quad \text{Eq. 6.6}$$

Then, the average mass weight is calculated following Eq. 6.7.

$$M_w = 64 \cdot DP_n + 196 \quad \text{Eq. 6.7}$$

In Table 6.4 are summarized the values of U%, DP_n and M_n of the telomers synthesized.

	U %	DP_n	M_w
CF₃I-TBPP-VDF1	5.2 %	18	1346
CF₃I-TBPP-VDF2	15.3 %	6	578
CF₃I-Perkadox-VDF1	6.2 %	17	1282
CF₃I-Perkadox-VDF2	16.4 %	10	834

Table 6.4. Percentage of defects, mean degree of polymerization and average molecular weight of the telomers obtained by telomerization of VDF in presence of CF₃I as chain transfer and TBPP or Perkadox[®] 16s as initiators.

Comparing the two fractions with higher M_w (CF₃I-TBPP-VDF1 and CF₃I-Perkadox-VDF1) few differences were noticed: using Perkadox[®] 16s as initiator a shorter chain is obtained (one VDF unit less), respect to TBPP telomer. Furthermore, CF₃I-Perkadox-VDF1 showed a little higher percentage of defect respect to CF₃I-TBPP-VDF1, but this behavior is evidenced also comparing the two lighter fractions CF₃I-TBPP-VDF2, and CF₃I-Perkadox-VDF2. Moreover, the latter telomer showed four monomer unit more than CF₃I-TBPP-VDF2. Conversely, a marked difference is detected for the values of conversion of VDF and CF₃I and yield, that are 71 % and 33 % when TBPP is used and 95 % and 60 % for Perkadox[®] 16s.

This trend can be derived by the different reactivity of Perkadox[®] 16s than TBPP, and it was confirmed monitoring the values of temperature and pressure during the telomerization reaction. Indeed, during the heating of the autoclave from the temperature of 20 °C to 75 °C (set point) the pressure arise gradually until 15 bar, than it stabilize itself during the reaction time, a successive pressure drop of about 8 bar indicates that the reaction has taken place. Conversely, using Perkadox[®] 16s and after the heating of the autoclave at 40 °C (the set point is 64 °C) the system increase autonomously and rapidly its temperature, until more than 80 °C. During this time it was necessary to control the temperature by an external cooling for 30 minutes, then the system stabilize itself. The pressure in this case arise readily following the temperature increasing, and as for the telomerization with TBPP, at the end of the reaction there was a pressure drop from 18 bar to about 1 bar, that means the reactant gasses (CF₃I and VDF) react almost completely, in fact only 2 grams of unreacted gas were released, with 95 % of conversion.

In conclusion, the remarkable difference between yield and conversion showed by the four telomers synthesized by radical telomerization of VDF in presence of CF₃I as chain transfer agent has confirmed the strong influence of the nature of the initiators chosen. This behavior is described in previous studies on the radical telomerization of VDF with branched or linear perfluoroalkyl iodides^{29,32-34}, telechelic diiodoperfluoroalkanes²⁸, or iodoperfluoropolyethers³⁵. The present study demonstrated the higher efficiency of *bis*(4-*tert*-butylcyclohexyl)peroxydicarbonate (Perkadox[®] 16s) as initiator compared to *tert*-butyl peroxyvalate (TBPP). Other authors reported the good efficiency of another initiator *tert*-amyl peroxyvalate³⁶ (TAPP) for the telomerization of VDF in presence of CF₃I as chain transfer, but in this case the yield rised up to 41 %. The excellent results obtained in the case of Perkadox[®] 16s contrast with the extremely high reactivity of this peroxide and makes it necessary to be careful to check the temperature and pressure of the system.

6.1.5 Telomerization of VDF with C₄F₉I as chain transfer

The telomerization of VDF in presence of C₄F₉I as chain transfer is carried out in a similar way as for the telomerization in presence of CF₃I, using TBPP as initiators. The goal of the

reaction is the synthesis of telomers with one or two VDF units, and try to use these telomers as reagent for further reactions, demonstrating the decreased reactivity of the inverse adduct respect to the normal adduct.

6.1.6 Telomerization of VDF using TBPP as initiator and C₄F₉I as chain transfer agent

The reaction was carried out in 600 mL Hastelloy autoclave equipped with inlet and outlet valves, a manometer, and a rupture disk, where were placed 29.7 g (0.171 mol) of *tert*-butyl peroxyvalate (TBPP), 227.7 g (0.658 mol) of 1-iodo-perfluorohexane and 50 mL of acetonitrile as solvent. Then, the autoclave was cooled, degassed, and pressurized with 10 bar of nitrogen to check the eventual leaks. Vacuum was performed to remove air. Then, the autoclave was left under vacuum for 15 minutes, after which, by double weighting, 84.2 g (1.32 mol) of VDF were introduced. Then the autoclave was progressively heated to 74 °C, it arise 26 bar. After 16 hours of reaction the pressure drop arrived to 18 bar, the autoclave was placed in an ice bath for about 30 minutes, and 22.5 g of unreacted VDF was released ($\chi = 73$ %). After the opening of the autoclave 148.3 g of slurry was obtained ($\eta = 47$ %). The slurry, was distilled, obtaining fractions of telomers with different molecular weight. Among them, were obtained 21.7 g of C₄F₉-(VDF)₁-I (b.p. 77 °C/20 mmHg) and 32.9 g of C₄F₉-(VDF)₂-I (b.p. 96 °C/20 mmHg), respectively. The ¹H NMR and ¹⁹F NMR characterization of the telomers are reported from Figure 6.4 to 6.7. Also, the mass spectra of the telomers are reported in Figure 6.8 and 6.9.

6.1.7 ¹H and ¹⁹F NMR of C₄F₉-(VDF)-I and C₄F₉-(VDF)₂-I telomers

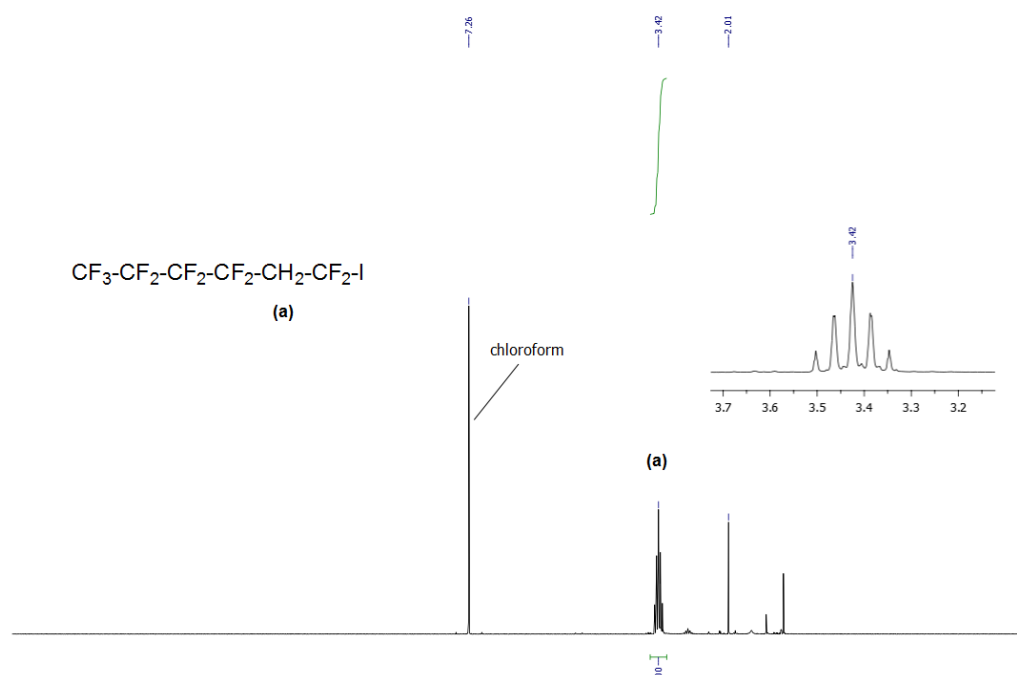


Figure 6.4. ¹H NMR of the C₄F₉-CH₂-CF₂-I telomer (recorded in CDCl₃).

1H NMR of $C_4F_9-CH_2-CF_2-I$ ($CDCl_3$) δ : 3.4 ppm (q, $^3J_{HF} = 16$ Hz, 2H, $-CF_2-\underline{CH}_2-CF_2-$).

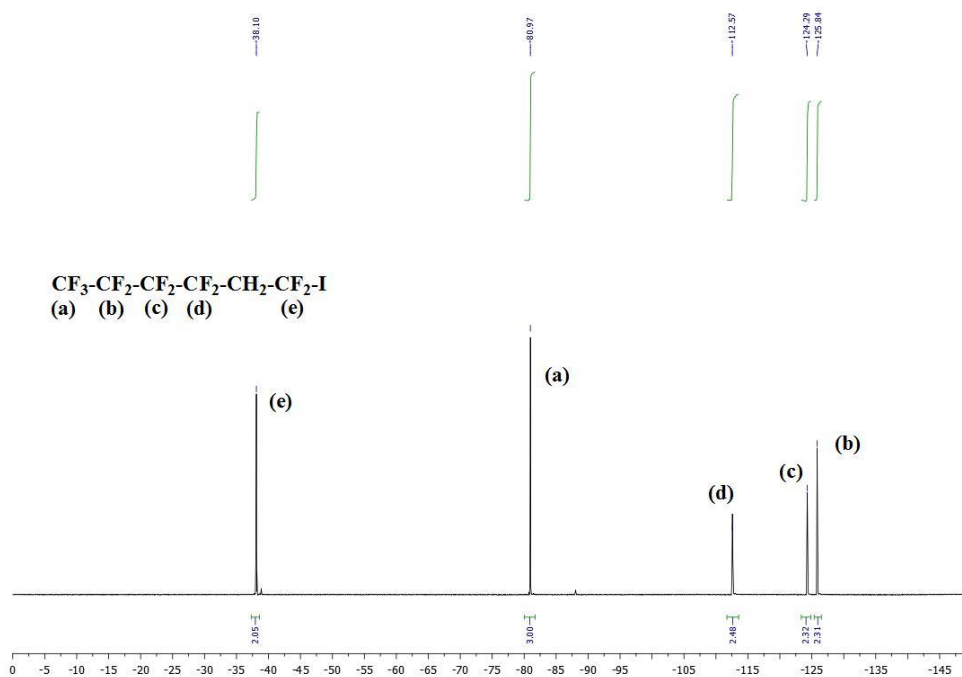


Figure 6.5. ^{19}F NMR of the $C_4F_9-CH_2-CF_2-I$ telomer (recorded in $CDCl_3$).

^{19}F NMR of $C_4F_9-CH_2-CF_2-I$ ($CDCl_3$) δ : -81.0 ppm (s, CF_3-CF_2-); -125.8 ppm (s, CF_3-CF_2-); -124.2 ppm (s, $CF_3-CF_2-CF_2-$), -122.6 ppm (s, $CF_3-CF_2-CF_2-$), -38.1 ppm (s, $-CF_2-I$).

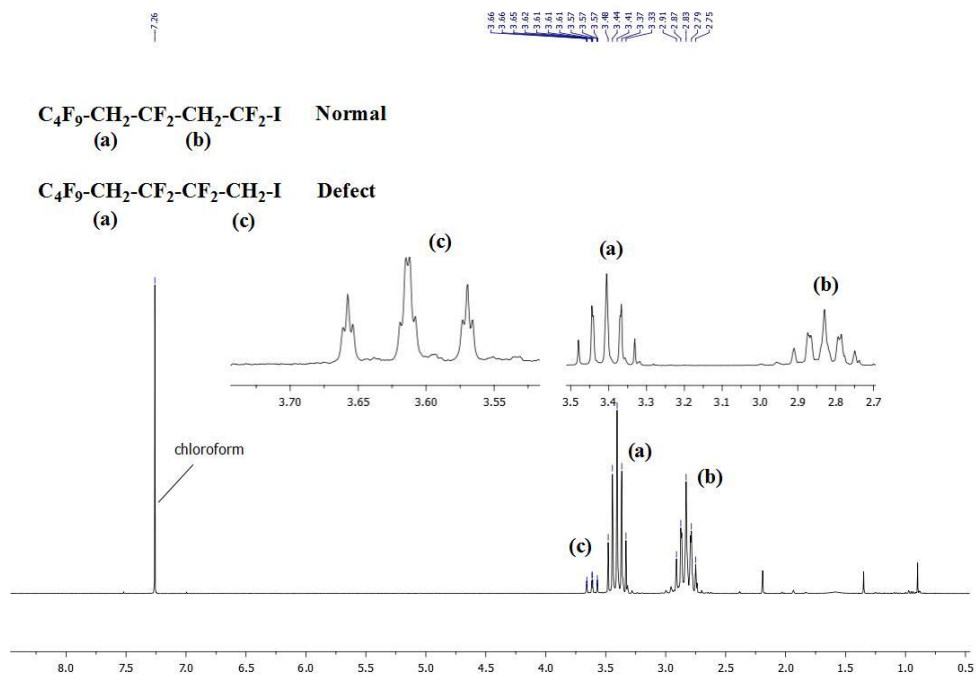


Figure 6.6. 1H NMR of the $C_4F_9-(C_2H_2F_2)-I$ telomer (recorded in $CDCl_3$).

^1H NMR of $\text{C}_4\text{F}_9\text{-CH}_2\text{-(C}_2\text{H}_2\text{F}_2\text{)-I}$ (CDCl_3) δ : 3.4 ppm (q, $^3J_{\text{HF}} = 16$ Hz, 2H, $-\text{CF}_2\text{-CH}_2\text{-CF}_2-$), 2.8 ppm (q, $^3J_{\text{HF}} = 16$ Hz, 2H, $-\text{CF}_2\text{-CH}_2\text{-CF}_2$, normal adduct); 3.6 ppm (tt, $^3J_{\text{HF}} = 16$ Hz, $^4J_{\text{HF}} = 4$ Hz, $\text{CF}_2\text{-CF}_2\text{-CH}_2\text{-I}$, reverse adduct).

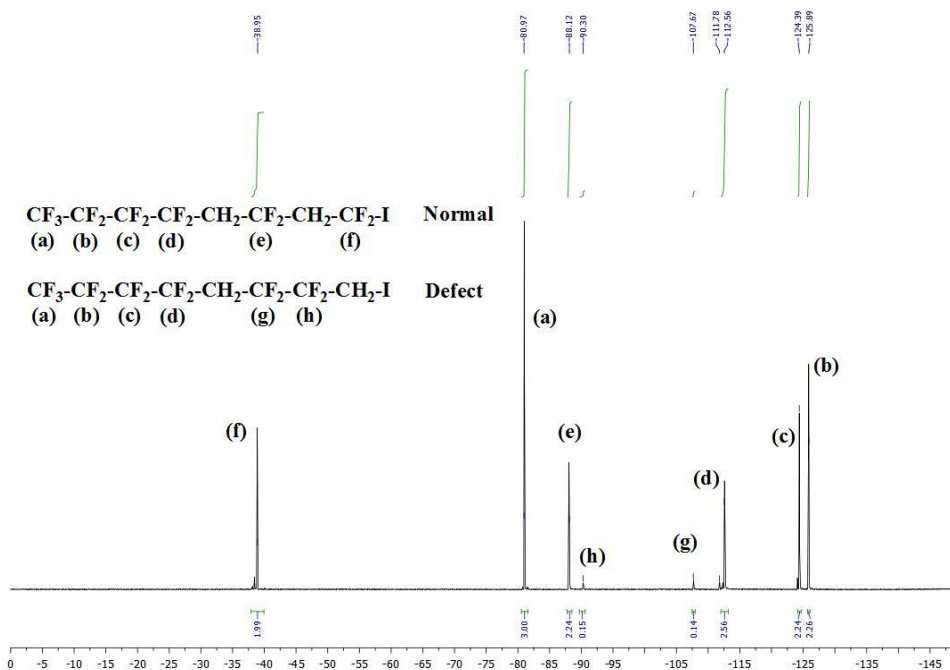
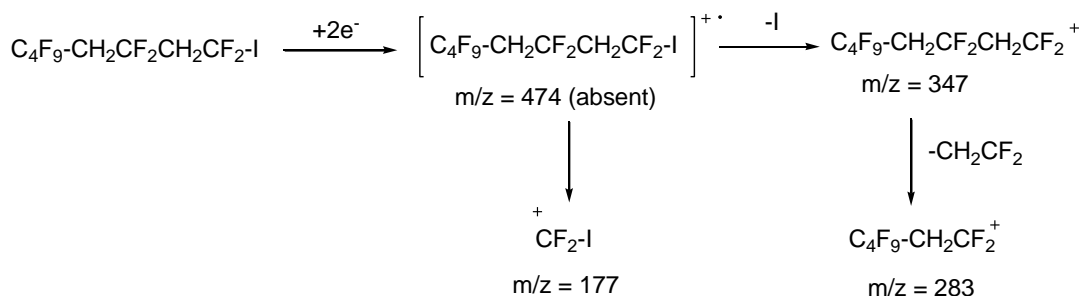


Figure 6.7. ^{19}F NMR of the $\text{C}_4\text{F}_9\text{-CH}_2\text{-CF}_2\text{-I}$ telomer (recorded in CDCl_3).

^{19}F NMR of $\text{C}_4\text{F}_9\text{-(C}_2\text{H}_2\text{F}_2\text{)-I}$ (CDCl_3) δ : -81.0 ppm (s, $\text{CF}_3\text{-CF}_2-$); -125.6 ppm (s, $\text{CF}_3\text{-CF}_2-$); -124.4 ppm (s, $\text{CF}_3\text{-CF}_2\text{-CF}_2-$), -112.6 ppm (s, $\text{CF}_3\text{-CF}_2\text{-CF}_2\text{-CF}_2\text{-CH}_2-$), -40.0 ppm (s, $-\text{CF}_2\text{-I}$, normal adduct), -107.8 ppm (s, $\text{C}_4\text{F}_9\text{-CH}_2\text{-CF}_2\text{-CF}_2\text{-CH}_2\text{I}$, reverse adduct), -90.3 ppm (s, $\text{C}_4\text{F}_9\text{-CH}_2\text{-CF}_2\text{-CF}_2\text{-CH}_2\text{I}$, reverse adduct).



Scheme 6.4. Possible fragmentation of $\text{C}_4\text{F}_9\text{-CH}_2\text{-CF}_2\text{-CH}_2\text{-CF}_2\text{-I}$.

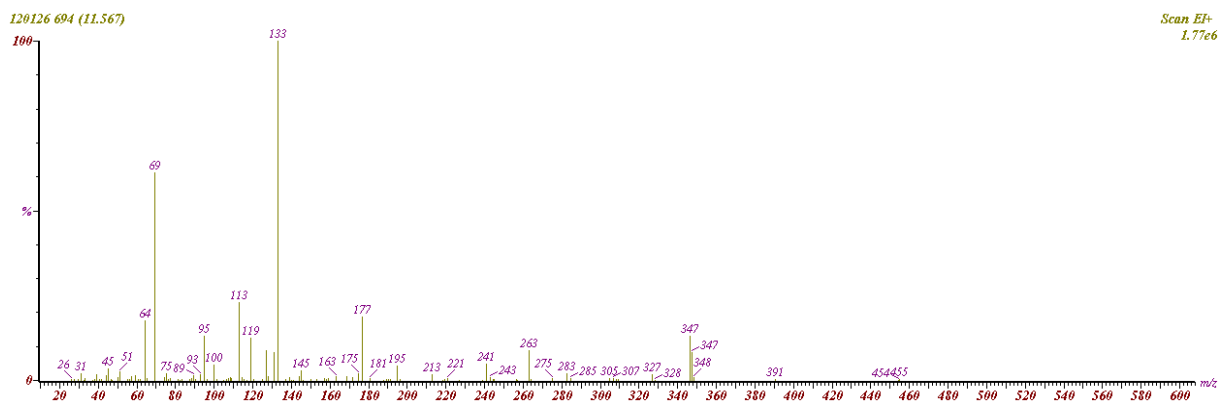
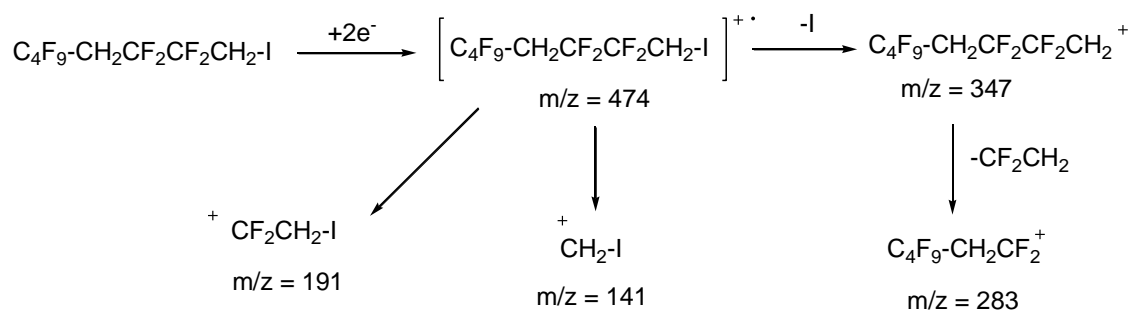


Figure 6.8. Mass fragmentation of $C_4F_9-CH_2-CF_2-CH_2-CF_2-I$.

Spectral data: MS m/z (rel. ab. %): 347 ($[M-I]^+$, 20%); 283 ($[M-CH_2CF_2I]^+$, 5%); 177 ($[CF_2I]^+$, 20%); 69 ($[CF_3]^+$, 60%).



Scheme 6.5. Possible fragmentation of $C_4F_9-CH_2-CF_2-CF_2-CH_2-I$.

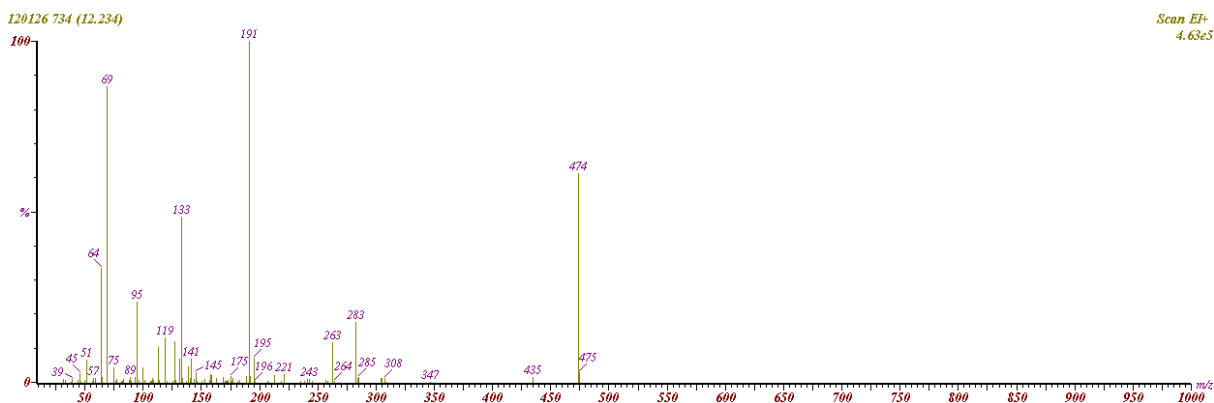
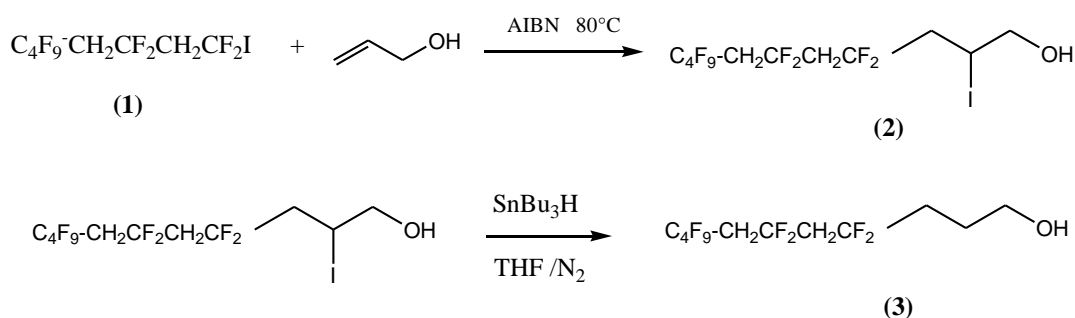


Figure 6.9. Mass fragmentation of $C_4F_9-CH_2-CF_2-CF_2-CH_2-I$.

Spectral data: MS m/z (rel. ab. %): 474 ($[M]^+$, 60%); 347 ($[M-I]^+$, 2%); 283 ($[C_4F_9CH_2CF_2]^+$, 20%); 191 ($[CF_2CH_2I]^+$, 100%); 69 ($[CF_3]^+$, 80%).

Synthesis of $C_4F_9-(VDF)_2-CH_2-CH_2-CH_2-OH$

The synthesis of a partially fluorinated alcohol with a vinylidene moiety was carried out in order to investigate the synthesis of a VDF telomer. The reaction involves two steps: first the addition of allyl alcohol to $C_4F_9-(VDF)_2-I$ telomer (**1**) followed by a reduction with tributylstannane as reported in Scheme 6.6.



Scheme 6.6. Scheme of the synthesis of $C_4F_9-(VDF)_2-CH_2-CH_2-CH_2-OH$ (**3**).

6.1.8 Materials

Allyl alcohol, tributyl stannane ($SnBu_3H$), tetrahydrofuran (THF), 2,2'-azobis(2-methylpropionitrile) (AIBN) was provided by Aldrich. $C_4F_9(VDF)_2I$ (**1**) was synthesized following the procedures reported above.

6.1.9 Synthesis of $C_4F_9-CH_2CF_2-CH_2CF_2-CH_2-CHI-CH_2-OH$ (**2**)

Allyl alcohol (1.0 g, 17.2 mmol) was added dropwise slowly to a mixture of $C_4F_9(VDF)_2I$ (5 g, 10.5 mmol) (**1**) and AIBN (3.0 mmol) at 85 °C. The reaction mixture was stirred for 48 h. The evolution of the reaction was monitored by gas chromatographic measurements. 0.5 g of AIBN were added every 2 hours until the complete consumption of the peak relative to the iodine reagent. The crude product was washed by water and chloroform to remove the excess of allyl alcohol. The organic layer was removed with a separating funnel and the solvent was removed by rotavapor obtaining 5 g of yellow oil (53 % yield).

6.1.10 Synthesis of $C_4F_9-CH_2CF_2-CH_2CF_2-CH_2-CH_2-CH_2-OH$ (**3**)

In a two necked round flask, equipped with condenser and magnetic stirrer, cooled with ice and saturated with nitrogen, 5 g of $C_4F_9-CH_2CF_2-CH_2CF_2-CH_2-CHI-CH_2-OH$ (**2**) and 10 mL of THF were dissolved with 0.8 g of AIBN. 2.5 mL of tributylstannane were dropwise added.

The mixture was initially stirred at room temperature and after was heated at 80 °C for 4 hours. The THF was removed washing the crude product with water and chloroform. The organic layer was separated and the chloroform was removed by vacuum. Two liquid layers were obtained, a white upper layer and a red lower layer. The product was recover by vacuum distillation (b.p. 80°C/0.2 mmHg) obtaining 3 g of white solid (78 % yield).

6.1.11 Chemical characterization of $C_4F_9-CH_2CF_2-CH_2CF_2-CH_2-CHI-CH_2-OH$ (**2**) and $C_4F_9-CH_2CF_2-CH_2CF_2-CH_2-CH_2-CH_2-OH$ (**3**)

Hereafter are reported the chemical characterization of $C_4F_9-CH_2CF_2-CH_2CF_2-CH_2-CHI-CH_2-OH$ (**2**) by 1H NMR (Figure 6.10), ^{19}F NMR (Figure 6.11).

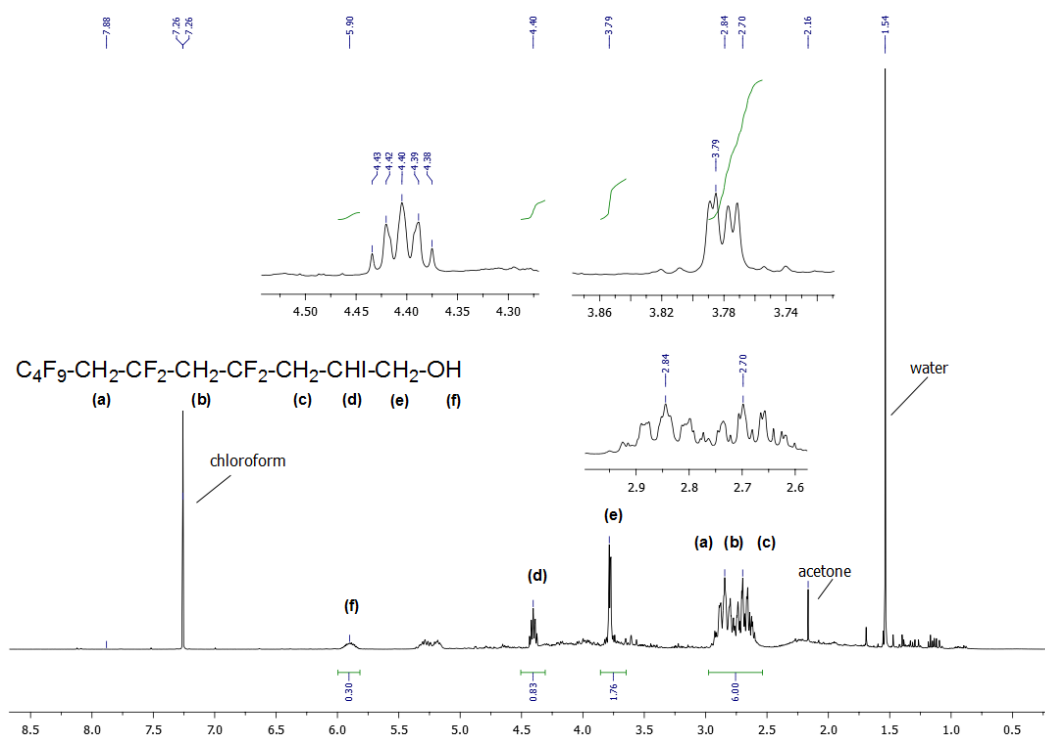


Figure 6.10. 1H NMR of the $C_4F_9-(VDF)_2-CH_2-CHI-CH_2-OH$ adduct (recorded in $CDCl_3$).

1H NMR of $C_4F_9-CH_2CF_2-CH_2CF_2-CH_2-CHI-CH_2-OH$, δ (in $CDCl_3$): 2.7 ppm (2H, m, $C_4F_9-CH_2$); 2.6 ppm (4H, m, $-CF_2-CH_2-CF_2-CH_2-$); 4.4 ppm (1H, q, $^3J_{HH} = 4.0$ Hz, $CH_2-CHI-CH_2-$); 3.8 ppm (2H, m, $CHI-CH_2-OH$); 5.9 ppm (1H, m, $-OH$).

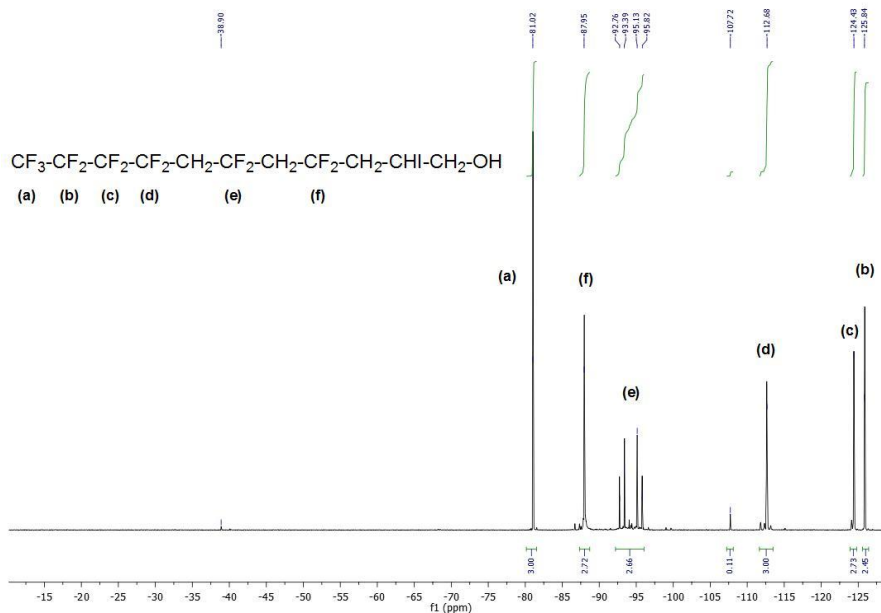


Figure 6.11. ^{19}F NMR of the $\text{C}_4\text{F}_9\text{-(VDF)}_2\text{-CH}_2\text{-CHI-CH}_2\text{-OH}$ adduct (recorded in CDCl_3).

^{19}F NMR of $\text{C}_4\text{F}_9\text{-CH}_2\text{CF}_2\text{-CH}_2\text{CF}_2\text{-CH}_2\text{-CHI-CH}_2\text{-OH}$, δ (in CDCl_3): -81.0 ppm (s, $\text{CF}_3\text{-CF}_2$); -125.8 ppm (s, $\text{CF}_3\text{-CF}_2$); -124.4 ppm (s, $\text{CF}_3\text{-CF}_2\text{-CF}_2$), -112.7 ppm (s, $\text{CF}_3\text{-CF}_2\text{-CF}_2\text{-CF}_2\text{-CH}_2$), -87.9 ppm (s, $\text{C}_4\text{F}_9\text{-CH}_2\text{-CF}_2$); -95.1 ppm (s, $\text{C}_4\text{F}_9\text{-CH}_2\text{-CF}_2\text{-CH}_2\text{-CF}_2$).

Hereafter are reported the chemical characterization of $C_4F_9-CH_2CF_2-CH_2CF_2-CH_2-CH_2-CH_2-OH$ (**2**) by 1H NMR (Figure 6.12), ^{19}F NMR (Figure 6.13) and the mass fragmentation (Figure 6.14)

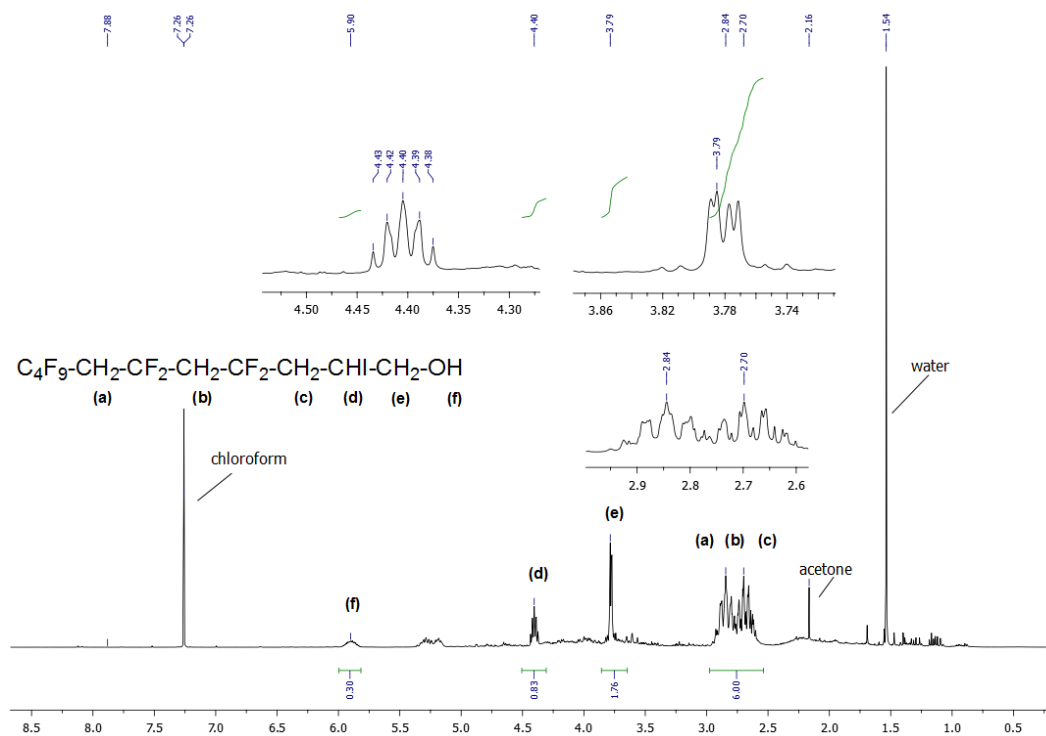


Figure 6.12. 1H NMR of the $C_4F_9-(VDF)_2-CH_2-CHI-CH_2-OH$ adduct (recorded in $CDCl_3$).

1H NMR of $C_4F_9-CH_2CF_2-CH_2CF_2-CH_2-CH_2-CH_2-OH$, δ (in $CDCl_3$): 2.7 ppm (2H, m, $C_4F_9-CH_2$); 2.6 ppm (4H, m, $-CF_2-CH_2-CF_2-CH_2-$); 1.8 ppm (2H, m, $CH_2-CH_2-CH_2-$); 3.6 ppm (2H, t, $^3J_{HH} = 6$ Hz, CH_2-CH_2-OH); 0.9 ppm (1H, m, $-OH$).

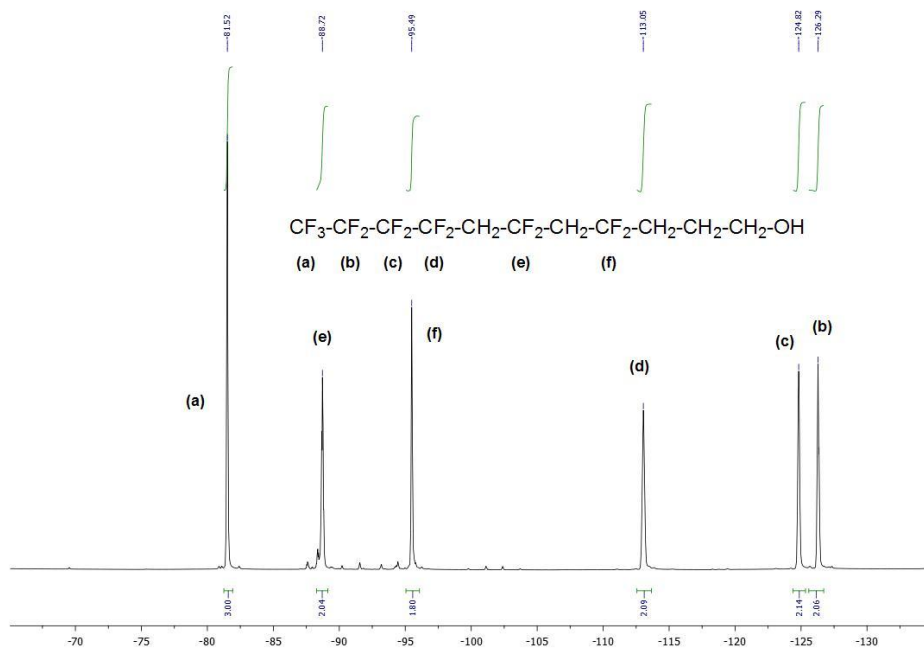
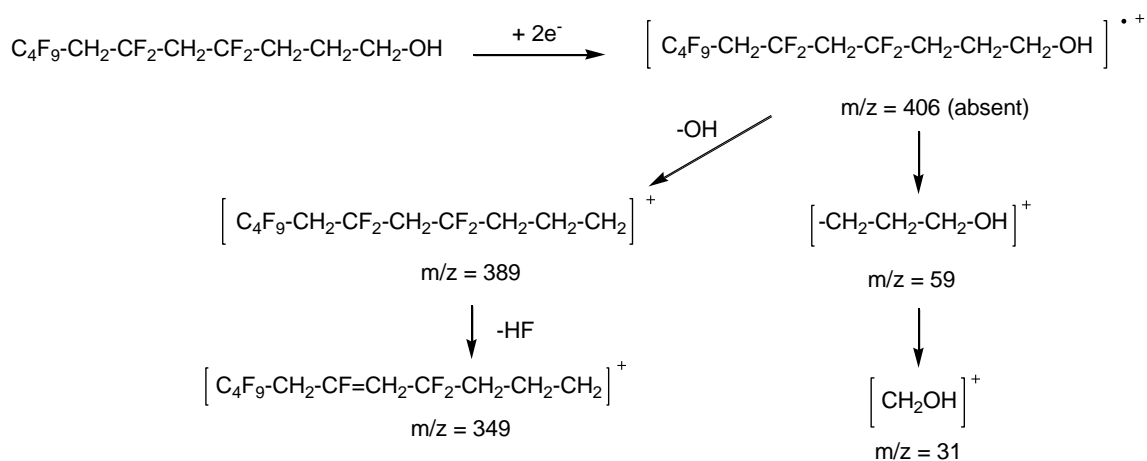


Figure 6.13. ^{19}F NMR OF $\text{C}_4\text{F}_9\text{-CH}_2\text{CF}_2\text{-CH}_2\text{CF}_2\text{-CH}_2\text{-CH}_2\text{-CH}_2\text{-OH}$ (recorded in CDCl_3).

^{19}F NMR of $\text{C}_4\text{F}_9\text{-CH}_2\text{CF}_2\text{-CH}_2\text{CF}_2\text{-CH}_2\text{-CH}_2\text{-CH}_2\text{-OH}$, δ (in CDCl_3): -81.5 ppm (s, $\text{CF}_3\text{-CF}_2$ -); -126.3 ppm (s, $\text{CF}_3\text{-CF}_2$ -); -124.8 ppm (s, $\text{CF}_3\text{-CF}_2\text{-CF}_2$ -), -113.0 ppm (s, $\text{CF}_3\text{-CF}_2\text{-CF}_2\text{-CF}_2\text{-CH}_2$ -), -88.7 ppm (s, $\text{C}_4\text{F}_9\text{-CH}_2\text{-CF}_2$ -); -95.5 ppm (s, $\text{C}_4\text{F}_9\text{-CH}_2\text{-CF}_2\text{-CH}_2\text{-CF}_2$ -).



Scheme 6.7. Possible fragmentation of $\text{C}_4\text{F}_9\text{-CH}_2\text{CF}_2\text{-CH}_2\text{CF}_2\text{-CH}_2\text{-CH}_2\text{-CH}_2\text{-OH}$.

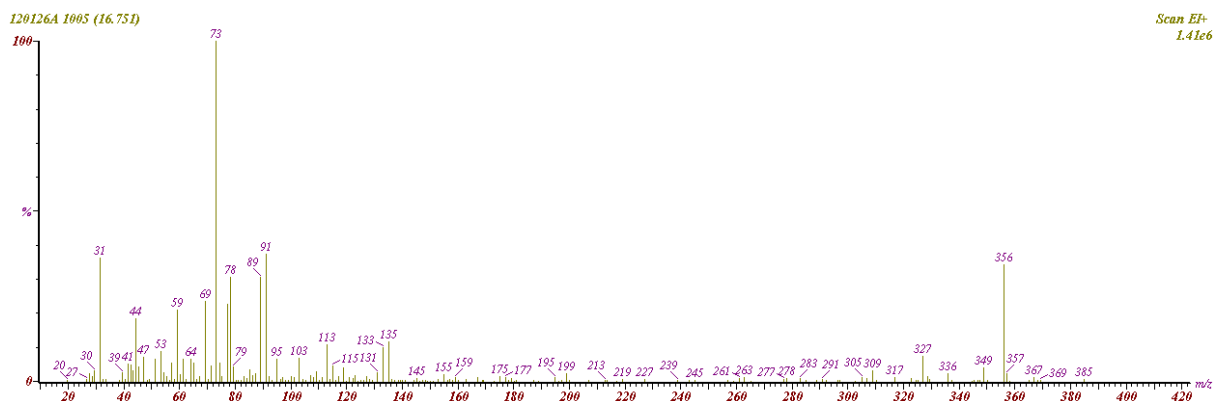


Figure 6.14. Mass fragmentation of $C_4F_9-(VDF)_2-CH_2-CH_2-CH_2-OH$.

Spectral data: MS m/z (rel. ab. %): 349 ($[M-OH-HF]^+$, 10%); 63 ($[CF_3]^+$, 20%); 59 ($[CH_2CH_2CH_2OH]^+$, 20%); 31 ($[CH_2OH]^+$, 30%).

Conclusion

The telomerisation of VDF in presence of C_4F_9I as chain transfer and TBPP as initiator is carried out with 73% of conversion of VDF and 47% of yield. After distillation different fractions of telomers were obtained. Among them, a monoadduct ($C_4F_9-CH_2CF_2-I$) and a diadduct ($C_4F_9-(C_2H_2F_2)_2-I$) were isolated and characterized by 1H NMR and ^{19}F NMR spectra. The characterization of the monoadduct evidenced the absence of the reverse telomer $C_4F_9-CF_2CH_2-I$, confirming the selectivity of the reaction of $C_4F_9\cdot$ radical on the VDF monomer. Conversely, the diadduct presents two species, one normal ($C_4F_9-CH_2CF_2-CH_2CF_2-I$) and one reverse ($C_4F_9-CH_2CF_2-CF_2CH_2-I$). The diadduct was used as reactant for the synthesis of the intermediate $C_4F_9-(VDF)_2-CH_2-CHI-CH_2-OH$ by reaction with allyl alcohol. The intermediate was reduced with *tert*-butyl stannane and $C_4F_9-(VDF)_2-CH_2-CHI-CH_2-OH$ was obtained.

The reaction with allyl alcohol evidenced the decreased reactivity of the reverse adduct compared to the normal one as evidenced by ^{19}F NMR spectra. In fact, the signal at -40 ppm, assigned to the $-CF_2-I$ fluorinated group of the normal $C_4F_9-VDF_2-I$ telomer, disappeared showing that a reaction happened. Conversely, signals of the inverse diadduct are still present after the reaction with allyl alcohol.

Appendix C: half-life of initiators

The half-life of a peroxide is defined as the time ($t_{1/2}$) needed for one half of a given quantity of peroxide in dilute solution (the solution can influence its decomposition) to decompose at a given temperature. The decomposition rate is first order (Eq. 6.8)

$$\frac{-d[I]}{dt} = k_d[I] \quad \text{Eq. 6.8}$$

Where $[I]$ is the initiator concentration [$\text{mol}\cdot\text{L}^{-1}$] and k_d is the first order rate constant, that is possible to calculate from the equation of Arrhenius:

$$k_d = Ae^{-E_a/RT} \quad \text{Eq. 6.9}$$

Where A is pre-exponential factor [s^{-1}], R is the constant of gases [$\text{J}\cdot\text{mol}^{-1}\cdot\text{K}^{-1}$], T is the temperature [K] and E_a is the activation energy [$\text{kJ}\cdot\text{mol}^{-1}$].

Integrating Eq. 6.8 with the following boundary conditions:

For initial state,

$$t_0 = 0; [I]_{(t_0=0)} = [I]_0 \quad \text{Eq. 6.10}$$

And for the final state,

$$t = t_{1/2}; [I]_{(t=t_d)} = [I]_0/2 \quad \text{Eq. 6.11}$$

We obtain

$$\ln(2) = k_d t_{1/2} \quad \text{Eq. 6.12}$$

And then:

$$t_{1/2} = \frac{\ln(2)}{k_d} \quad \text{Eq. 6.13}$$

The higher the temperature corresponding to the half-life, more stable is the initiator. Half-life temperatures can vary based on the manner in which they are determined, especially the solvent used.

Bibliography

- (1) Timmerman, R. *J. Polym. Sci.* **1962**, 6, 456-460.
- (2) Gorlitz, M.; Minke, R.; Trautvetter, W.; Weisberger, G. *Angew. Makromol. Chem.* **1973**, 29/30, 137-162.
- (3) Dohany, J.E.; Humphrey, J.S. *Encycl. Polym. Sci. Eng.* **1989**, 17, 532-548.
- (4) Ameduri, B.; Boutevin, B., *Well Architected Fluoropolymers: Synthesis, Properties and Applications*. 2004, Elsevier: Amsterdam.
- (5) Ameduri, B. *Chem. Rev.* **2009**, 109, 6632-6686.
- (6) Governal, R.A. *Semicond. Int.* **1994**, July, 176-180.
- (7) Henley, M. *Ultrapure Water* **1995**, May/June, 15-20.
- (8) Robinson, D.; Seiler, D.A. *Potential Application For Kynar Flex PVDF in the Nuclear Industry*. in *Proceedings American Glovebox Society*. 1993. Seattle, WA 16-19 August.
- (9) Moggi, G.; Caratto, A.; Bonardelli, P.; Monti, C. U.S. 4,739,024, **1988**, Montefluos S.P.A.
- (10) Ameduri, B. *Macromolecules* **2010**, 43, 10163-10184.
- (11) Ameduri, B.; Boutevin, B.; Guida-Pietrasanta, F.; Manseri, A.; Ratsimihéty, A.; Caporiccio, G., *Use of Fluorinated Telomers for the Obtaining of Hybrid Fluorosilicones*. Vol. 2 1999. pp. 67-79.
- (12) Tatemoto, M.; Suzuki, T.; Tomoda, M.; Furukawa, Y.; Ueta, Y.; De. Patent 2,815,187, **1978**,
- (13) Oka, M.; Tatemoto, M., *Vinylidene fluoride-hexafluoropropylene copolymer having terminal iodines*. Contemporary Topics in Polymer Science, ed. W.J.; Tsuruta Bailey, T. 1984, Plenum Press: New York. pp. 763-781.
- (14) Tatemoto, M. *Int. Poly. Sc. Tech.* **1985**, 12, 85-98.
- (15) Tatemoto, M.; Nakagawa, T. Japanese Patent 61,049,327, **1986**,
- (16) David, G.; Boyer, C.; Tonnar, J.; Ameduri, B.; Lacroix Desmazes, P.; Boutevin, B. *Chem. Rev.* **2006**, 106, 3936-3962.
- (17) Boutevin, B. *J. Polym. Sci.: Part A: Polym. Chem.* **2000**, 38, 3235-3243.
- (18) Tedder, J.M.; Walton, J.C. *Adv. Phys. Org. Chem.* **1978**, 16, 51-86.
- (19) Tedder, J.M.; Walton, J.C. *Tetrahedron* **1980**, 36, 701-707.
- (20) Okafo, E.N.; Whittle, E. *Int. J. Chem. Kinet.* **1975**, 7, 287-300.
- (21) Low, H.C.; Tedder, J.M.; Walton, J.C. *J. Chem. Soc., Faraday Trans. 1* **1976**, 72, 1707-1714.
- (22) Sloan, J.P.; Tedder, J.M.; Walton J.C. *J. Chem. Soc., Faraday Trans. 1* **1973**, 69, 1143-1152.

- (23) McMurray, N.; Tedder J.M.; Vertommen, L.L.T.; Walton J.C. *J. Chem. Soc.: Perkin Trans. 2* **1976**, 63-67.
- (24) Sloan, J.P.; Tedder, J.M.; Walton, J.C. *J. Chem. Soc.: Perkin Trans. 2* **1975**, 63-67.
- (25) Ashton, D.S.; Mackay A.F.; Tedder, J.M.; Tipney, D.C.; Walton J.C. *J. Chem. Soc.: Chem. Comm.* **1973**, 14, 496-497.
- (26) Chambers, R.D.; Hutchinson, J.; Mobbs, R.H.; Musgrave, W.K.R. *Tetrahedron* **1964**, 20, 497-506.
- (27) Apsey, G.C.; Chambers, R.D.; Salisbury, M.J., Moggi, G. *J. Fluorine Chem.* **1988**, 40, 261-282.
- (28) Manseri, A.; Ameduri, B.; Boutevin, B.; Caporiccio, G.; Chambers, R.D.; Wright, A.P. *J. Fluorine Chem.* **1995**, 74, 59-66.
- (29) Balague, J.; Ameduri, B.; Boutevin, B.; Caporiccio, G. *J. Fluorine Chem.* **2000**, 104, 253-268.
- (30) Hauptschein, M.; Braid, M.; Lawlor, F.E. *J. Am. Chem. Soc.* **1958**, 80, 846-851.
- (31) Hauptschein, M.; Oesterling, R.E. *J. Am. Chem. Soc.* **1960**, 82, 2868-2871.
- (32) Balague, J.; Ameduri, B.; Boutevin, B.; Caporiccio, G. *J. Fluorine Chem.* **1995**, 70, 215-223.
- (33) Guiot, J.; Ameduri, B.; Boutevin, B. *Macromolecules* **2002**, 35, 8694-8706.
- (34) Ameduri, B.; Ladaviere, C.; Delholme, F.; Boutevin, B.; Caporiccio, G. *Macromolecules* **2004**, 37, 7602-7609.
- (35) Gelin, M.P.; Ameduri, B. *J. Polym. Sci, Part A: Polym. Chem.* **2003**, 41, 160-169.
- (36) Montefusco, F.; Bongiovanni, A.; Priola, A.; Ameduri, B. *Macromolecules* **2004**, 37, 9804-9813.

Chapter 7. Instruments

In this chapter are described the instruments and experimental conditions used for the characterization of the products synthesized.

Nuclear Magnetic Resonance

^1H NMR (250 or 400 MHz) and ^{19}F (250 or 400 MHz) and ^{13}C NMR (250 or 400 MHz) spectroscopies: the NMR spectra were recorded on Bruker, AC 250 and AC 400 instruments, using deuterated chloroform or deuterated tetrahydrofuran as the solvents and tetramethylsilane (TMS) (or CFCl_3) as the references for ^1H (or ^{19}F) nuclei, respectively. Coupling constants and chemical shifts are given in Hz and ppm, respectively. The experimental conditions for recording ^1H (^{19}F) NMR spectra were as follows: flip angle = 90° (30°), acquisition time = 4.5s (0.7 s), pulse delay = 2 s (5 s), number of scans = 16 (64), and pulse width = $5 \mu\text{s}$ for ^{19}F NMR. 2D-heterocorrelated ^1H - ^{13}C experiment were performed using a VSP-400 5 mm z-gradient probe in the reverse detection conditions. The proton and carbon assignments were obtained by standard chemical shift correlations and confirmed by 2D homo- and hetero-correlated measurements.



Figure 7.1. NMR apparatus.

Infrared and GC-MS

Infrared spectroscopy measurements were performed in transmission with a spectrometer Nicolet Avatar 10 P. The accuracy was $\pm 2 \text{ cm}^{-1}$. GC/MS spectra were measured on a Carlo Erba Instrument MFC 500/QMD1000 using a silica fused capillary PS264 column (30 m x 0.25 mm) on a Finnigan Mat TSQ7000 (capillary column 30 m x 0.32 mm). Typical conditions were: temperature program 60 °C for 2 min, 10 °C min^{-1} to 280 °C. Helium was used as the gas carrier 1 mL min^{-1} .



Figure 7.2. IR spectrometer.

Surface characterizations

The static, advancing and receding contact angles were assessed using a KRÜSS GmbH *EasyDrop*, Drop Shape Analysis System, with a measuring range of 1-180°, volume of one drop of water: 5 μL , volume of one drop of diiodomethane: 2 μL , with a monochrome interline CCD, 25/30 fps camera with halogen lamp. The contact angles were determined using KRÜSS DSA1 v1.91 program. The values given in this present paper were obtained from the average of 10 measurements.



Figure 7.3. Tensiometer KRÜSS GmbH EasyDrop.

The polymer film obtained for the contact angles assessments was formed using the spin coater (Karl Suss Technique SA apparatus, CT60 model). A solution of 20 mg of 4'-nonafluorobutyl styrene in 2 mL of THF was placed on a 20 mm x 20 mm x 1 mm of quartz substrate. The substrate surface was covered using a pipette and followed by spinning at 1000 rpm for three minutes to spread and form a uniform thin film over the substrate (Figure 7.4).

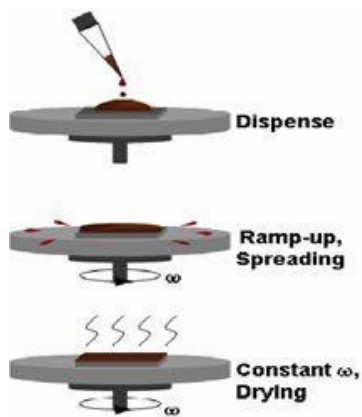


Figure 7.4. Spin-coating.

During the static contact angle determination, the size of the drop did not alter during the measurement. During the assessments of the advancing angle, the syringe needle remained in the drop. Advancing and receding contact angles were determined by the needle-syringe method, also carried out on the same polymer samples using a stainless steel needle

connected with an automatically microliter syringe (diameter of the needle 0.5 mm). The water introduction and its withdrawal were monitored by a video camera that recorded the profile during the process. All calculation methods were based on the sessile drop method, while the surface energies calculation were assessed by the Owens-Wendt method (see Appendix A).

Gas chromatography (GC)

Gas chromatography analyses were performed with a GC1000 DPC (Digital Pressure Control), Dani Instruments. The column is 15 m long, with 0.25 mm of internal diameter, stationary phase: PS 264. , mobile phase: helium with a flow of 26 mL · min⁻¹. Temperature of the column 60 °C, injector temperature 250 °C, detector temperature 250 °C. The initial temperature was 60 °C and the final temperature was 250 °C, $\Delta T/\Delta t = 15^\circ\text{C} \cdot \text{min}^{-1}$.



Figure 7.5. Gas chromatography detector.

Gel permeation chromatography (GPC)

Gel permeation chromatography (GPC) was performed using a Spectra-Physics apparatus equipped with a set of two PLgel 5 μm MIXED-C columns from Polymer Laboratories. The eluent was pure THF at a flow rate of 0.8 mL min^{-1} . The calibration curve was established using monodispersed PS standards from Polymer Laboratories.

Thermogravimetric analyses (TGA)

Thermogravimetric analyses (TGA) were carried out with a TGA 51 apparatus from TA instruments, under air, at the heating rate of $10 \text{ }^\circ\text{C min}^{-1}$ from room temperature up to a maximum of $500 \text{ }^\circ\text{C}$. The sample size was 15 mg.

Differential scanning calorimetry

Differential scanning calorimetry (DSC) measurements were conducted using a Pyris 1 apparatus from Perkin Elmer. Scans were recorded at a heating rate of $20 \text{ }^\circ\text{C min}^{-1}$ from -100 to $+150 \text{ }^\circ\text{C}$ and values of T_g and T_m were assessed from the second cycle. The sample weight was 10 mg.

General conclusion

Fluorinated compounds are attractive materials because of their unique properties, such as low polarizability, high hydro- and oleophobicity, high thermal and chemical resistance, resistance to oxidation and hydrolytic decomposition, low flammability, low refractive index and low dielectric constants.

Because of these outstanding properties, fluorinated compounds have been extensively used since mid-50's in the synthesis of low-surface energy protective coatings for different surfaces (metals, paper, stone, wood, leather, textiles to name a few).

Molecules having long fluorinated moieties (at least 8 to 12 completely fluorinated carbon atoms) show highly ordered structures due to the liquid crystal behavior of the rigid fluorinated side group, but they are persistent in the environment and have strong bioaccumulative effects. This arises from the extreme stability of the perfluorinated chain which cannot degrade under enzymatic or metabolic decomposition. As a consequence of the EPA's 2010/2015 PFOA Stewardship Program which aims to the complete elimination of long-chain perfluorochemicals by 2015 an urging need to find out alternatives has become a real challenge.

The use of shorter chain is detrimental to surface properties because of the partial or complete loss of highly structured liquid crystal phases. One of the strategies adopted to increase the molecular rigidity of short chain fluorinated telomers is the introduction of a phenyl or biphenyl group as rigid molecular spacer.

Polymers bearing fluorinated substituents connected to the polymer backbone by means of a phenyl group show improved surface properties due to the enhanced self-assembly behavior of the semifluorinated side group. In order to investigate this alternative, in this work a new short-chain fluorinated monomer, 4'-nonafluorobutyl styrene, has been first synthesized and then polymerized using different polymerization techniques.

The synthesis of 4'-nonafluorobutyl-styrene was achieved in three steps: fluoroalkylation of bromo acetophenone, reduction of 4'-nonafluorobutyl acetophenone and, finally, dehydration of the latter, in the presence of KHSO_4 , enabled us to synthesize the desired monomer. The synthesis of 4'-nonafluorobutylacetophenone was achieved by the cross-coupling reaction and optimized by changing experimental conditions. It was demonstrated that the use of an aprotic polar solvent is compulsory for the success of the reaction. Further the optimum $[\text{solvent}]_0 / [1\text{-iodo-perfluorobutane}]_0$ molar ratio is 4 and only the use of copper led to the formation of the desired product. Moreover, among the complexing ligands used (2,2'-bipyridine, HMTETA, PMTETA), 2,2'-bipyridine gave the best results both for conversion (99 %) and yield (73 %), when the reaction was carried out at 100 °C.

Subsequently, the 4'-nonafluorobutyl styrene was polymerized. For the first time, the iodine transfer polymerization (ITP) of 4'-nonafluorobutyl styrene, controlled by 1-

iodoperfluorohexane has been reported and compared to the conventional radical one. As expected, polymers obtained by ITP displayed more narrow polydispersity index (PDI = 1.13) than those achieved by conventional radical polymerization (PDI = 1.30). Thermal stability of these polymers was satisfactory, and 10% of the weight loss under air was achieved at 305 °C. The kinetic of radical homopolymerization enabled to assess the k_p^2/k_t value ($3.62 \cdot 10^{-2} \text{ l} \cdot \text{mol}^{-1} \cdot \text{sec}^{-1}$ at 80 °C). Measurements of both static and dynamic contact angles in the presence of water and diiodomethane were performed on spin-coated surfaces with poly(4'-nonafluorobutyl styrene) achieved from both strategies. Values of contact angles evidenced the satisfactory hydro- and oleophobicity of synthesized polymers, and no significant differences were detected between polymers synthesized by ITP and those obtained by conventional radical polymerization. Conversely, an increase of hysteresis in polymers with lower polydispersity ($47^\circ \pm 2^\circ$) compared to those with higher PDI ($18^\circ \pm 2^\circ$) was observed. The results obtained suggest a strong correlation between PDI values and surface properties of poly(4'-nonafluorobutyl styrene).

In the last part of the thesis, the telomerisation of VDF in presence of $\text{C}_4\text{F}_9\text{I}$ as chain transfer and TBPP as initiator was carried out with 73% of conversion of VDF and 47% of yield. After distillation, different fractions of telomers were obtained. Among them, a monoadduct ($\text{C}_4\text{F}_9\text{-CH}_2\text{CF}_2\text{-I}$) and a diadduct ($\text{C}_4\text{F}_9\text{-(C}_2\text{H}_2\text{F}_2)_2\text{-I}$) were isolated and characterized by ^1H NMR and ^{19}F NMR spectra. The characterization of the monoadduct evidenced the absence of the reverse telomer $\text{C}_4\text{F}_9\text{-CF}_2\text{CH}_2\text{-I}$, confirming the selectivity of the reaction of $\text{C}_4\text{F}_9\cdot$ radical on the VDF monomer. Conversely, the diadduct presents two species, one called "normal" ($\text{C}_4\text{F}_9\text{-CH}_2\text{CF}_2\text{-CH}_2\text{CF}_2\text{-I}$) and one called "reverse" ($\text{C}_4\text{F}_9\text{-CH}_2\text{CF}_2\text{-CF}_2\text{CH}_2\text{-I}$). The diadduct was used as reactant for the synthesis of the alcohol $\text{C}_4\text{F}_9\text{-(VDF)}_2\text{-CH}_2\text{-CHI-CH}_2\text{-OH}$ obtained by radical addition of diadduct to allyl alcohol followed by the reduction with *tert*-butyl stannate.

The reaction with allyl alcohol evidenced the decreased reactivity of the reverse adduct compared to the normal one as evidenced by ^{19}F NMR spectra. In fact, the signal at -40 ppm, assigned to the $\text{-CF}_2\text{-I}$ fluorinated group of the normal $\text{C}_4\text{F}_9\text{-VDF}_2\text{-I}$ telomer, disappeared showing that a reaction happened. Conversely, signals of the inverse diadduct are still present after the reaction with allyl alcohol, demonstrating the less reactivity of the reverse adduct.

Ringraziamenti

Giunto alla conclusione di questo lavoro desidero ringraziare il Prof. Conte per la sua disponibilità e supporto fornito durante l'attività di ricerca svolta in questi tre anni.

Desidero ringraziare in modo particolare il Dr. Alessandro Zaggia, che mi ha fatto da guida e da maestro, fornendomi tutti gli strumenti e le conoscenze necessarie per completare il mio percorso formativo.

Ringrazio il Dr. Gennifer Padoan, che ha condiviso con me i primi due anni di dottorato, per avermi aiutato nelle prime fasi di sperimentazione in laboratorio.

Ringrazio il Prof. Bruno Ameduri, direttore di ricerca presso l'École Nationale Supérieure de Chimie de Montpellier, per avermi ospitato e seguito durante il periodo di ricerca svolto all'estero.

Ringrazio il Dr. Paolo Sgarbossa e il Dr. Alfonso Venzo, per avermi aiutato nella fase di sintesi e di caratterizzazione dei prodotti sintetizzati.

Un sentito ringraziamento alla mia famiglia per essermi stata accanto fino ad oggi e senza la quale non sarei riuscito a raggiungere gli obiettivi sinora prefissati.

Infine ringrazio tutti coloro che mi hanno sostenuto, sia in ambito scientifico che "extra-scientifico" per avere reso piacevoli le ore trascorse insieme.